The Occurrence of Residual Biological and Chemical Hazards in Recovered Struvite from Blackwater

by

Rachel Ashley Yee

A thesis submitted in partial fulfillment of the requirements for the degree of

Master of Science

in

Environmental Engineering

Department of Civil and Environmental Engineering

University of Alberta

Abstract

Phosphorus is an essential element in several industries such as agriculture and a requirement for growth. Dwindling phosphate rock sources thus requires the security of new phosphorus sources to maintain future populations. On the other hand, wastewater contains a considerable amount of nutrients that are often released into the receiving environment. To reduce the eutrophication that results from effluent release and secure a new phosphorus source, nutrient recovery from treated wastewater can be an attractive option. Phosphorus and nitrogen recovery in the form of struvite ($MgNH_4PO_4 \cdot 6H_2O$) has been identified as a product easily precipitated from wastewater effluent and could help alleviate phosphorus pressures by acting as a slow release fertilizer.

More specifically, anaerobic digestion of source-diverted blackwater has been shown to provide a good source for energy and nutrient recovery. However, since source-diverted blackwater lacks the dilution typically associated with municipal wastewater, the concentration of hazards would be expected to be much higher. Potential hazards of concern include microbial pathogens, antimicrobial resistance genes (ARGs), pharmaceuticals and heavy metals. Though struvite precipitation from wastewater is not a new process, the level of risk associated with applying recovered struvite to agriculture has not been well characterized. A full analysis of pilot and full scale struvite samples in comparison to lab produced struvite shows that all samples can be identified as struvite regardless of their source. However, further examination into the co-precipitation that occurs shows that a more complex matrix such as blackwater would produce a product with reduced purity as bacteria, viruses, ARGs and other macro- and micronutrients can be detected.

Additionally, many water chemistry conditions have been identified as optimal conditions for enhancing the precipitation process, but the consideration of hazard co-precipitation has not been taken into account. This study shows that pH of 9, 1.5:1 Mg^{2+}:PO_4^{3-} molar ratio and $MgCl_2$ dosing rate of 24 mL•min^{-1} are most optimal for enhanced phosphorus recovery and reduced co-precipitation from blackwater. Furthermore, it is shown that the post-processing methods, such as drying would be required to further reduce the risk presented by viable bacterial cells.

Preface

The contents of this thesis are my original work, with the contribution of several individuals listed below. The research shown in this thesis was conducted under the supervision of Dr. Yang Liu and Dr. Nicholas Ashbolt, both of which have made significant contributions to all areas of this project.

Candis Scott and Graham Banting (School of Public Health, University of Alberta) contributed to the development of the molecular methodology described and used in Chapter 3, 4 and 5. The *uidA* and *entero1* qPCR assays were previously developed and optimized by Candis Scott and Graham Banting (School of Public Health, University of Alberta) and Candis Scott solely developed the method for *cpn60* detection.

Nancy Price (School of Public Health, University of Alberta) contributed to the development of microbiological methodology described and used in Chapter 3, 4 and 5. The *C. perfringens* wastewater isolate used in the project was isolated by Nancy Price.

Mats Leifels, School of Public Health, was solely responsible for method development and virus detection described in Chapter 4.

Lastly, a version of Chapter 4 and 5 have been prepared for journal publication.

Acknowledgement

The work presented in this thesis could not have been accomplished without the support and expertise of a large number of people in my life.

First and foremost, I would like to thank my supervisors Dr. Yang Liu and Dr. Nicholas Ashbolt for their supervision, advice and guidance from the early stages of research to putting this thesis together. I am grateful for the opportunity to work on such an integrated project and for the skills they have allowed me to develop as a part of their groups.

A big thanks to all past and present group members in the Liu and Ashbolt group for the support throughout my time in the lab. I feel fortunate to have had the opportunity to work with members of both groups who diversified my knowledge. Special thanks to Candis Scott and Nancy Price for all the molecular and microbiological training and technical support. I would also like to thank Johnathon Shim for helping with experiments in the lab and Weiduo Hao for helping program the titrator.

I would like to acknowledge the University of Alberta service labs that assisted with several different types of sample analyses and the funding sources (NSERC-CRD, City of Edmonton/EPCOR Water Services and Alberta Innovates) for allowing this research to occur. I also gratefully acknowledge Dr. Tong Yu for being a part of my exam committee.

Lastly, I would not be here without my family's love and encouragement. My parents have supported me through everything I have pursued and no doubt will continue to support me in my future endeavours. I would also like to thank my husband, Huy, for his never-ending support and love and for making Edmonton feel like home. I could not have asked for a better partner to share my accomplishments and life with. I must also thank our dog, Robin, for all the cuddles on the rough days.

Table of Contents

List of Tables

List of Figures

List of Abbreviations

AMR – Antimicrobial resistance

ARB – Antimicrobial resistant bacteria

ARG – Antimicrobial resistance genes

BGM – Blue green monkey

CFIA – Canadian Food Inspection Agency

CFU – Colony forming unit

EDS – Energy dispersive X-ray spectroscopy

EV - Enteroviruses

FIB – Fecal indicator bacteria

HAdV – Human adenoviruses

HGT – Horizontal gene transfer

ICC – Integrated cell culture

ICP-OES – Induced coupled plasma optical emission spectrometry

ICSD – Inorganic crystal structure database

MATH - Microbial adhesion to hydrocarbons

MAP - Magnesium ammonium phosphate

MGE – Mobile genetic element

MPN – Most probable number

NoV GII – Norovirus G11

QMRA – Quantitative microbial risk assessment

qPCR – Quantitative polymerase chain reaction

SEM – Scanning electron microscope

TSA – Trypticase soy agar

TSB – Trypticase soy broth

WWTP – Wastewater treatment plant

XPS – X-ray photoelectron spectroscopy

XRD – X-ray diffraction

Chapter 1 – Introduction

1.1 Overview of Phosphorus Scarcity

Phosphorus (P) is an essential element for living organisms and agricultural production, however, is a limiting nutrient. It has allowed for increased global food production that is necessary to sustain Earth's population (Mayer et al. 2016). Phosphate rock is the dominant source of available phosphorus that can be utilized as a phosphorus fertilizer (Cordell and Neset 2014). The accessible phosphate rock reserves are currently limited to China, the US and Morocco (Cordell et al. 2009). There are several social, economic and environmental factors that control the accessibility of the phosphate rock and the need to secure new sources.

Despite the beneficial use of phosphorus in the agricultural industry, a large amount of residual phosphorus is lost thus accelerating water pollution. Increased levels of phosphorus in water can cause the phenomenon of eutrophication to elevate, which leads to uncontrolled algal growth that can impact water supplies (Mayer et al. 2016). Impacted by eutrophication is the natural water chemistry which reduces the water quality for aquatic life and recreational use (USEPA 1998).

With phosphate rock sources and water pollution becoming a global issue, reuse and recovery appears to be an attractive alternative. For the agricultural industry, P recovery and reuse will be critical in maintaining future food supplies as well as minimizing economic and political issues that revolve international food supply. By recovering, receiving waters will also contain lower levels of phosphorus that will ultimately improve water quality by reducing eutrophication effects (Mayer et al. 2016).

1.2 Overview of Struvite in Wastewater Treatment Plants (WWTPs)

Struvite scaling in pipes is a common occurrence and a costly endeavor for WWTPs to overcome. There are many factors and conditions that can induce the rate of scaling, such as CO_2 stripping that occurs within treatment plants, which can increase the pH and lead to struvite scaling (Le Corre et al. 2009). Chemical additions of alum and ferric chloride (Mamais et al. 1994) into treatment plants have been done as a way to remove phosphorus

that would otherwise induce scaling. Recovery of struvite that already occurs in WWTPs assists in alleviating limited phosphorus source, but is also economically valuable, easy to implement and efficient for recovery (Shih et al. 2017).

1.3 Overview of Potential Hazards

There are several potential hazards, both of chemical and biological nature, that are not the means of determining treatment efficiency. Chemical hazards can exist as inorganic elements, micropollutants and pharmaceutical and personal care products. Inorganic elements, such as sodium, iron and copper are often present in WWTPs and may not always be completely removed. For water reuse, the inorganic elements remaining in the effluent could present a potential risk depending on end use. The application of struvite recovered from wastewater for agricultural purposes could affect crop production as metals in excess levels can be toxic to plant growth. Additionally, metal presence can reduce the purity of struvite. Pharmaceuticals in the form of antibiotics can also be problematic as antibiotic by-products can be excreted. Current treatment regimens do not directly measure these types of chemicals, so the removal efficiency is not well known.

Biological hazards exist as bacteria, viruses, protozoa and helminths. Fecal indicator bacteria (FIB) including *Escherichia coli* and *Enterococcus* spp. are often measured as a way to evaluate treatment efficiency and pathogen removal. Spore forming bacteria, such as *Clostridium perfringens* are also concerning as their spores are resistant to disinfection processes. With antibiotics in wastewater, the development of antibiotic resistance can occur. Antibiotic resistant bacteria (ARB) are responsible for many clinical infections and are the main reason why antibiotics are becoming less effective. In addition to bacterial presence within waste streams, viruses are also a concern as they tend to be more stable despite their need for a host. As discussed, several hazards exist within wastewater and utilization of treated effluent for reuse purposes can pose a public health concern that requires further consideration.

1.4 Overall Objectives, Hypothesis and Thesis of Structure

The overall objective of this study was to determine if there is a need for future risk assessments on struvite recovered from blackwater and if there are conditions that reduce co-precipitation of other wastewater components in struvite. To achieve this goal, specific objectives were developed for this research as follows:

1. Optimize methods for microbial risk detection.

   Bacterial isolates recovered from wastewater were used to develop qPCR methods for ARG detection and used as a tool in determining co-precipitation of bacteria and ARGs required to achieve objective 1 and 2 as listed below.

2. Evaluate wastewater recovered struvite from pilot and full scale plants.

   Hypothesis: Treatment efficiency of WWTPs typically depends only on a few parameters and with the complexity of wastewater, it is predicted that metals and pathogens can co-precipitate and be detected in the final struvite product regardless of feed source and processing methods. It is also predicted that a concentrated source of wastewater, such as blackwater would result in higher co-precipitation capabilities due to a higher residual concentration of nutrients and potential hazards.

3. Evaluate the impact of struvite precipitation conditions on phosphorus recovery and metal/microbial co-precipitation from blackwater.

   Hypothesis: As hazard co-precipitation could occur, it is predicted that there will be an optimal condition by altering pH, Mg^{2+}:PO_4^{3-} and $MgCl_2$ dosing rate (deemed important factors) that promotes enhanced recovery with reduced co-precipitation. A more basic environment would increase struvite precipitation, but would also readily affect cell viability appearing more attractive for reduced microbial co-precipitation. Increased presence and rate of Mg^{2+} addition would also increase struvite recovery, but could also impact metal co-precipitation through crystal formation interference.

Chapter 1 provides an overview of relevant information to the project and describes the problem, objectives and organization of the thesis. Following is Chapter 2 which is a literature review of struvite, its reported recovery from wastewater and a review of important hazards present in wastewater. Chapter 3 describes the detailed method development for culture methods and antibiotic resistance qPCR assays used for further experiments and addresses the first objective. Furthermore, this study was divided into two main parts to address the second and third objective above. The first involved a full analysis on struvite samples recovered from pilot and full scale plants. More specifically, the objective of the first part of the study (detailed in Chapter 4) were as follows:

- To develop and utilize methods that assess the physical, chemical and biological characteristics of commercial struvite products recovered from wastewater.

The second part of the study examines changes in water chemistry conditions that are relevant to struvite precipitation to determine optimized conditions for phosphorus recovery with minimized co-precipitation. The specific objectives of the second part of the study (detailed in Chapter 5) were as follows:

- To assess the effects of pH (ranges from 7-9), Mg^{2+}:PO_4^{3-} molar ratio (ranges from 1:1– 2:1) and $MgCl_2$ dosing rate (ranges from 0.1 – 24 mL/min) on the phosphorus recovery of struvite from synthetic wastewater representative of anaerobically digested blackwater.

- To assess hazard partitioning from the liquid to solid phase of the struvite precipitation process at the tested conditions. Fecal indicator bacteria (FIB) – *E. coli*, *E. faecalis* and *C. perfringens* with known antimicrobial resistance gene (ARG) markers and a mixture of metals were assessed for their detection in the recovered product.

Both Chapter 4 and 5 are presented as technical papers titled “Evaluated Microbial and Chemical Hazards in Commercial Struvite Recovered from Wastewater” and “Nutrient Recovery from Source-Diverted Blackwater: Optimization for Enhanced Phosphorus Recovery and Reduced Hazard Co-precipitation”, respectively, where a version of the chapter will be submitted for publication. Lastly, Chapter 6 summarizes the conclusions of the study and recommendations for future work. It must also be noted that information could be repeated throughout this thesis given it has been prepared as a paper-based thesis.

1.5 References

Cordell D, Neset TSS. 2014. Phosphorus vulnerability: A qualitative framework for assessing the vulnerability of national and regional food systems to the multi-dimensional stressors of phosphorus scarcity. Glob. Environ. Chang. 24:108–122.

Cordell D, Schmid-Neset T, White S, Drangert J-O. 2009. Preferred future phosphorus scenarios: A framework for meeting long-term phosphorus needs for global food demand. Ashley K, Mavinic D, Koch F, editors. London, UK: IWA Publishing.

Le Corre KS, Valsami-Jones E, Hobbs P, Parsons SA. 2009. Phosphorus recovery from wastewater by struvite crystallization: a review. Crit. Rev. Environ. Sci. Technol. 39:433–477.

Mamais D, Pitt PA, Cheng YW, Loiacono J, Jenkins D, Wen Y. 1994. Digesters determination to control in anaerobic of ferric chloride precipitation digesters dose struvite sludge. Water Environ. Res. 66:912–918.

Mayer BK, Baker LA, Boyer TH, Drechsel P, Gifford M, Hanjra MA, Parameswaran P, Stoltzfus J, Westerhoff P, Rittmann BE. 2016. Total value of phosphorus recovery. Environ. Sci. Technol. 50:6606–6620.

Shih Y-J, Abarca RRM, de Luna MDG, Huang Y-H, Lu M-C. 2017. Recovery of phosphorus from synthetic wastewaters by struvite crystallization in a fluidized-bed reactor: Effects of pH, phosphate concentration and coexisting ions. Chemosphere 173:466–473.

USEPA. 1998. National Strategy for the Development of Regional Nutrient Criteria.

Chapter 2 - Literature Review

2.1 Phosphorus

Phosphorus is a key element essential for all living organisms and is required in many industries such as agriculture (Song et al. 2007; Le Corre et al. 2009). The current source of phosphorus lies within phosphate rock, which is a non-renewable resource (Mehta and Batstone 2013; Kemacheevakul et al. 2015). Current phosphate rock reserves are limited to China, the US and Morocco and are quickly depleting (Cordell et al. 2009). With phosphate rock reserves confined to only a few places, transportation and energy costs can also be significant (Cordell et al. 2009). Additionally, the decrease in availability will result in a gap between supply and demand. Shown in Figure 2.1 are scenarios depicting how phosphate rock reserves could impact future phosphorus demands. Despite which scenario occurs, phosphate rock supply will decrease and result in decreased phosphorus availability.

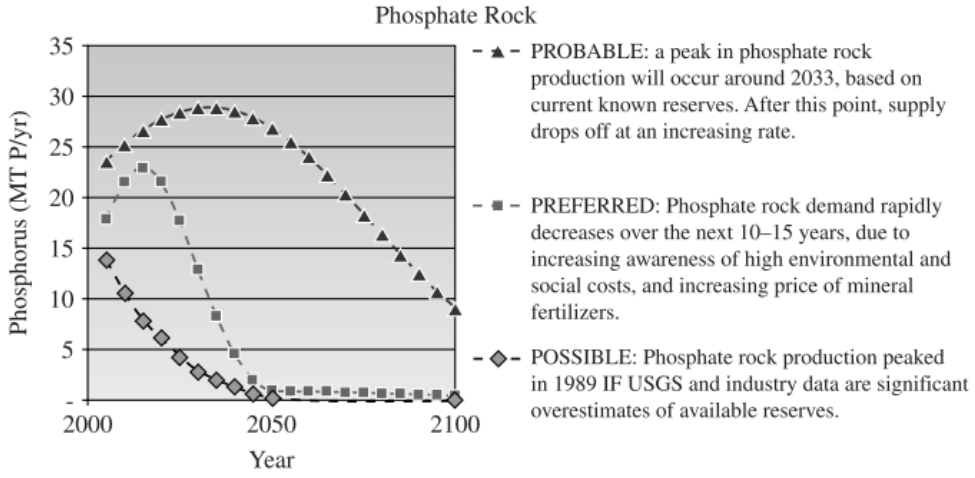

Figure 2.1 The contribution of phosphate rock in future phosphorus demand (Cordell et al. 2009).

At all points in the system from mining phosphate rock to discharge into the environment, the loss of phosphorus can exist and will negatively impact the environment. Eutrophication is a problem that can occur due to an excessive amount of phosphorus release into the receiving environment. It results in overgrowth of aquatic plants, typically algae that in turn depletes oxygen in the water and reduces the potential for light penetration into the water

(Rahman et al. 2014). In this case, a large amount of phosphorus is lost and the deoxygenation of receiving waters from enhanced plant growth ultimately affects the rest of the ecosystem (Mayer et al. 2016; Tang 2016). Formation of algal blooms from excess nitrogen and phosphorus in receiving waters can reduce the available oxygen levels.

Figure 2.2 depicts a simple schematic that tracks where mined phosphate eventually ends up. The cycle of water reuse and associated benefits can be observed from the schematic.

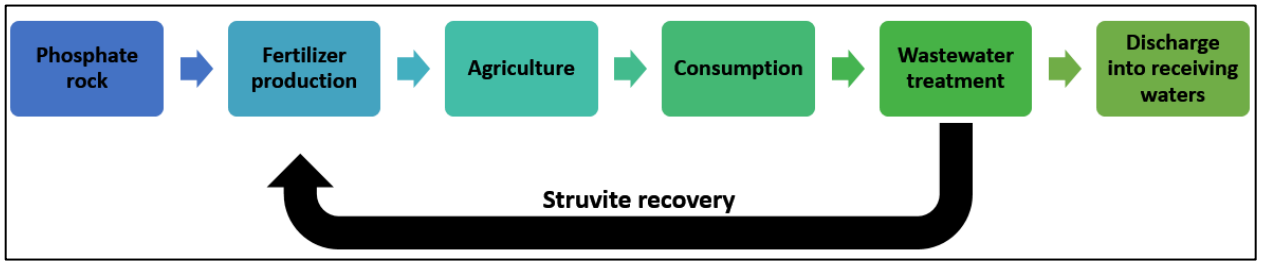

Figure 2.2 Simple schematic of phosphorus source and end use.

With issues of limited phosphate rock and eutrophication due to effluent discharge, nutrient recovery appears to be an attractive option to help alleviate issues posed by phosphorus and to promote water reuse.

2.2 Wastewater

2.2.1 Anaerobic Treatment of Blackwater

Municipal wastewater collected in centralized systems often consist of a mixture of waste streams, including blackwater and greywater. Blackwater is the wastewater stream collected from toilets and therefore contains a high concentration of nutrients, organics, chemical compounds and pathogens, though the composition of blackwater is very dependent on the demographics and thus can be variable (Kujawa-Roeleveld and Zeeman 2006; Gallagher and Sharvelle 2010). Figure 2.3 depicts the distribution of COD, nitrogen, phosphorus and potassium in various wastewater streams with urine and faeces together dominating in nitrogen, phosphorus and potassium, thus showing that the largest amount of nutrient availability would occur from a blackwater source.

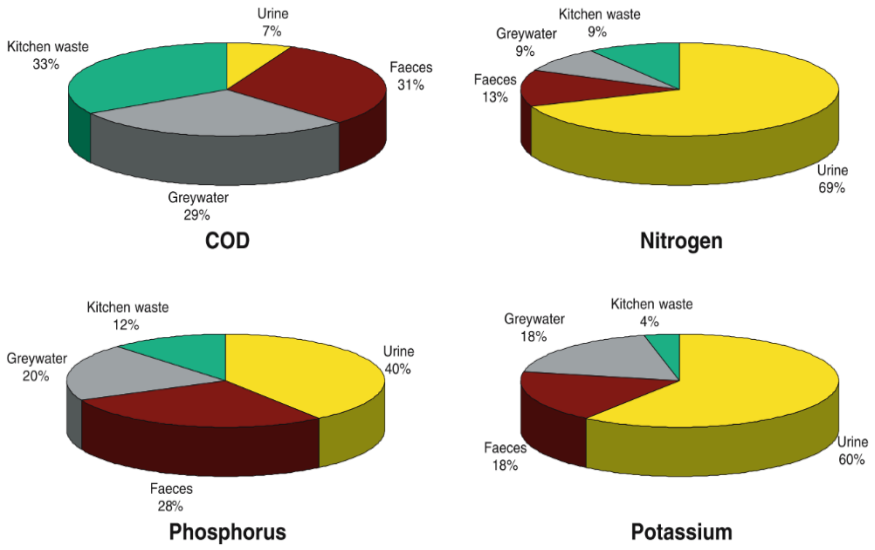

Figure 2.3 COD, nitrogen, potassium and phosphorus distribution in wastewater streams (Kujawa-Roeleveld and Zeeman 2006).

With knowledge of the large nutrient load in blackwater, source-diverted blackwater could be favourable in promoting nutrient recovery (Gallagher and Sharvelle 2010). Furthermore, source-diverted blackwater has a high organic loading that makes it favourable for anaerobic treatment (Gallagher and Sharvelle 2010). Anaerobic digestion of blackwater can produce a methane biogas that can be used as a renewable energy source (Gallagher and Sharvelle

2010). The process of anaerobic digestion assists in the solubilisation of organic phosphorus and nitrogen into phosphate and ammonia respectively (Mehta and Batstone 2013). Thus, the effluent of anaerobically treated blackwater has been shown to contain soluble nutrients, such as phosphorus and nitrogen that can be recovered as a fertilizer (Gallagher and Sharvelle 2010; de Graaff, Temmink, Zeeman, and Buisman 2011; de Graaff, Temmink, Zeeman, van Loosdrecht, et al. 2011). Table 2.1 shows the effluent composition of blackwater following anaerobic digestion from an upflow anaerobic sludge blanket (UASB) reactor.

Table 2.1 Published UASB effluent composition (de Graaff et al. 2010).

		Day 1 – 518		Day 519 – 951	
	Unit	UASB effluent	s.d.	UASB effluent	s.d.
pH	-	7.6	0.13	7.4	0.17
COD_{total}	[gCOD/L]	2.4	0.84	1.2	0.34
COD_{SS}	[gCOD/L]	0.43	0.43	0.10	0.08
$COD_{colloidal}$	[gCOD/L]	0.53	0.27	0.21	0.07
$COD_{soluble}$	[gCOD/L]	1.5	0.39	0.90	0.21
VFA	[gCOD/L]	0.36	0.30	0.14	0.18
BOD_5	[g/L]	0.87	0.24	0.48	0.06
HCO_3^-	[gC/L]	1.4	0.14	0.87	0.10
TN	[gN/L]	1.8	0.22	1.2	0.12
NH_4-N	[gN/L]	1.5	0.19	1.0	0.18
TP	[gP/L]	0.13	0.015	0.094	0.018
TP soluble	[gP/L]	0.103	0.010	0.070	0.011
PO_4-P	[gP/L]	0.092	0.011	0.069	0.013

s.d. = standard deviation

Studies examining the treatment of blackwater via an UASB reactor show that there is a high COD removal as well as a log reduction in *E. coli* and fecal coliforms. Despite that, the effluents typically do not meet the standards for reuse and discharge without further post-treatment (Kujawa-Roeleveld and Zeeman 2006). A study examining the concentrations of select micropollutants in influent blackwater show that the concentrations are higher than the values expected for municipal wastewater (Butkovskyi et al. 2017). Post treatment with an UASB reactor results in an effluent with residual micropollutants (Butkovskyi et al. 2017). It has also been suggested that UASB treatment of blackwater could potentially remove heavy metals to improve treatment efficiency (Gell et al. 2011).

2.2.2 Metals in Wastewater

Metals in wastewater are chemical concerns as discharge of high metal concentrations can be toxic to the environment. As treatment systems are not specifically designed for metal removal, the fate of metals and their removal through processes are not well characterized. Metal concentrations can also be highly dependent on the source of the wastewater, where industrial waste is more likely to contain a higher concentration of metals than municipal wastewater (Drozdova et al. 2015). Thus, the influent and effluent concentrations will be highly variable between WWTPs. Due to the higher concentrations observed in industrial wastewater, it is not surprising that there are more strict regulations regarding metals prior to discharge.

Metal removal in municipal wastewater has been examined by measuring the metal concentrations in dissolved and particulate phases at different phases of treatment (Choubert et al. 2011). The major cations that are found in wastewater are K, Mg and Ca with micronutrients including Mn, Fe, Co, Cu, Mo and Ni (Thanh et al. 2016). In anaerobic digestion, trace metals are essential for the growth of microbes that assist with the digestion process. Micronutrients as mentioned above are required for enzyme functioning associated with the success of anaerobic digestion. It has been shown that the major cations K, P and N are typically preserved through the process (Legros et al. 2017). Furthermore, anaerobic digestion is capable of altering the speciation of metals, specifically Cu and Zn (Legros et al. 2017).

Since metals are not biodegradable or volatile, their removal during treatment is not particularly high. Additionally, it was shown that the following metals – Ti, Cr, Cd, Cu, Zn, Sn, Pb, Fe, Ag and Al – could be absorbed to particulates and removed at an efficiency of around 75% through biological treatment (Choubert et al. 2011). On the other hand, metals such as B, Li, Rb and Mo had low absorption capabilities, while Ni, Se, Ba and U resulted in moderate absorption and removal through biological treatment (Choubert et al. 2011). Tertiary treatment was also shown to improve the removal efficiency following secondary treatment (Choubert et al. 2011). Despite these results, it can be concluded that metals will not be fully removed given the current treatment systems and upgrades to current processes

would be required (Choubert et al. 2011). Given this, knowledge that metals will be present in the effluent needs to be taken into consideration prior to discharge into receiving waters or with the intent to reuse.

2.2.3 Pathogens in Wastewater

Wastewater can act as a reservoir for pathogens that are known causes of waterborne diseases and infections. These diseases and infections often occur through waterborne pathogens upon the exposure to affected water sources. The infectious dose and the stability of the pathogen will dictate the harm that it can induce and is highly dependent on the pathogen of interest (Ajonina et al. 2015).

The current processes of wastewater treatment have been highly beneficial in treating wastewater to a level that meets water quality standards. All treatment plants follow a set of guidelines to ensure the effluent meets the standards. Fecal indicator bacteria (FIB) are often used to assess the treatment efficiency as related to pathogen removal. However, other pathogens and biological hazards pose several problems in regards to the effectiveness of these treatment processes. Included in this list are the biological hazards that are already present in wastewater streams, but are typically not used as a measure of treatment efficiency. Examples are spore forming bacteria, viruses, protozoa and helminths.

E. coli is a FIB that is used to indicate the presence of pathogenic microbes and fecal contamination (Wose Kinge et al. 2010). The level of pathogenicity of *E. coli* specifically lies on a spectrum as some strains are commensal, while others are responsible for causing disease (Ajonina et al. 2015; Bajaj et al. 2016). Though they are commonly tested and isolated from waste streams, *E. coli* only represents a very low percentage of the total coliforms that could be present (Johnson and Atheesha 2013; Ajonina et al. 2015). It has also been suggested that *E. coli* may not be suitable indicators for enteric pathogen detection, though *E. coli* is commonly used for treatment efficiency (Johnson and Atheesha 2013). Similarly to *E. coli*, enterococci are ubiquitous bacteria and also excreted at high densities that are also classified as FIB. They are gram positive bacteria that are capable of surviving

in adverse environmental conditions, thus making them a good option as an indicator of treatment efficiency.

Though *E. coli* and *Enterococcus* spp. are more frequently tested for treatment efficiency, *Clostridia* spp. can also be found in wastewater. Their ability to form spores makes them persistent through treatment processes and could be a better indicator for pathogen detection (Lucena et al. 2004; De Sanctis et al. 2017). Detection of *C. perfringens* shows that the log removal is typically much lower than other indicator organisms (Wen et al. 2009; Ajonina et al. 2015) A study has shown that removal of spores due to irreversible adsorption may be the best method for increased log reduction, however, it is more likely that detachment could occur (Wen et al. 2009). When compared to *E. coli*, *C. perfringens* is more persistent in wastewater over time (Vierheilig et al. 2013). Furthermore, the detection of spores can also be delayed following an outbreak downstream (Vierheilig et al. 2013).

Viruses are also typically found in wastewater in numbers as high as 10^{13} viral particles per gram of stool (Lizasoain et al. 2018) and can thus be the cause of environmental contamination and a number of waterborne diseases. They are relatively stable under environmental stresses which makes them resistant to treatment processes (Johnson and Atheesha 2013). Use of the above mentioned FIB as indicators for virus presence has recently not been well supported as recent studies have shown that there is a weak correlation between bacteria and virus reduction following treatment (Harwood et al. 2005; Payment and Locas 2011). Some important human enteric viruses include norovirus genogroup II (NoV GII) and human adenovirus (HAdV), which can be excreted in high concentrations (Iaconelli et al. 2017). In particular, NoV is a major contributor to gastroenteritis, with the genogroup II most frequently associated with disease in clinical cases and is more persistent in wastewater (Haramoto et al. 2018; Lizasoain et al. 2018). HAdV has been suggested as an indicator of sewage contamination due to its prevalence, occurrence in the environment and resistance to environmental stresses (Johnson and Atheesha 2013; Iaconelli et al. 2017). Regardless, the efficacy of WWTPs processes typically does not fully remove all virus particles.

Protozoa are abundant in wastewater and can be pathogenic as well as non-pathogenic. Included in this group of organisms are ciliates, flagellates and amoeba. They play an important role in clarification of the effluent and function in the process of carbon mineralization and as bacteria grazers (Madoni 2011). The observed carbon mineralization is more likely to play a larger role in high substrate conditions. Increased numbers of protozoa can also be related to increased nitrification per cell as protozoa can affect the growth of bacteria (Madoni 2011). Thus, protozoa are useful in nitrogen, phosphorus and carbon cycles. Protozoa within anaerobic treatment processes have not been widely investigated. One study shows that protozoan counts can be correlated to COD removal and sludge activity (Priya et al. 2007), but further studies would be required to confirm the role of protozoa in anaerobic treatment. Though, this group can assist in wastewater treatment, parasitic protozoa have been linked to cause gastroenteritis. Examples of parasitic protozoa include *Cryptosporidium* spp. and *Giardia intestinalis* (Berglund et al. 2017). *Cryptosporidium* spp. and *Giardia intestinalis* are typically eliminated from infected hosts and can persist as they are released in states that make them more resilient to changing environments (Berglund et al. 2017). It has been noted that *Cryptosporidium* spp. is typically linked to waterborne outbreaks and is therefore not detected unless an outbreak occurs, whereas a high removal rate of *Giardia intestinalis* has been observed (Berglund et al. 2017). During outbreaks, *Cryptosporidium* spp. and *Giardia* can be excreted at numbers as high as 10^9-10^{10} oocysts (*Cryptosporidium* spp.) and cysts (*Giardia*) per day and can persist through treatment processes (Risebro et al. 2007). As literature pertaining to protozoan counts in anaerobically treated wastewater is limited, it remains unclear as to the role they play.

Another group found in wastewater are helminths, which could be problematic as they could persist in the environment. There are several types of helminths, each with their own life cycle that reproduce through eggs. The eggs are the infective agent of helminths and are of greater concern than the worm life stage (Jimenez-Cisneros 2006). They are more difficult to inactivate with treatment processes such as chlorine, UV or ozone treatment than other microorganisms typically found in wastewater (Jimenez-Cisneros 2006). Furthermore, survival of helminths in wastewater are relatively low as they require a host. However, only a low number of eggs are required to reach the infectious dose. Within soil and crops, the

survival time of helminth ova has been reported to be much longer than bacteria, viruses and protozoan oocyts (Jimenez-Cisneros 2006). The conditions of anaerobic digestion have been shown to alter the stage of *Ascaris lumbricoides* ova and can thus play a major role in reducing their potential infectivity post treatment (Manser et al. 2015). Exposure to anaerobic conditions causes the ova to remain in a dormant stage or be unembryonated (Manser et al. 2015). The digestion process can assist in physically damaging the ova, thus capable of reducing the viability (Manser et al. 2015).

Current wastewater treatment standards involve detection of FIB to assess the treatment efficiency and potential contamination in the effluent. Several techniques, including culture methods and molecular methods, have been employed to detect FIB, such as *E. coli* and enterococci in wastewater streams. The advantage of molecular methods is that cultural bias is avoided (Luby et al. 2016). Despite that, there are also limitations to molecular methods including the difficulty in assessing the functionality and cell viability (Luby et al. 2016). Molecular methods can be used to determine cell concentration, however, detection of a certain target may not indicate if the gene is functional or mutated (Luby et al. 2016). It can also be difficult to determine if the entire gene is intact or the state of the cell (Luby et al. 2016). Other indicators are often used for enteric viruses as methods for virus detection are often expensive and labour intensive (Johnson and Atheesha 2013). Additionally, methods with the ability to detect low numbers is required as few viral particles can be sufficient enough to cause infection/disease and culturing methods can be slow (Johnson and Atheesha 2013).

2.2.4 Antibiotic Resistance in Wastewater

To date, many different natural and synthetic antibiotics have been developed for use predominantly in medicine and agriculture. Each antibiotic falls into a different class that is typically classified based on their mechanism of action. The mechanism of action of each antibiotic class varies in addition to whether they act in a broad or narrow spectrum. Increasing levels of resistance to current antibiotics force the development of new antibiotics

and the combination of multiple antibiotics for treatment. Table 2.2 lists some of the common antibiotics that are used. In addition to a difference in mechanism of action, antimicrobial resistance genes (ARGs) within the bacteria have been identified as ways for microbes to become resistant.

Table 2.2 List of Common Antibiotics (Hooper 2001; Said et al. 2015).

Antibiotic Class	Antibiotic Sub-class	Antibiotic	Mechanism of Action	Broad or Narrow Spectrum	Commonly Studied Genes
Beta-lactams	Penicillin	Ampicillin	Inhibits and disrupts synthesis of bacterial cell wall	Broad	*bla_{TEM}* *bla_{CTX-M}* *bla_{SHV}*
		Amoxicillin			
	Cephalosporin	Cefazolin (1st gen)		Broad	
		Cefoxitin (2nd gen)			
		Cefotaxmine (3rd gen)			
		Ceftazidime (4th gen)			
	Carbapenem	Meropenem		Broad	
Fluoroquinolones		Ciprofloxacin	Affects DNA synthesis	Broad	*qnrA* *qnrB* *qnrS*
		Levofloxacin			
Tetracyclines		Tetracycline	Affects protein synthesis	Broad	*tetO* *tetW* *tetA*
Sulfonamides		Sulfamethoxazole	Inhibition of metabolic processes that affect growth and replication	Narrow	*sul(I)* *sul(II)*
Macrolides		Erythromycin	Affects protein synthesis	Broad	*ermB*
Glycopeptides		Vancomycin	Inhibits synthesis of bacterial cell wall by substrate binding	Narrow	*vanA* *vanB*
Amphenicol		Chloramphenicol	Affects protein synthesis	Broad	*catA*
Aminoglycosides		Kanamycin	Affects protein synthesis	Narrow	*aph(3)-IIIa* *aac(6')-Ie-aph(2")-Ia* *ant(6)-Ia*
		Streptomycin			
		Gentamicin			
		Tobramycin			

AMR is a common area of concern in clinical settings, but antibiotics are also commonly used in agriculture, thus are frequently detected in WWTPs. The persistence of antibiotics residing in the effluent of WWTPs is a relatively new area of research as the spread of AMR has become a global health concern. Due to the wide range of antibiotic consumption, the antibiotic presence in WWTPs will vary based on demographics and location. In many instances, consumed antibiotics are not fully metabolized and thus can be detected in WWTPs and presents an outlet for AMR. Comparisons of specific antibiotic persistence in wastewater effluents have been conducted with reports suggesting that some antibiotics are more prone to degradation and removal via wastewater treatment processes than others (Yang et al. 2014; Guo et al. 2017). Though it is inevitable that the antibiotics listed in Table 2.2 will be detected downstream of use, there are some specific antibiotics and ARGs that have appeared to be more prevalent in wastewater. In addition to observing that some antibiotics persist through treatment more than others, specific AMR within bacteria, such as vancomycin-resistant enterococci have become a growing clinical concern. Commonly observed antibiotics in wastewater include tetracycline, vancomycin and trimethoprim where the removal rates are variable between cases (Michael et al. 2013; Li et al. 2014).

Tetracycline is a member of the tetracycline family and is classified as a broad-spectrum antibiotic. Several studies have reported high detection levels of tetracycline in WWTP effluents (Miao et al. 2004). Calcium and other metal ion complexes with tetracycline can form within wastewater treatment plants and thus sorption mechanisms may be more useful for removal (Michael et al. 2013). The *tetA* gene is one of many gene clusters of the tetracycline group and has been commonly identified in wastewater treatment plants and the receiving environment (Borjesson et al. 2009). Studies on *E. coli* isolates from WWTPs show that tetracycline prevalence is particularly high, but even more so when the water is treated (Ferreira Da Silva et al. 2007). Similar patterns between raw and treated water have been reported for *Enterococcus* spp. isolates to ciprofloxacin (Da Silva et al. 2006). Since there are a wide range of genes associated with tetracycline with conjugation and mobile elements being the most common form of gene transfer, tetracycline resistance is not specific to any single type of bacteria (Chopra and Roberts 2001). Despite that, *tetA* is one of the

tetracycline genes limited to gram negative bacteria, hence their prevalence in *E. coli* (Chopra and Roberts 2001).

Vancomycin is a narrow spectrum glycopeptide antibiotic that affects the synthesis of cell wall cross linking (Miller et al. 2014). Cell wall synthesis is prevented via peptidoglycan chain cross-linking that occurs due to the binding of the glycopeptide to peptidoglycan precursor (Miller et al. 2014). The observation of highly resistant vancomycin *Enterococcus* spp. in clinical settings has been important as it is responsible for nosocomial infections (Da Silva et al. 2006). Therefore, the examination of antibiotic resistance in WWTPs related to vancomycin in enterococci could result in important information pertaining to the spread of these highly resistant strains. Similarly to other ARGs, several clusters have been identified in relation to vancomycin with *vanA* being the most frequently observed cause of vancomycin resistance (Miller et al. 2014). Clinical isolates have also expressed varying levels of resistance through the *vanB* gene, which has some similarities to *vanA* (Woodford et al. 1995; Miller et al. 2014). Though *vanA* and *vanB* genes have some similarities, there are some differences in the functionality of the genes (Miller et al. 2014). The sensor kinase and response regulator are not closely related and thus their gene activation differs (Miller et al. 2014). Additionally, both *vanA* and *vanB* rely on mobile elements that are transferred between enterococci (Cetinkaya et al. 2000; Miller et al. 2014). They can be found on both plasmids or chromosomes, unlike some other vancomycin resistance genes that are limited to the chromosome (Van Hoek et al. 2011). As there are a number of reservoirs that could increase the number of transposition events, it is not surprising that *vanB* resistance in *Clostridium* spp. has also been previously reported (Bender et al. 2016).

There are several mechanisms in which AMR can be spread between organisms. Genetic material can be passed on via transformation, transduction, conjugation or transposition. Transformation occurs when DNA is directly taken up by recipients. This method of gene transfer is often observed in environmental samples as DNA can be directly taken up from the environment. Once within the cell, the gene cassette can be incorporated within a plasmid or recombine with the host's genome (Culyba et al. 2015). Transduction typically occurs through the use of phages in which the phage that infects the cell carries the gene cassette.

Conjugation occurs when DNA is exchanged between contact of different species. Lastly, transposition occurs when mobilization of DNA occurs within the genome of an organism. Transposons are typically associated with the mechanism of HGT. Integrons are mobile genetic elements (MGEs) that do not confer resistance themselves, but are important in the dissemination of AMR as they allow for the transfer of gene cassettes between cells (Berglund et al. 2015; Gillings 2017). As a result, horizontal gene transfer (HGT) could allow for increased levels of ARB within the environment (Baquero et al. 2008). Though examining specific gene targets can be valuable, integron presence could be a strong predictor in the AMR spread. Class 1 integrons are the most frequently observed integron class related to AMR (Dillon et al. 2005). The 5'-CS to 3'-CS region are variable regions where the inserted cassettes for varying antibiotic resistance can be found (Jones et al. 2001; Dillon et al. 2005). The *intI1* gene is often found at increased levels in the effluent of WWTPs (Di Cesare et al. 2016) and is thought to be a driver for AMR spread.

With antibiotics persisting in receiving environments, the development of ARB can occur from the acquisition of gene cassettes that confer resistance. Multi-drug resistance is becoming more problematic as many of the above mentioned antibiotics are proving to be ineffective and with gene transfer playing a large role. In addition to the presence of residual antibiotic products and ARGs, there are several other factors that can influence the spread of AMR. When bacteria are in close proximity to each other, the high density can increase the probability of gene transfer (Karkman et al. 2018). Additionally, the occurrence of anti-restriction proteins in plasmids and transposons can help overcome the host's system, thus allowing survival and persistence (Van Hoek et al. 2011). Lack of detection of the plasmids and transposons can also increase the ability for acquired resistance (Van Hoek et al. 2011).

As a result, the development of ARB has become a growing public health concern. Intensive research has been conducted on resistance developed in FIB, such as *E. coli* and *Enterococcus* spp. likely due to the ease of their detectability, though AMR in other bacteria have also been readily studied. The ability for these organisms to acquire new resistance mechanisms can be problematic, though the development of resistance intrinsically can also occur (Said et al. 2015). Bacteria that can grow in the presence of antibiotics carry ARGs

that function by affecting cell processes (Luby et al. 2016). For example, treatment for infections caused my enterococci typically consists of penicillin or vancomycin with an aminoglycoside to induce a synergistic approach (Said et al. 2015). Thus, it is not surprising that aminoglycoside and vancomycin resistant enterococci have been shown to be common isolates related to human infection (Said et al. 2015).

2.3 Struvite

2.3.1 Struvite Properties

Phosphorus in the form of phosphates can be recovered and reused as products such as fertilizers and insecticides (Le Corre et al. 2009). Recovery of phosphates, particularly from a wastewater source can be useful in helping replenish the diminishing phosphate rock reserves. The precipitation of struvite from wastewater sources is becoming a more promising process for the recovery of phosphate to reduce and reuse phosphorus remaining in treated effluents.

Struvite (also known as magnesium ammonium phosphate (MAP)) is a crystalline compound that consists of magnesium, ammonium and phosphate at equal molar amounts in addition to six water hydrates (Rahaman et al. 2008). Thus, the formation of struvite occurs under the following chemical equation (Le Corre et al. 2009):

$$Mg^{2+} + NH_4^+ + H_nPO_4^{3-n} \leftrightarrow MgNH_4PO_4 \cdot 6H_2O + nH^+ \qquad \text{[Equation 1]}$$

By mass, the composition of struvite is 44 % H_2O, 39 % PO_4^{3-}, 10 % Mg^{2+} and 7 % NH_4^+ (Gell et al. 2011). Struvite has been intensively studied and therefore many properties have been determined and reported (Table 2.3).

Table 2.3 Properties of Struvite.

Property	Value	Reference
Molecular Formula	$MgNH_4PO_4 \cdot 6H_2O$	
Molecular Weight	247.42 g/mol	
Specific Gravity	1.7	
Cell dimensions	a = 6.941 ± 0.002 Å b = 6.137 ± 0.002 Å c = 11.199 ± 0.004 Å	(Tansel et al. 2018)
Mean bond lengths	P-O: 1.543 Å Mg-H_2O: 2.081 Å H_2O-H: 0.792 Å H_2O interaction: 2.630 -3.141 Å N-O: 2.800 Å	(Tansel et al. 2018)
Reported K_{sp} values	2.51×10^{-13}	(Stumm and Morgan 1981)

The arrangement of NH_4^+, Mg^{2+}, PO_4^{3-} and H_2O can be depicted in Figure 2.4. It can be seen that hydration shells form around Mg^{2+} and hydrogen bonds are the predominant bonds in crystal formation. It should also be noted that shorter bonds correlate with stronger bonds and the energy required to break the strong bonds is much higher.

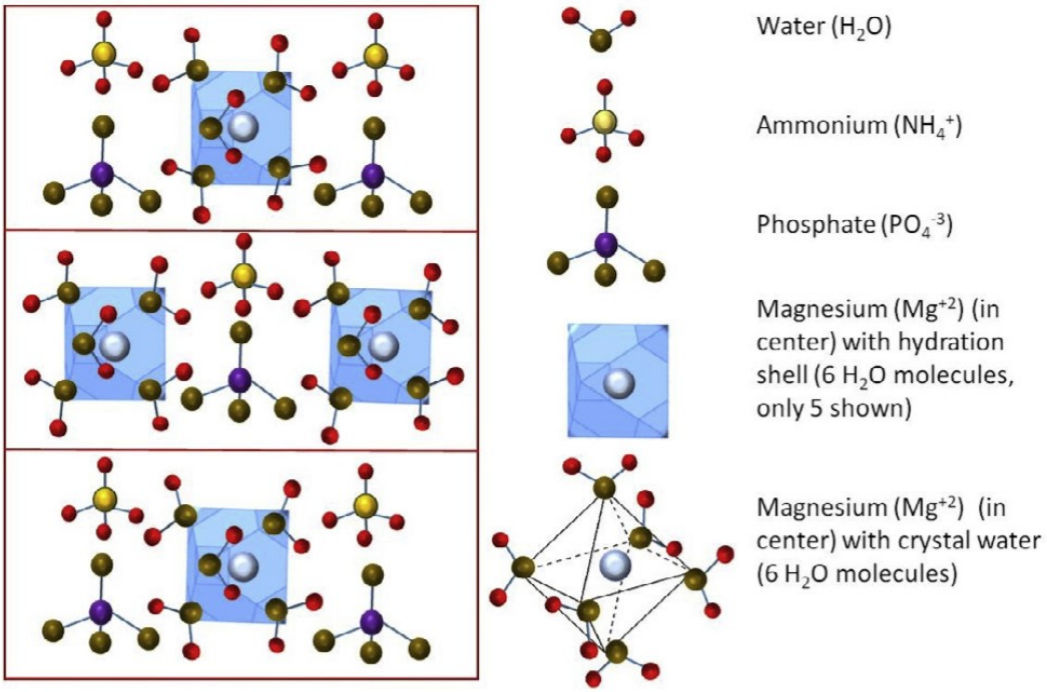

Figure 2.4 Arrangement of ionic groups in formation of struvite crystals (Tansel et al. 2018).

2.3.2 Struvite Nucleation and Crystallization

Struvite formation occurs in two stages known as nucleation and crystal growth. The crystallization process is a thermodynamically unstable process that moves towards the two stages for stabilization (Mehta and Batstone 2013). Nucleation refers to the combination of ions to initiate the birth of the crystal (Le Corre et al. 2009). Specifically, primary nucleation refers to the appearance of the first crystal nuclei, followed by secondary nucleation where the nuclei form when other nuclei are present in the system (Mehta and Batstone 2013; Rahman et al. 2014). In the case of struvite, the contact of Mg^{2+}, NH_4^+, and PO_4^{3-} at concentrations greater than supersaturation allow for cluster formation that induces the nucleation step (Huang et al. 2011, Ohlinger et al. 1999). The supersaturation level is reached when the calculated values are below the minimum solubility product (K_{so}) (Rahman et al. 2014). On the other hand, the solution is undersaturated when the calculated value is above K_{so}. The K_{sp} is typically calculated based on the concentration of ions present in solution (Huang et al. 2011). Use of the super saturation value can assist in predicting the induction time, which is the time required between achieving super saturation and the nucleation step (Rahman et al. 2014).

Following nucleation, crystal growth occurs to form larger crystals (Le Corre et al. 2009), which occurs when the rate of crystal growth exceeds the rate of nucleation (Huang et al. 2011). When this occurs, the activation energy for nucleation to occur is too great compared to the activation energy required for ion deposition on the surface of the crystals (Huang et al. 2011). The rate of the nucleation and crystallization steps will greatly impact the growth kinetics and morphology of the crystal.

Several studies have been done to examine the parameters that affect struvite crystallization. These parameters include pH, Mg:P ratio, supersaturation, mixing and temperature. With these parameters, the kinetics of struvite formation can be altered and compared. It has also been shown that pH, temperature and other ions can control the supersaturation ratio (Fattah 2012). In one instance, the mixing strength has shown to dictate the crystal growth rate (Ohlinger et al. 1999). The ion presence can play a large role in the nucleation and growth stages of crystal formation as they can affect the bonding that occurs, specifically the strength

of the hydrogen bonds and for the formation of salt bridges (interactions involving hydrogen bonding and ionic bonding) (Tansel et al. 2018). Increased presence of PO_4^{3-} and NH_4^+ increase the likelihood of salt bridges to form, thus strengthening the hydrogen bonds (Tansel et al. 2018).

2.3.3 Struvite Morphology

Struvite is a crystalline compound that is typically white in colour (Rahaman et al. 2008). The morphology of the crystals have been described from various types of waste streams and processes. In many cases irregular shaped crystals have been described (Rahman et al. 2014). Twinned dendritic and tabular crystals have been previously observed from synthetic wastewater studies (Mehta and Batstone 2013) in addition to orthorhombic structures (Kim et al. 2007). With varying water chemistry conditions, the crystal morphology could easily present a more elongated, needle-like structure (Mehta and Batstone 2013). The tabular crystals have the more uniform shape with a smaller risk of fracturing into smaller fragments and is therefore the preferred shape (Mehta and Batstone 2013). Figure 2.5 shows a few images of the differences in morphology of struvite recovered from varying waste streams.

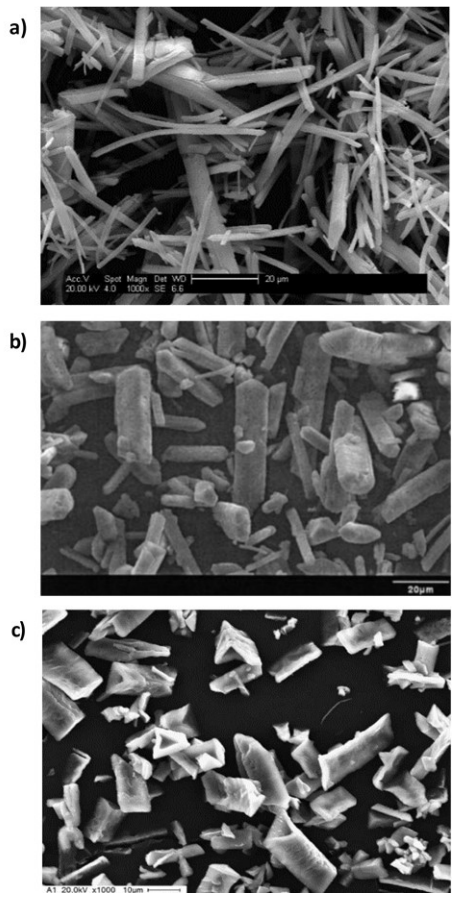

Figure 2.5 Different reported morphological shapes of struvite crystals.
a) (Le Corre et al. 2007); b) (Wang et al. 2005); c) (Huchzermeier and Tao 2012).

There are a number of factors that affect struvite morphology. These include the ion interactions, pH, temperature and time (Tansel et al. 2018). As a result, it is possible that other compounds (as discussed in Chapter 2.4) similar to struvite may form under the given conditions. Irregular growth patterns can occur as a result of other ions co-precipitating.

Commercial struvite products, such as Crystal Green® are usually in the form of granules (Degryse et al. 2017). The granular form of struvite is often recommended for agricultural use as powders dissolve much quicker and therefore has reduced plant availability (Degryse et al. 2017). Thus, the morphology can be important as it can assist in determining the effectiveness as a fertilizer. Currently, limited data exists on the morphology in relation to the phosphorus release and availability upon application.

2.3.4 Struvite Recovery from Wastewater

Within anaerobic sludge digesters in particular, struvite precipitation is a common problem that WWTPs often have to deal with due to the high pH that is generally observed post-digestion in comparison to the treatment steps prior to the digester (Laridi et al. 2005). Initial observations of struvite within a treatment system was first solved by diluting the digested sludge stream until pumps were installed and the diameter of pipes decreased (Parsons and Doyle 2002). Though struvite is not a new problem, it can be costly for WWTPs. With the process of digestion solubilizing the components of struvite, the ability to reach equilibrium occurs for struvite formation (Mamais et al. 1994). This formation typically occurs within the supernatant recycle lines and pumps (Rahaman et al. 2008) where blocked pipes can increase pumping costs and energy requirements (Parsons and Doyle 2002). Decreased pipe diameters also reduces the plant capacity as it takes longer for sludge to move through the system (Parsons and Doyle 2002). The adherence of crystals to sludge particles and the surfaces of the treatment system can result in pipes becoming clogged and the equipment such as pumps and aerators to foul (Fattah 2012). Re-circulation of the effluent can also result in residual phosphorus levels that accumulate and increases the phosphorus load (Fattah 2012). With re-circulation and limited nutrient removal, the efficiency of treatment will decline and maintenance of the system can be impacted (Le Corre et al. 2009; Fattah 2012).

Due to the natural occurrence of struvite formation, methods to reduce and eliminate the problem have been investigated. Mitigation options that have been suggested mainly consist of using chemicals as a control mechanism. Chemicals act to affect the solubility, crystal growth mechanisms and act as dispersants (Parsons and Doyle 2002). As mentioned above, dilution of the sludge stream was initially done, but was not a long lasting solution (Parsons and Doyle 2002). To impact solubility, pH can be adjusted to reduce the precipitation process. This requires the additional cost of acids and/or base to control the pH as the ions present for struvite formation still remain in solution (Parsons and Doyle 2002). Impacting crystal growth can be done by the addition of inhibitor compounds to reduce scaling formation, but the process has not been well studied and optimized (Parsons and Doyle 2002). Metal salts, such as alum or ferric chloride are can be dosed to minimize precipitation

by the removal of phosphate via the formation of vivianite ($Fe_3(PO_4)_2 \bullet 8H_2O$) instead (Mamais et al. 1994). Additionally, side stream treatment has been shown to be an efficient method to control struvite precipitation within plants as the treatment and processing required for the end product is not overly extensive (Fattah 2012). Despite these methods to help alleviate the issues revolving struvite formation, it can be a costly endeavor as labour and materials must be taken into consideration in addition to the offline time of certain parts of the treatment train (Fattah 2012).

With struvite already forming in WWTPs, it appears that nutrient recovery in the form of struvite could be a solution to help eliminate struvite build up within treatment plants, but also a way to utilize the nutrients in other industries that require new reserves to be secured to maintain their current output. In particular, struvite can be used in agriculture as a slow release fertilizer, which is advantageous due to the inability to leach like other conventional fertilizers (Fattah 2012). Additionally, the economic incentive greatly supports the idea for recovery of nutrients over traditional thoughts of devising methods for complete elimination of the issue.

As nutrient recovery is becoming an attractive process to implement post treatment, commercialization of the process has already occurred. Table 2.4 highlights some of the operational processes occurring worldwide.

Table 2.4 Current phosphorus recovery technologies.

Technology	Company	Operation Location	Process Specifics	Reference
Pearl® process	Ostara Nutrient Recovery Technologies Inc.	Worldwide	Fluidized bed reactor with magnesium addition following Wasstrip® process	(Ostara Nutrient Recovery Technologies Inc. 2017)
AirPrex® process	Berliner Wasserbetriebe	Germany and the Netherlands	Aeration with CO_2 stripping and $MgCl_2$ addition	(P-Rex 2015)
Crystalactor®	DHV	China	Fluidized bed crystallizer that is cylindrical with $Mg(OH)_2$ addition	(Metcalf & Eddy Inc. et al. 2014)
NuReSys® process	Akwadok/NuReSys	Belgium and the Netherlands	Aerated CO_2 stripping tank followed by mechanically stirred crystallizer with NaOH and $MgCl_2$ addition	(Metcalf & Eddy Inc. et al. 2014)
Phosnix® process	Unitika Ltd	Japan	Aerated cylindrical reactor with conical bottom, CO_2 stripping and NaOH and $Mg(OH)_2$ addition	(Metcalf & Eddy Inc. et al. 2014)
PHOSPAQ™	Paques®	Netherlands	Aerated reactor with MgO addition	(Paques 2017)
Cone-shaped fluidized bed crystallizer	Multiform Harvest Inc.	United States	Fluidized bed crystallizer that is conical with NaOH and $MgCl_2$ addition	(Metcalf & Eddy Inc. et al. 2014)

While several processes already exist at pilot and full scale levels, lab scale studies have been conducted to identify optimal conditions for varying waste streams. Several studies have focused on struvite formation from separated urine sources. Urine has been mostly studied as it has been thought to be more sterile than when mixed with faeces and thus less treatment is required prior to reuse (Cordell et al. 2009). Others have identified optimal conditions using treated municipal wastewater where dilution factors greatly reduce the hazard levels.

As anaerobic treatment can provide both an energy and nutrient recovery mechanism, there have also been several studies examining the conditions optimal for struvite recovery from anaerobically digested effluent as seen in Table 2.5. In addition to removing phosphorus, nitrogen through NH_4^+ removal can also be a target. NH_4^+ concentrations in wastewater are typically in excess in comparison to Mg^{2+} and PO_4^{3-}. Therefore, to achieve maximum NH_4^+ removal, the addition of a magnesium and phosphorus source is required, however would increase the operational costs (Huang et al. 2011). The goal of previous studies described in Table 2.5 can be seen by the choice of chemical additions. The wastewater sources differ in many cases, but provides a basis for the conditions that appear to be the most important for practical applications.

Table 2.5 Published literature examining factors that affect struvite precipitation in wastewater streams from anaerobic digestion.

Source	Type of reactor	Factors examined	Range	Chemical Source	Optimal conditions	Reference
Raw BW	Batch reactor	Mg^{2+}:PO_4^{3-} molar ratio	1.1:1 1.3:1 1.5:1	MgO	1.1:1, but if sedimentation time is shorter, then 1.3:1	(Alp et al. 2008)
		pH	9, 10, 11	NaOH	9.5	
		Mixing time (mins)	15, 20, 30		15	
		Settling time (mins)	30-60		30	
Raw WW from anaerobic digester effluent of NPW	Batch reactor	Mg^{2+}:PO_4^{3-} molar ratio	0.9:1 – 1.3:1	$MgSO_4$ Na_2HPO_4	1.3:1:1 (low residual PO_4-P, but high $Mg_3(PO_4)_2$), therefore 1:1:1 is optimal	(Huang et al. 2012)
			2.5:1 – 4:1	Brucite H_3PO_4	2:1 or 2.5:1	
		pH	7.0, 7.5, 8.0, 8.5, 9.0	NaOH	8.5-9.0	
		Mixing time (hrs)	1.5 hrs (brucite)		Dependent on chemicals	
		Settling time (mins)	20		20	
Anaerobic digestion of primary and thickened waste activated sludge	Piolet-scale MAP reactor	Mg^{2+}:PO_4^{3-} molar ratio	1:1.3	55% w/w $Mg(OH)_2$ + 42% w/w H_2O	1:1.3	(Munch and Barr 2001)
		pH	8.5-9		8.5	
UASB pretreated poultry manure wastewater	Lab scale batch study – beaker with magnetic stirrer	Mg^{2+}:NH^{4+}: PO_4^{3-} molar ratio	1.2:1:1 1.5:1:1 1:1:1.2 1:1:1.5 0.5:1:1 0.8:1:1	$MgCl_2 \cdot 6H_2O$ + KH_2PO_4 $MgSO_4 \cdot 7H_2O$ + $NaHPO_4 \cdot 7H_2O$	$MgCl_2 \cdot 6H_2O$+ KH_2PO_4 1.5:1:1 increased removal but due to cost 1:1:1 was sufficient	(Yetilmezsoy and Sapci-Zengin 2009)

			1:1:0.5 1:1:0.8	MgO + 85%H_3PO_4		
		pH	4.45-11	NaOH	9.0	
		Mixing time (min)	15		15	
		Settling time (mins)	30		30	
		Temperature	25°C			
Anaerobic pretreated molasses-based industrial WW	Batch reactor	Mg^{2+}:NH^{4+}: PO_4^{3-} molar ratio	1:1:1 1.2:1:1 1.4:1:1 1.2:1:1.2 1:1:1.2			(Türker and Çelen 2011)
		pH	7.5, 8.0, 8.5, 9.0	NaOH or HCl		
		Temperature	37˚C			
UASB treating BW from vacuum toilet system	CSTR (100 L) into settling tank (750 L)	Mg^{2+}:NH^{4+}: PO_4^{3-} molar ratio	Not indicated	H_3PO_4 and $MgCl_2$	Not indicated	(Gell et al. 2011)
		pH	8.6	NaOH	8.6	
		Temperature	35°C			

2.3.5 Effects of pH

Based on the chemical equation, the importance of the pH can be observed as an acidic environment would promote dissociation of struvite. In turn, a pH below 6 does not result in struvite formation (Huang et al. 2011). Subsequently, as H^+ ions are being produced, the pH of the solution will lower as more precipitation occurs and a shift in equilibrium is observed (Le Corre et al. 2009; Tang 2016). Though struvite can precipitate in pH ranges from 7-11, it has been shown that a pH in the range of 8.5-9.5 is optimal for increased growth rate and precipitation (Mehta and Batstone 2013; Tang 2016; Kim et al. 2017). Additionally, increased pH results in increased supersaturation, a parameter that has been identified important for crystallization (Mehta and Batstone 2013). The pH can also play a role in the purity of the precipitate (Kim et al. 2017) as determined by other compounds that could potentially precipitate. Figure 2.6 shows the solubility curves of struvite and other compounds that can form when pH is altered. Shown is that struvite predominately forms when the pH is above 8 (Shih et al. 2017).

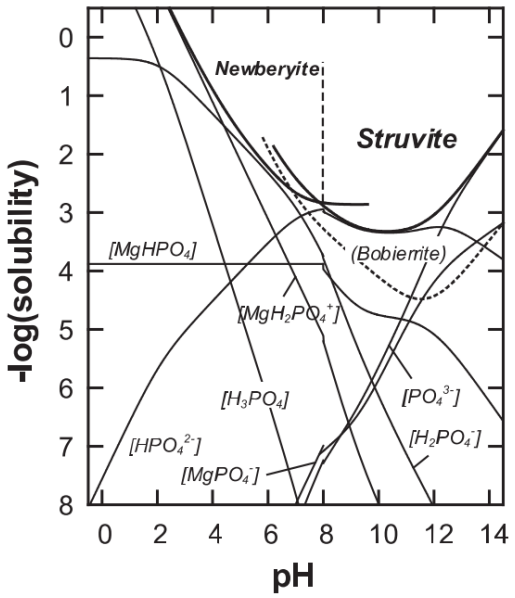

Figure 2.6 Solubility curve based on solubility products (Shih et al. 2017).

As there is a large pH range in which struvite could precipitate at, the precipitation will largely depend on the interactions of ions and the system at certain conditions.

2.3.6 Effects of Mg^{2+}:PO_4^{3-} Molar Ratio

A 1:1:1 molar ratio between Mg^{2+}, NH_4^+ and PO_4^{3-} is required, in which Mg^{2+} is often the limiting reagent (Le Corre et al. 2005). The NH_4^+ concentration in the effluent is typically much higher than Mg^{2+} and PO_4^{3-} (Fattah 2012) and typically both Mg^{2+} and PO_4^{3-} sources would need to be added to completely remove NH_4^+ (Kim et al. 2017). The reported ratios that are optimal for recovery slightly differ depending on the feedstock tested, but it has been suggested that increased phosphorus recovery can occur with a molar ratio greater than 1:1:1 (Kim et al. 2017). Furthermore, the concentration of the ions will be highly dependent on the influent concentration and the treatment efficiency. The importance of the feed source for recovery is observed when comparing the ion interactions that could occur in a controlled laboratory system versus a complex system, such as wastewater.

As Mg^{2+} is often limiting, the addition of a magnesium source, such as $MgCl_2 \cdot H_2O$, $Mg(OH)_2$ or $MgSO_4 \cdot 7H_2O$ (Karabegovic et al. 2013) is often required to reach an appropriate molar ratio. Though MgO and $Mg(OH)_2$ are typically chosen as it is inexpensive and has the capability of acting as a magnesium source as well as increasing the pH, the limited solubility of MgO in water makes it more difficult for nutrient recovery (Li et al. 2012; Degryse et al. 2017). $MgCl_2$ is water soluble and can react quickly for precipitation resulting in a pure product (Degryse et al. 2017).

The feeding sequence of the reagents for magnesium addition and pH control can also impact struvite precipitation. As there are several chemical reactions that can occur with a complex matrix, the adjustment of pH prior to the magnesium addition can cause other side reactions to occur. The result was a high residual PO_4^{3-} concentration, likely due to the formation of $Mg(OH)_2$. The addition of magnesium and phosphate reagents prior to the pH adjustment increased the recovery through struvite and produced a product that was more pure (Kim et al. 2007).

2.3.7 Effect of Seeds

As discussed, crystal formation requires two stages with the nucleation stage needed for initial crystal growth as struvite cannot precipitate otherwise. Though altering water chemistry conditions can promote nucleation, precipitation can occur more rapidly with a nucleus that is already seeded within the system (Wang et al. 2006). The lack of seed can promote growth on surfaces of the treatment plant. Studies comparing precipitation with and without a seed show that the phosphorus removal is enhanced when a seed is present (Wang et al. 2006). The type of seed can also play a role where struvite crystals resulted in better phosphorus removal than use of granite or quartz sand as a seed (Wang et al. 2006). The specific gravity of the material plays a large role as the surface area and number of particles increases with low specific gravity, thus explaining why struvite is more optimal as a seed. Presence of a seed can also increase the crystal size as a nucleus is already present for struvite precipitation to occur (Wang et al. 2006). The amount of seeding can also be an important factor as high amounts of seeding can favour crystal growth over crystal nucleation and accelerate precipitation and crystal size (Kim et al. 2007). On the other hand, there appears to be an optimal seeding amount for maximum phosphorus removal. It has been shown that when exceeding a certain seeding threshold, the phosphate removal decreases (Tang 2016). One stage addition of seeds has shown to favour phosphorus recovery as nucleation on the seed surface can occur more rapidly when the seed is added immediately at once, thus subsequent additions of seed does not have a significant effect (Tang 2016).

2.4 Co-precipitation in Struvite

With wastewater being such a complex matrix, it is likely that due to the common ion effect, other ions will co-precipitate with struvite (Türker and Çelen 2011). Ca^{2+} has been shown to be a competitor ion to Mg^{2+} in the formation of struvite. Previous studies have shown that Ca^{2+} at varying concentrations can impact growth, purity and size of struvite (Le Corre et al. 2005). It has been shown that the Mg^{2+}:Ca^{2+} concentration can be integral in determining the morphology of the crystal as well as the compound produced. Le Corre and colleagues demonstrated that high Ca^{2+} concentrations inhibits struvite growth resulting in smaller crystals (Le Corre et al. 2005; Liu and Qu 2017). Additionally, it was shown that amorphous

calcium phosphate is likely to form in these high Ca^{2+} ion situations, thus reducing the amount of crystalline compound produced (Le Corre et al. 2005). The induction time for struvite precipitation increases when calcium is present as calcium carbonate and calcium phosphate form (Le Corre et al. 2005). Higher Ca^{2+} concentrations that Mg^{2+} also results in decreased average crystal sizes (Le Corre et al. 2005). XRD patterns are shown to produce more background noise as compared to struvite production without Ca^{2+} presence. The ability to identify the crystalline structure also becomes more difficult with co-precipitates occurring (Le Corre et al. 2005). Low Ca^{2+} concentrations results in co-precipitates forming near and over the surface of struvite crystals, however amorphous material forms when Ca^{2+} concentrations become much higher limiting struvite formation (Le Corre et al. 2005).

There are a number of potential inorganic compounds and salts that can be formed from the presence of PO_4^{3-} ions. Though formation is highly dependent on the reaction kinetics, there is a potential for compounds to form as seen in Table 2.6.

Table 2.6 List of compounds that can form in the system with struvite.

Compounds	Chemical Reaction Equation	K_{sp}	Reference
Newberyite	$Mg^{2+} + H_2PO_4^{2-} + 3H_2O \leftrightarrow MgHPO_4 \bullet 3H_2O + 3H^+$	$1.51x10^{-6}$	(Shih et al. 2017)
Cattiite	$3Mg^{2+} + 2HPO_4^{2-} + 22H_2O \leftrightarrow Mg_3(PO_4)_2 \bullet 22H_2O + 2H^+$	$7.94x10^{-24}$	(Taylor et al. 1963)
Bobierrite	$3Mg^{2+} + 2HPO_4^{2-} + 8H_2O \leftrightarrow Mg_3(PO_4)_2 \bullet 8H_2O + 2H^+$	$6.31x10^{-26}$	(Shih et al. 2017)
Brucite	$Mg^{2+} + 2OH^- \leftrightarrow Mg(OH)_2$	$1.40x10^{-9}$	(Al-hamzah et al. 2015)
Hazenite	$2\ Mg^{2+} + K^+ + Na^+ + 2PO_4^{3-} + 14H_2O \leftrightarrow Mg_2KNa(PO_4)_2 \bullet 14H_2O$	No reported value	
Potassium struvite	$Mg^{2+} + K^+ + PO_4^{3-} + 6H_2O \leftrightarrow MgKPO_4 \bullet 6H_2O$	$1.00x10^{-11}$	(Bennett et al. 2017)
Nesquehonite	$Mg^{2+} + CO_3^{2-} + 3H_2O \leftrightarrow MgCO_3 \bullet 3H_2O$	$6.56x10^{-6}$	(Stumm and Morgan 1981)
Magnesite	$MgCO_3 \leftrightarrow Mg^{2+} + CO_3^{2-}$	$3.50x10^{-8}$	(Stumm and Morgan 1981)

In addition to the potential precipitation of the above compounds, other ions that can be found include H_3PO_4, $H_2PO_4^-$, HPO_4^{2-}, $MgPO_4^-$, $MgH_2PO_4^+$ and $MgHPO_4$ and can be present depending on the pH (Huang et al. 2011) as described in Figure 2.7. The availability of other ions can also affect the purity of struvite as it can replace the key components of struvite. NH_4^+ can be substituted by ions such as K^+, Rb^+ or Cs^+, while Mg^{2+} can be replaced by Ca^{2+}, Zn^{2+} of Cd^{2+} (Tansel et al. 2018). This would result in a similar appearance to struvite, but the elemental composition would differ. Additionally, the radius of the ion could affect the stability of the formed crystal (Tansel et al. 2018).

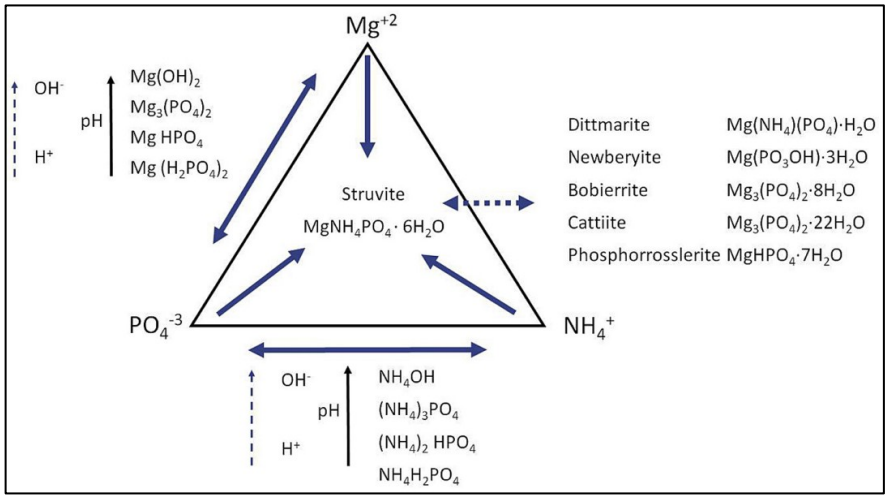

Figure 2.7 Interaction of Mg^{2+}, PO_4^{3-} and NH_4^+ ions (Tansel et al. 2018).

Physical mechanisms such as heating and drying can transform struvite into some of the other compounds listed in Table 2.6. These potential transformations are highlighted in Figure 2.7 and 2.8 with dittmarite, bobierrite, newberyite, amorphous P and magnesium pyrophosphate being the dominate species (Bhuiyan et al. 2008). The breaking and rearrangement of bonds during the transformations can result in a release of NH_3 and H_2O molecules (Tansel et al. 2018). These transformations could be important in the steps following precipitation as drying in particular is typically used (Figure 2.8).

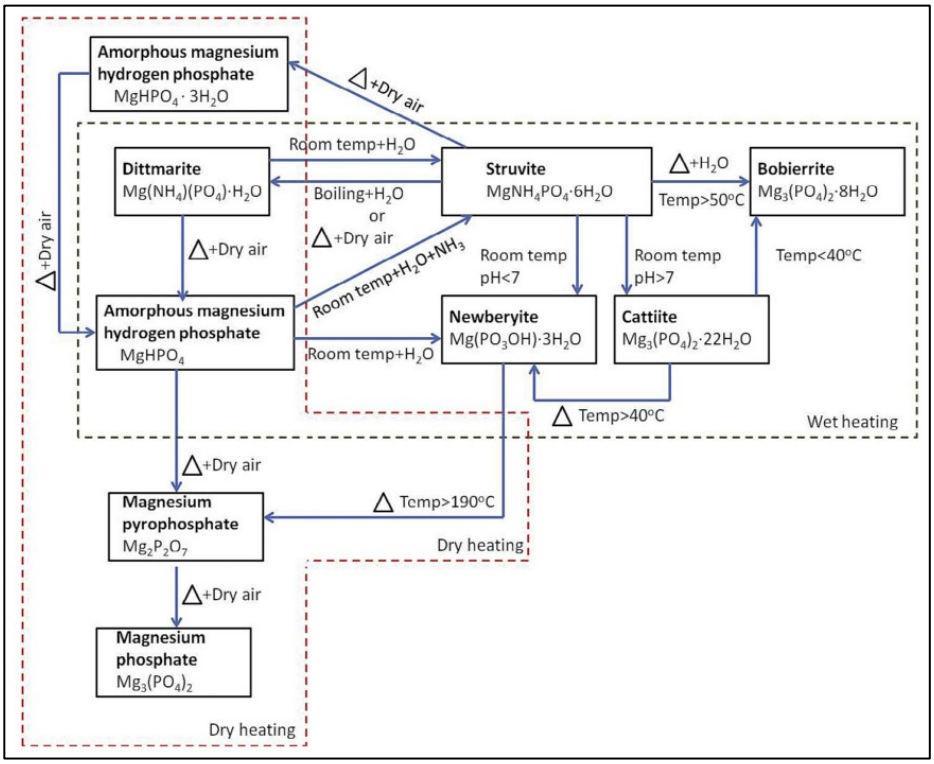

Figure 2.8 Possible transformation mechanisms of various phases associated with struvite from physical factors such as temperature and drying (Tansel et al. 2018).

In addition to the inorganic compounds that could potentially co-precipitate depending on water chemistry conditions, biological hazards can co-precipitate and be even more problematic. It is thought that struvite recovered from urine would be free of microbial co-precipitation as there are little traces of fecal contamination. However, a study using surrogates (Phage ϕX174 and *Ascaris suum* eggs) for human viruses and helminths show that accumulation occurs within struvite recovered from urine (Decrey et al. 2011). Another study on struvite formation from urine showed that there was an accumulation of bacteria in struvite during the collection process (Bischel et al. 2016). However, upon further processing of struvite, it was observed that higher drying temperatures resulted in increased inactivation (Bischel et al. 2016). Thus, regardless of the feed, residual microbes from wastewater treatment can potentially end up in struvite with the need for other mechanisms to reduce the risk involved.

As antibiotic residuals are often found in wastewater, adsorption of molecules within struvite can occur. In particular, it has been shown that tetracycline adsorption can occur, but is highly dependent on pH where a pH of 9 increases the adsorption capabilities (Başakçılardan-Kabakcı et al. 2007). Though extensive studies have not been conducted on all residuals, the purity of struvite can be hindered by other molecules that are not removed by wastewater treatment processes. Subsequently, the presence of antibiotic residuals can help lead to the development of ARB and increase the prevalence of ARGs. A study examined the ARG profile of struvite and its effects on the soil, rhizosphere and phylloshpere upon application for *Brassica* growth (Chen et al. 2017). There was an overlap of ARGs within the soil, rhizosphere and phyllosphere with an observed increase upon struvite application leaves (Chen et al. 2017). Additional tests showed that consumption of the *Brassica* could be a potential public health concern through the connection of microbes within the roots and leaves (Chen et al. 2017). Research investigating the co-precipitation of the above discussed biological hazards as well as viruses and protozoa is currently limited.

2.5 References

Ajonina C, Buzie C, Rubiandini RH, Otterpohl R. 2015. Microbial pathogens in wastewater treatment plants (WWTP) in Hamburg. J. Toxicol. Environ. Health 78:381–387.

Al-hamzah AA, Smith EJ, Fellows CM. 2015. Inhibition of homogeneous formation of magnesium hydroxide by low-molar-mass poly(acrylic acid) with different end-groups. Ind. Eng. Chem. Res. 54:2201–2207.

Alp Ö, Yazgan B, Söhmen U, Gulyas H, Otterpohl R. 2008. Recovery of phosphorus as struvite from source-separated blackwater.

Bajaj P, Singh NS, Virdi JS. 2016. Escherichia coli β-lactamases: what really matters. Front. Microbiol. 7:1–14.

Baquero F, Martínez JL, Cantón R. 2008. Antibiotics and antibiotic resistance in water environments. Curr. Opin. Biotechnol. 19:260–265.

Başakçılardan-Kabakcı S, Thompson A, Cartmell E, Le Corre K. 2007. Adsorption and precipitation of tetracycline with struvite. Water Environ. Res. 79:2551–2556.

Bender JK, Kalmbach A, Fleige C, Klare I, Fuchs S, Werner G. 2016. Population structure and acquisition of the vanB resistance determinant in German clinical isolates of Enterococcus faecium ST192. Sci. Rep. 6:1–13.

Bennett AM, Lobanov S, Koch FA, Mavinic DS. 2017. Improving potassium recovery with new solubility product values for K-struvite. J. Environ. Eng. Sci. 12:93–103.

Berglund B, Dienus O, Sokolova E, Berglind E, Matussek A, Pettersson T, Lindgren PE. 2017. Occurrence and removal efficiency of parasitic protozoa in Swedish wastewater treatment plants. Sci. Total Environ. 598:821–827.

Berglund B, Gengler S, Batoko H, Wattiau P, Errampalli D, Leung K, Cassidy MB, Kostrzynska M, Blears M, Lee H, et al. 2015. Environmental dissemination of antibiotic resistance genes and correlation to anthropogenic contamination with antibiotics. J. Microbiol. Methods 113:28564–28574.

Bhuiyan MIH, Mavinic DS, Koch FA. 2008. Thermal decomposition of struvite and its phase transition. Chemosphere 70:1347–1356.

Bischel HN, Schindelholz S, Schoger M, Decrey L, Buckley CA, Udert KM, Kohn T. 2016. Bacteria inactivation during the drying of struvite fertilizers produced from stored urine. Environ. Sci. Technol. 50:13013–13023.

Borjesson S, Dienues O, Jarnheimer P-A, Olsen B, Matussek A, Lindgren P-E. 2009. Quantification of genes encoding resistance to aminoglycosides, beta-lactams and

tetracyclines in wastewater environments by real-time PCR. Int. J. Environ. Health Res. 19:219–230.

Butkovskyi A, Leal LH, Zeeman G, Rijnaarts HHM. 2017. Micropollutants in source separated wastewater streams and recovered resources of source separated sanitation. Environ. Res. 156:434–442.

Cetinkaya Y, Falk P, Mayhall CG. 2000. Vancomycin-resistant enterococci. Clin. Microbiol. Rev. 13:686–707.

Chen Q, An X, Zhu Y, Su J, Gillings MR, Ye Z. 2017. Application of struvite alters the antibiotic resistome in soil, rhizosphere, and phyllosphere. Environ. Sci. Technol. 51:8149–8157.

Chopra I, Roberts M. 2001. Tetracycline antibiotics: mode of action, applications , molecular biology, and epidemiology of bacterial resistance. Microbiol. Mol. Biol. Rev. 65:232–260.

Choubert JM, Pomiès M, Martin Ruel S, Coquery M. 2011. Influent concentrations and removal performances of metals through municipal wastewater treatment processes. Water Sci. Technol. 63:1967–1973.

Cordell D, Schmid-Neset T, White S, Drangert J-O. 2009. Preferred future phosphorus scenarios: A framework for meeting long-term phosphorus needs for global food demand. Ashley K, Mavinic D, Koch F, editors. London, UK: IWA Publishing.

Culyba MJ, Mo CY, Kohli RM. 2015. Targets for Combating the Evolution of Acquired Antibiotic Resistance. Biochemistry 54:3573–3582.

Da Silva MF, Tiago I, Verissimo A, Boaventura RA, Nunes OC, Manaia CM. 2006. Antibiotic resistance of enterococci and related bacteria in an urban wastewater treatment plant. FEMS Microbiol. Ecol. 55:322–329.

Decrey L, Udert KM, Tilley E, Pecson BM, Kohn T. 2011. Fate of the pathogen indicators phage ΦX174 and Ascaris suum eggs during the production of struvite fertilizer from source-separated urine. Water Res. 45:4960–4972.

de Graaff MS, Temmink H, Zeeman G, Buisman CJN. 2010. Anaerobic treatment of concentrated black water in a UASB reactor at a short HRT. Water 2:101–119.

de Graaff MS, Temmink H, Zeeman G, Buisman CJN. 2011. Energy and phosphorus recovery from black water. Water Sci. Technol. 63:2759–2765.

de Graaff MS, Temmink H, Zeeman G, van Loosdrecht MCM, Buisman CJN. 2011. Autotrophic nitrogen removal from black water: calcium addition as a requirement for settleability. Water Res. 45:63–74.

Degryse F, Baird R, da Silva RC, McLaughlin MJ. 2017. Dissolution rate and agronomic effectiveness of struvite fertilizers – effect of soil pH, granulation and base excess. Plant Soil 410:139–152.

De Sanctis M, Del Moro G, Chimienti S, Ritelli P, Levantesi C, Di Iaconi C. 2017. Removal of pollutants and pathogens by a simplified treatment scheme for municipal wastewater reuse in agriculture. Sci. Total Environ. 580:17–25.

Di Cesare A, Eckert EM, D'Urso S, Bertoni R, Gillan DC, Wattiez R, Corno G. 2016. Co-occurrence of integrase 1, antibiotic and heavy metal resistance genes in municipal wastewater treatment plants. Water Res. 94:208–214.

Dillon B, Thomas L, Mohmand G, Zelynski A, Iredell J. 2005. Multiplex PCR for screening of integrons in bacterial lysates. J. Microbiol. Methods 62:221–232.

Drozdova J, Raclavska H, Skrobankova H. 2015. A survey of heavy metals in municipal wastewater in combined sewer systems during wet and dry weather periods. Urban Water J. 12:131–144.

Fattah KP. 2012. Assessing struvite formation potential at wastewater treatment plants. Int. J. Environ. Sci. Dev. 3:548–552.

Ferreira Da Silva M, Vaz-Moreira I, Gonzalez-Pajuelo M, Nunes OC, Manaia CM. 2007. Antimicrobial resistance patterns in Enterobacteriaceae isolated from an urban wastewater treatment plant. FEMS Microbiol. Ecol. 60:166–176.

Gallagher N, Sharvelle S. 2010. Decentralized anaerobic treatment of blackwater: a sustainable development technology concept for urban water management. World Environ. Water Resour. Congr.:4118–4128.

Gell K, Ruijter FJ d., Kuntke P, Graaff M De, Smit AL. 2011. Safety and effectiveness of struvite from black water and urine as a phosphorus fertilizer. J. Agric. Sci. 3:67–80.

Gillings MR. 2017. Class 1 integrons as invasive species. Curr. Opin. Microbiol. 38:10–15.

Guo J, Li J, Chen H, Bond PL, Yuan Z. 2017. Metagenomic analysis reveals wastewater treatment plants as hotspots of antibiotic resistance genes and mobile genetic elements. Water Res. 123:468–478.

Haramoto E, Kitajima M, Hata A, Torrey JR, Masago Y, Sano D, Katayama H. 2018. A review on recent progress in the detection methods and prevalence of human enteric viruses in water. Water Res. 135:168–186.

Harwood VJ, Levine AD, Scott TM, Chivukula V, Lukasik J, Farrah SR, Rose JB. 2005. Validity of the indicator organism paradigm for pathogen reduction in reclaimed water and public health protection. Appl. Environ. Microbiol. 71:3163–3170.

Hooper DC. 2001. Mechanisms of action of antimicrobials: focus on fluoroquinolones. Clin. Infect. Dis. 32:S9–S15.

Huang H, Song Q, Wang W, Wu S, Dai J. 2012. Treatment of anaerobic digester effluents of nylon wastewater through chemical precipitation and a sequencing batch reactor process. J. Environ. Manage. 101:68–74.

Huang HM, Song QW, Xu CL. 2011. The mechanism and influence factors of struvite precipitation for the removal of ammonium nitrogen. Adv. Mater. Res. 189–193:2613–2620.

Huchzermeier MP, Tao W. 2012. Overcoming challenges to struvite recovery from anaerobically digested dairy manure. Water Environ. Res. 84:34–41.

Iaconelli M, Muscillo M, Della Libera S, Fratini M, Meucci L, De Ceglia M, Giacosa D, La Rosa G. 2017. One-year surveillance of human enteric viruses in raw and treated wastewaters, downstream river waters, and drinking waters. Food Environ. Virol. 9:79–88.

Jimenez-Cisneros BE. 2006. Helminth ova control in wastewater and sludge for agricultural reuse. In: Encylopedia of Life Support Systems. Vol. II. p. 12.

Johnson L, Atheesha G. 2013. Water quality indicators: bacteria, coliphage, enteric viruses. Int. J. Environ. Res. Public Health 23:484–506.

Karabegovic L, Uldal M, Werker A, Morgan-Sagastume F. 2013. Phosphorus recovery potential from a waste stream with high organic and nutrient contents via struvite precipitation. Environ. Technol. 34:871–883.

Karkman A, Do TT, Walsh F, Virta MPJ. 2018. Antibiotic resistance genes in waste water. Trends Microbiol. 26:220–228.

Kemacheevakul P, Chuangchote S, Otani S, Matsuda T, Shimizu Y. 2015. Effect of magnesium dose on amount of pharmaceuticals in struvite recovered from urine. Water Sci. Technol. 72:1102–1110.

Kim D, Min KJ, Lee K, Yu MS, Park KY. 2017. Effects of pH, molar ratios and pre-treatment on phosphorus recovery through struvite crystallization from effluent of anaerobically digested swine wastewater. Environ. Eng. Res. 22:12–18.

Kim D, Ryu H-D, Kim M-S, Kim J, Lee S-I. 2007. Enhancing struvite precipitation potential for ammonia nitrogen removal in municipal landfill leachate. J. Hazard. Mater. 146:81–85.

Koeleman JGM, Stoof J, Van der bijl MW, Vandenbroucke-Grauls CMJE, Savelkoul PHM. 2001. Identification of epidemic strains of Acinetobacter baumannii by integrase

gene PCR. J. Clin. Microbiol. 39:8–13.

Kujawa-Roeleveld K, Zeeman G. 2006. Anaerobic treatment in decentralised and source-separation-based sanitation concepts. Rev. Environ. Sci. Biotechnol. 5:115–139.

Laridi R, Auclair JC, Benmoussa H. 2005. Laboratory and pilot-scale phosphate and ammonium removal by controlled struvite precipitation following coagulation and flocculation of swine wastewater. Environ. Technol. 26:525–536.

Le Corre KS, Valsami-Jones E, Hobbs P, Jefferson B, Parsons SA. 2007. Struvite crystallisation and recovery using a stainless steel structure as a seed material. Water Res. 41:2449–2456.

Le Corre KS, Valsami-jones E, Hobbs P, Parsons SA. 2005. Impact of calcium on struvite crystal size, shape and purity. J. Cryst. Growth 283:514–522.

Le Corre KS, Valsami-Jones E, Hobbs P, Parsons SA. 2009. Phosphorus recovery from wastewater by struvite crystallization: a review. Crit. Rev. Environ. Sci. Technol. 39:433–477.

Legros S, Levard C, Marcato-Romain CE, Guiresse M, Doelsch E. 2017. Anaerobic digestion alters copper and zinc speciation. Environ. Sci. Technol. 51:10326–10334.

Li J, Cheng W, Xu L, Strong PJ, Chen H. 2014. Antibiotic-resistant genes and antibiotic-resistant bacteria in the effluent of urban residential areas, hospitals, and a municipal wastewater treatment plant system. Environ. Sci. Pollut. Res. 22:4587–4596.

Li Z, Ren X, Zuo J, Liu Y, Duan E, Yang J, Chen P, Wang Y. 2012. Struvite precipitation for ammonia nitrogen removal in 7-aminocephalosporanic acid wastewater. Molecules 17:2126–2139.

Liu Y, Qu H. 2017. Interplay of digester supernatant composition and operating pH on impacting the struvite particulate properties. J. Environ. Chem. Eng. 5:3949–3955.

Lizasoain A, Tort LFL, García M, Gillman L, Alberti A, Leite JPG, Miagostovich MP, Pou SA, Cagiao A, Razsap A, et al. 2018. Human enteric viruses in a wastewater treatment plant: evaluation of activated sludge combined with UV disinfection process reveals different removal performances for viruses with different features. Lett. Appl. Microbiol. 66:215–221.

Luby E, Ibekwe AM, Zilles J, Pruden A. 2016. Molecular methods for assessment of antibiotic resistance in agricultural ecosystems: prospects and challenges. J. Environ. Qual. 45:441–451.

Lucena F, Duran AE, Morón A, Calderón E, Campos C, Gantzer C, Skraber S, Jofre J. 2004. Reduction of bacterial indicators and bacteriophages infecting faecal bacteria in

primary and secondary wastewater treatments. J. Appl. Microbiol. 97:1069–1076.

Madoni P. 2011. Protozoa in wastewater treatment processes: a minireview. Ital. J. Zool. 78:3–11.

Mamais D, Pitt PA, Cheng YW, Loiacono J, Jenkins D, Wen Y. 1994. Digesters determination to control in anaerobic of ferric chloride precipitation digesters dose struvite sludge. Water Environ. Res. 66:912–918.

Manser ND, Wald I, Ergas SJ, Izurieta R, Mihelcic JR. 2015. Assessing the fate of Ascaris suum ova during mesophilic anaerobic digestion. Environ. Sci. Technol. 49:3128–3135.

Mayer BK, Baker LA, Boyer TH, Drechsel P, Gifford M, Hanjra MA, Parameswaran P, Stoltzfus J, Westerhoff P, Rittmann BE. 2016. Total value of phosphorus recovery. Environ. Sci. Technol. 50:6606–6620.

Mehta CM, Batstone DJ. 2013. Nucleation and growth kinetics of struvite crystallization. Water Res. 47:2890–2900.

Metcalf & Eddy Inc., Tchobanoglous G, Stensel HD, Tsuchihashi R, Burton F. 2014. Wastewater engineering - treatment and resource recovery.

Miao XS, Bishay F, Chen M, Metcalfe CD. 2004. Occurrence of antimicrobials in the final effluents of wastewater treatment plants in Canada. Environ. Sci. Technol. 38:3533–3541.

Michael I, Rizzo L, McArdell CS, Manaia CM, Merlin C, Schwartz T, Dagot C, Fatta-Kassinos D. 2013. Urban wastewater treatment plants as hotspots for the release of antibiotics in the environment: a review. Water Res. 47:957–995.

Miller WR, Munita JM, Arias CA. 2014. Mechanisms of antibiotic resistance in enterococci. Expert Rev. Anti. Infect. Ther. 12:1221–1236.

Munch E V., Barr K. 2001. Controlled struvite crystallisation for removing phosphorus from anaerobic digester sidestreams. Water Res. 35:151–159.

Ohlinger BKN, Member S, Young TM, Member A, Schroeder ED. 1999. Kinetics effects on preferential struvite accumulation in wastewater. J. Environ. Engin 125:730–737.

Ostara Nutrient Recovery Technologies Inc. 2017. Ostara delivers a complete resource recovery solution.

P-Rex. 2015. AirPrex® Struvite crystallization in sludge.

Paques. 2017. PHOSPAQ ™ Sustainable phosphorus recovery.

Parsons SA, Doyle JD. 2002. Struvite scale formation and control. Water Sci. Technol.

49:177–182.

Payment P, Locas A. 2011. Pathogens in water: value and limits of correlation with microbial indicators. Ground Water 49:4–11.

Priya M, Haridas A, Manilal VB. 2007. Involvement of protozoa in anaerobic wastewater treatment process. Water Res. 41:4639–4645.

Rahaman MS, Ellis N, Mavinic DS. 2008. Effects of various process parameters on struvite precipitation. Water Sci. Technol. 57:647–654.

Rahman MM, Salleh MAM, Rashid U, Ahsan A, Hossain MM, Ra CS. 2014. Production of slow release crystal fertilizer from wastewaters through struvite crystallization - a review. Arab. J. Chem. 7:139–155.

Risebro HL, Doria MF, Andersson Y, Medema G, Osborn K, Schlosser O, Hunter PR. 2007. Waterborne transmission of protozoan parasites: a worldwide review of outbreaks and lesson learnt. J. Water Health 5:1–18.

Said L Ben, Klibi N, Lozano C, Dziri R, Ben Slama K, Boudabous A, Torres C. 2015. Diversity of enterococcal species and characterization of high-level aminoglycoside resistant enterococci of samples of wastewater and surface water in Tunisia. Sci. Total Environ. 530–531:11–17.

Shih Y-J, Abarca RRM, de Luna MDG, Huang Y-H, Lu M-C. 2017. Recovery of phosphorus from synthetic wastewaters by struvite crystallization in a fluidized-bed reactor: Effects of pH, phosphate concentration and coexisting ions. Chemosphere 173:466–473.

Song Y, Yuan P, Zheng B, Peng J, Yuan F, Gao Y. 2007. Nutrients removal and recovery by crystallization of magnesium ammonium phosphate from synthetic swine wastewater. Chemosphere 69:319–324.

Stumm W, Morgan JJ. 1981. Aquatic chemistry. Wiley-Interscience.
Tang P. 2016. Effects of solution pH and seed material on MAP crystallization. Int. J. Environ. Prot. Policy 4:171–177.

Tansel B, Lunn G, Monje O. 2018. Struvite formation and decomposition characteristics for ammonia and phosphorus recovery: a review of magnesium-ammonia-phosphate interactions. Chemosphere 194:504–514.

Taylor a. W, Frazier a. W, Gurney EL. 1963. Solubility products of magnesium ammonium and magnesium potassium phosphates. Trans. Faraday Soc. 59:1580–1584.

Thanh PM, Ketheesan B, Yan Z, Stuckey D. 2016. Trace metal speciation and bioavailability in anaerobic digestion: a review. Biotechnol. Adv. 34:122–136.

Türker M, Çelen I. 2011. Chemical equilibrium model of struvite precipitation from anaerobic digester effluents. Turkish J. Eng. Environ. Sci. 35:39–48.

Van Hoek AHAM, Mevius D, Guerra B, Mullany P, Roberts AP, Aarts HJM. 2011. Acquired antibiotic resistance genes: an overview. Front. Microbiol. 2:1–27.

Vierheilig J, Frick C, Mayer RE, Kirschner AKT, Reischer GH, Derx J, Mach RL, Sommer R, Farnleitner AH. 2013. Clostridium perfringens is not suitable for the indication of fecal pollution from ruminant wildlife but is associated with excreta from nonherbivorous animals and human sewage. Appl. Environ. Microbiol. 79:5089–5092.

Wang J, Burken JG, Zhang X. 2006. Effect of seeding materials and mixing strength on struvite precipitation. Water Environ. Res. 78:125–132.

Wang J, Burken JG, Zhang X, Surampalli R. 2005. Engineered struvite precipitation: impacts of component-ion molar ratios and pH. J. Environ. Eng. 131:1433–1440.

Wen Q, Tutuka C, Keegan A, Jin B. 2009. Fate of pathogenic microorganisms and indicators in secondary activated sludge wastewater treatment plants. J. Environ. Manage. 90:1442–1447.

Woodford N, Morrison D, Johnson AP, Bateman AC, Hastings JG, Elliott TS, Cookson B. 1995. Plasmid-mediated vanB glycopeptide resistance in enterococci. Microb. Drug Resist. 1:235–240.

Wose Kinge CN, Ateba CN, Kawadza DT. 2010. Antibiotic resistance profiles of Escherichia coli isolated from different water sources in the Mmabatho locality, Northwest Province, South Africa. S. Afr. J. Sci. 106:44–50.

Yang Y, Li B, Zou S, Fang HHP, Zhang T. 2014. Fate of antibiotic resistance genes in sewage treatment plant revealed by metagenomic approach. Water Res. 62:97–106.

Yetilmezsoy K, Sapci-Zengin Z. 2009. Recovery of ammonium nitrogen from the effluent of UASB treating poultry manure wastewater by MAP precipitation as a slow release fertilizer. J. Hazard. Mater. 166:260–269.

Chapter 3 - Fecal Indicator Bacterial Detection and qPCR Method Development

3.1 Introduction

To assess bacterial viability and AMR in future experiments, methods for analysis needed to be developed and optimized. This chapter outlines the materials and methods used to obtain purified *E. coli*, *Enterococcus* spp. and *C. perfringens* wastewater isolates, to optimize qPCR methods for bacterial and antimicrobial resistance genes as well as quantify viable cells.

3.2 Materials and Methods

3.2.1 Culturing Methods

Selective media was used as per manufacturer's instructions to isolate bacteria from wastewater samples. Rebecca CF Waters (Biomerieux, France) and pre-made x-gluc agar plates (Thermo Fisher Scientific, USA) were used for *E. coli* isolation, while Slanetz and Bartley (Oxoid, USA) was used for *Enterococcus* spp. isolation. An inoculation loop was submerged into positive Colilert and Enterolert Quanti-trays 2000® (IDEXX, USA) sampled from post grit and post UV steps from the Bonnybrook and Pine Creek wastewater treatment plants in Calgary, AB. Samples were streaked onto the selective mediums and incubated overnight at their respectable temperatures (37 °C for *E. coli* and 42 °C for *Enterococcus* spp.). *E. coli* colonies appeared blue on the Rebecca CF Waters and x-gluc medium (Figure 3.1a) while *Enterococcus* spp. colonies appeared maroon on the Slanetz and Bartley medium (Figure 3.1c). Coliform growth where pure *E. coli* colonies could not be identified are shown in Figure 3.1b.

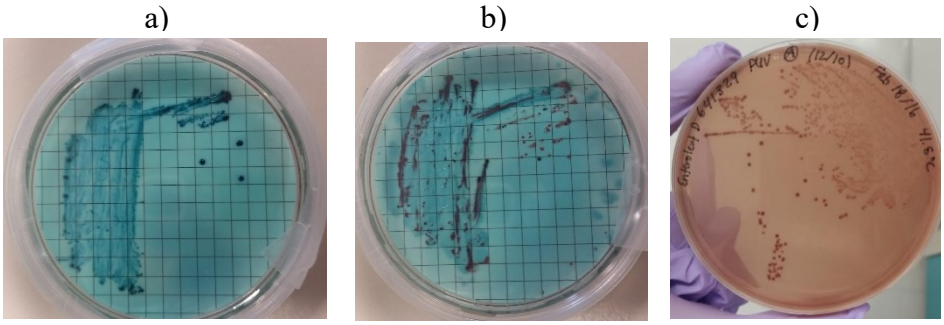

Figure 3.1 Process of obtaining pure *E. coli* and *Enterococcus* spp. isolates from wastewater samples via culturing. a) Purified *E. coli* isolate (blue colonies); b) Coliform growth from sample (red colonies); c) Purified *Enterococcus* spp. isolate.

From the incubated agar plates, colonies that appeared to represent the target organism were continually re-streaked onto the selective medium until a pure culture was obtained. Upon confirmation of pure cultures, non-selective media - Trypticase soy agar (TSA) (Becton Dickinson, USA) and trypticase soy broth (TSB) (Becton Dickinson, USA) - was used to carry out further culturing. The pure cultures were stored in 10 % sterile glycerol and kept frozen at -80 °C until further use.

CM0587 Perfringens agar base (TSC & SFP) media (Thermo Scientific, USA) with 85 mg/L 4-methylumbelliferyl phosphate (Invitrogen, USA) was used to culture and purify *C. perfringens* from environmental samples. The plates were incubated 18-20 h at 37 °C in an anaerobic box. *C. perfringens* isolates were purified and propagated by Nancy Price (School of Public Health, University of Alberta) for use in qPCR method development and viability assays described in Chapter 4 and 5.

3.2.2 Antibiotic Susceptibility Test Methods

The culture method was used to test the level of antibiotic resistance within the *E. coli* and *Enterococcus spp.* isolates previously cultured from the wastewater samples in Chapter 3.2.1. The pure culture was grown on TSA overnight at 37 °C and a colony was inoculated into a tube containing ~8 mL of TSB that was incubated on a shaker for 3-4 h at 37 °C. The culture was adjusted to the 0.5 McFarland standard prior to applying with a swab onto a TSA plate. Within minutes of applying the culture, the antibiotic discs (Becton Dickinson, USA) – vancomycin (5 µg), ciprofloxacin (5 µg), trimethoprim (5 µg), tetracycline (30 µg), streptomycin (10 µg), ampicillin (10 µg) and cefatoxime (30 µg) - were dispensed onto the inoculated agar plate and incubated overnight at 37 °C. The diameter of the lawn formed on the plates were compared to the CLSI standards to determine their resistance level.

Results of the culture based antibiotic susceptibility tests on various *E. coli* and *Enterococcus* spp. wastewater isolates indicated the presence of some antibiotic resistant microorganisms in the Calgary wastewater treatment plants. The results shown in Table 3.1 and 3.2 are not interpreted as overall levels of ARB presence in wastewater. Instead, these results along with a literature review are indicative of the possible antibiotics that could be present and could be of interest for future studies. Trimethoprim resistance was commonly observed in both *E. coli* and *Enterococcus* spp. isolates. Streptomycin and ciprofloxacin resistance were also commonly observed. Additionally, though vancomycin was not tested for all *Enterococcus* spp. isolates, it should be noted that vancomycin-resistant enterococci is increasing on the list of important antimicrobial resistant organisms (U.S. Centers for Disease Control and Prevention 2013).

Table 3.1 Results of antibiotic susceptibility test on *E. coli* isolates (Calgary Colilert samples).

Sample ID	Ampicillin	Tetracycline	Streptomycin	Cefatoxime	Trimethoprim	Ciprofloxacin
ATCC 25922	QC	QC	QC	QC	QC	QC
201444327 PUV (4)	S	S	I	S	S	S
201444327 PUV (2)	S	S	I	S	S	S
201444323 PG B (3)	S	R	I	S	R	S
201444323 PG A (7)	I	S	I	S	S	S
641329 PUV B (8)	S	S	I	S	S	S
641318 2 (9)	S	S	I	S	R	S
Post UV #2 I1 (10)	S	S	I	S	S	S
Post UV #2 I2 (11)	S	S	I	S	S	S
Pre UV #2 I1 (12)	S	S	I	S	S	S
Pre UV #2 I2 (13)	R	R	R	S	R	R
Pre UV #2 I3 (14)	R	R	R	S	R	R
201444323 PG (1)	I	S	I	S	R	S
201444352 PUV 8 (5)	S	R	I	S	R	S
201444327 PUV A (6)	S	S	I	S	R	S

Index: S = susceptible; I = intermediate; R = resistant; Q = quality control

Table 3.2 Results of antibiotic susceptibility test on *Enterococcus* spp. isolates (Calgary Enterolert samples).

Sample ID	Ampicillin	Tetracycline	Streptomycin	Cefatoxime	Trimethoprim	Ciprofloxacin	Vancomycin
201444252 PUV (5)	S	S	S	S	R	I	NT
201444346 PG #1 (1)	S	S	S	S	R	I	NT
641326 PG C #2 (4)	S	S	I	R	R	S	NT
Prim eff #3 I1 (15)	S	S	S	S	R	S	NT
Prim eff #3 I2 (16)	S	S	S	S	R	S	NT
Prim eff #3 I3 (17)	S	S	S	S	R	S	NT
201444352 PUV Dil D (6)	S	S	S	S	R	I	NT
641329 PUV B #1 (7)	S	S	S	S	R	S	NT
641329 PUV B #2 (8)	S	S	S	S	R	S	NT
641326 PG B #1 (9)	S	S	R	S	R	I	NT
641326 PG B #2 (10)	S	S	R	S	R	I	NT
201444346 PG D (11)	S	R	R	R	R	S	NT
201444346 PG E #2 (2)	S	S	I	S	R	S	I
641326 PG C #2 (3)	S	S	R	R	R	S	I
201444346 PG C (12)	S	S	I	I	R	I	R
201444352 PUV Dil C #1 (13)	S	S	I	I	R	I	I
201444352 PUV Dil C #2 (14)	S	I	I	I	R	I	R

Index: S = susceptible; I = intermediate; R = resistant; NT = not tested

3.2.3 qPCR Assay Development

Fecal indicator bacteria, *E. coli* and *Enterococcus* spp., along with *C. perfringens* were the bacterial isolates of interest. The assay for *uidA* (Taskin et al. 2011) and *entero1* (US. EPA 2012) were previously optimized in the Neumann lab (School of Public Health, University of Alberta) by Candis Scott and Graham Banting.

Assays for *cpn60* (*C. perfringens*), *tetA* (tetracycline), *vanB* (vancomycin) and *intI1* (class 1 integron) required development. *C. perfringens* was identified based on the *cpn60* gene and was developed by Candis Scott (School of Public Health, University of Alberta) and validated with a wild *C. perfringens* isolate that was isolated by Nancy Price (School of Public Health, University of Alberta) with the above described *C. perfringens* culture method. The *tetA* assay was validated with a wild *E. coli* isolate (identified as *E. coli* wastewater isolate #1) obtained from wastewater, while the class 1 integron gene, *intI1* was validated with another wild *E. coli* isolate (identified as *E. coli* wastewater isolate #2). The *vanB,* assay was validated with ATCC *E. faecalis* 51299. Previously published primer/probe sets were initially selected and tested on a PCR gel to determine its suitability for qPCR and to identify a positive control from the wastewater isolates available. Table 3.3 shows the primer and probe sequences of the gene targets that were initially tested on a PCR gel. It should also be noted the *C. perfringens* isolate used for qPCR development and in Chapter 4 and 5 presented tetracycline resistance, though no gene target was developed.

Table 3.3 List of published primer and probe sequences used to develop ARG qPCR assays.

Target	Primer	Sequence (5' → 3')	Amplicon size (bp)	Reference
C. perfringens	*cpn60* - F	AAATGTAACAGCAGGGGCA	139	(Karpowicz et al. 2010)
	cpn60 - R	TGAAATTGCAGCAACTCTAGC		
Tetracycline	*tetA* – F	CAGCCTCAATTTCCTGACGGGCTG	96	(Borjesson et al. 2009)
	tetA – R	GAAGCGAGCGGGTTGAGAG		
Vancomycin	*vanB* - F	ACCCTGTCTTTGTGAAG	121	(Mirzaei et al. 2013)
	vanB - R	GAAATCGCTTGCTCAAT		
Class 1 Integron	*intI1* – F	CAGTGGACATAAGCCTGTTC	160	(Dillon et al. 2005)
	intI1 - R	CCCGAGGCATAGACTGTA		

DNA from pure isolates obtained from culturing above were extracted using the boiling method where pure cultures grown for a few hours at 37 °C were placed on a heat block set at 95 °C for 15 mins. Following extraction, all samples were stored at -20 °C until required. These extracted samples were run on a PCR gel with the primers listed in Table 3.3 to identify a positive control. Figures 3.2 show examples of the PCR gel results of testing the above mentioned primer sets (Table 3.3) for each gene target. The presence of a band with the correct corresponding base pair length represented a positive result.

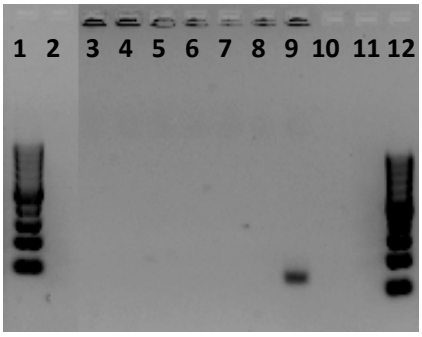

Figure 3.2 PCR gel results from testing *vanB* primer set (Table 3.3).
(1) 100 bp ladder; (2) Blank; (3-9*) Enterococcus* spp. isolates; (10-11) Blank; (12) 100 bp ladder.

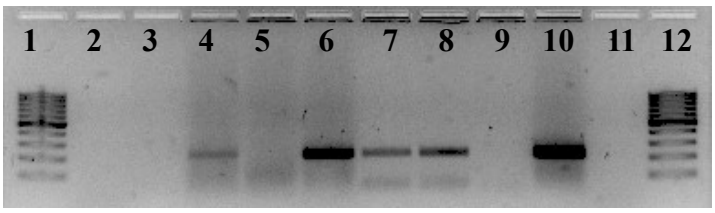

Figure 3.3 PCR gel results from testing *intI1* primer set (Table 3.3).
(1) 100 bp ladder; (2) Blank; (3-6) *E. coli* isolates; (7-9) *Enterococcus* spp. isolates; (10) *E. coli* isolate; (11) Blank; (12) 100 bp ladder.

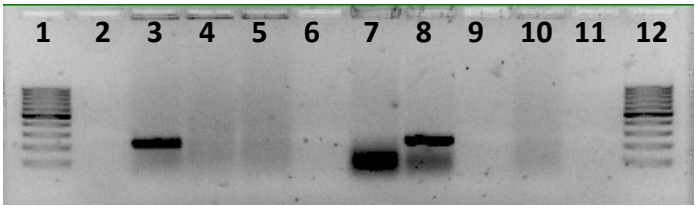

Figure 3.4 PCR gel results from testing *tetA* primer set (Table 3.3).
(1) 100 bp ladder; (2) Blank; (3-10) *E. coli* isolates; (11) Blank; (12) 100 bp ladder.

The gel products of potential positive controls were submitted to the Applied Genomics Core (TAGC) at the University of Alberta for Sanger sequencing and the results were used in conjunction with the NCBI database (https://blast.ncbi.nlm.nih.gov/Blast.cgi) to confirm that the PCR product matched the expected target. With the sequence, the Primer Express 3.0 program (Thermo Fisher Scientific, USA) was used to re-design a primer and probe set for each gene target that would be better suited for use in the TaqMan® qPCR assay. All primer/probe sets were synthesized by Integrated DNA Technologies (USA), diluted with nuclease-free water (Invitrogen, USA) and stored at -20 °C until used. The primers and probes developed for qPCR assays used in this project are as seen in Table 3.4.

Table 3.4 List of primer and probe sequences used for qPCR assays for bacteria and ARG detection.

Target	Primer/Probe	Sequence (5' → 3')	Amplicon size (bp)	Reference
E. coli	*uidA* - F	CGC AAG GTG CAC GGG AAT A	143	(Taskin et al. 2011)
	uidA - R	CAG GCA CAG CAC ATC AAA GAG A		
	uidA - P	[FAM] ACC CGA CGC GTC CGA TCA CCT [MGBNFQ]		
***Enterococcus* spp.**	*entero1*- F	GAG AAA TTC CAA ACG AAC TTG	90	(US. EPA 2012)
	entero1 - R	CAG TGC TCT ACC TCC ATC ATT		
	*entero*1 - P	[FAM] TGG TTC TCT CCG AAA TAG CTT TAG GGC TA [TAMRA]		
C. perfringens	*cpn60* - F	AAA TGT AAC AGC AGG GGC A	139	This study
	cpn60 - R	TGA AAT TGC AGC AAC TCT AGC		
	cpn60 - P	[FAM] ATG TCT TCT TTT CCA TTT ACA GGC TTA GAA [MGBNFQ]		
Tetracycline (*E. coli*)	*tetA* – F	CCT GCC TGG ACA ACA TTG CT	71	This study
	tetA – R	CCC GAT CAT GGT CCT GCT T		
	tetA - P	[FAM] CAT TCC GAT GCC ACC C [MGBNFQ]		
Vancomycin (*E. faecalis*)	*vanB* - F	ACG GTC AGG TTC GTC CTT TG	69	This study
	vanB - R	GCT TCT ATC GCA GCG TTT AGT TC		
	vanB - P	[FAM] CGT AAC CAA AGT AAA CAG TAC G [MGBNFQ]		
Class 1 Integron (*E. coli*)	*intI1* – F	GCC GAG GTC TTC CGA TCT C	69	This study
	intI1 - R	TGC TGT TCT TCT ACG GCA AGG T		
	intI1 - P	[FAM] CAG GGC AGA TCC GTG CA [MGBNFQ]		
Internal Amplification Control	IAC - P	CTA ACC TTC GTG ATG AGC AAT CG	200	(Deer et al. 2010)
	IAC - R	GAT CAG CTA CGT GAG GTC CTA C		
	IAC - P	[VIC] AGC TAG TCG ATG CAC TCC AFT CCT CCT [MGBNFQ]		

To further optimize the qPCR assay, standards were required to enable quantification of gene copies in the samples. Plasmid cloning was done using the previously identified positive controls by extracting gel products as outlined in the Qiagen gel extraction kit (Qiagen, USA). The TOPO TA Cloning kit (Invitrogen, USA) was used for ligation into a PCR™2.1-TOPO® vector and transformed into chemically competent TOPO10F' One Shot® *E. coli* cells. Plasmid prep was conducted with the Qiagen QIAprep Spin Miniprep kit (Qiagen, USA) and the DNA concentration was determined using the Qubit (Thermo Fisher Scientific, USA). A restriction digest using EcoR1 (Thermo Fisher Scientific, USA) was done to verify the gene insert within the plasmid. Confirmation of successful cloning can be identified by the presence of two bands, where the top band represents the plasmid and the second represents the gene target insert (Figure 3.5).

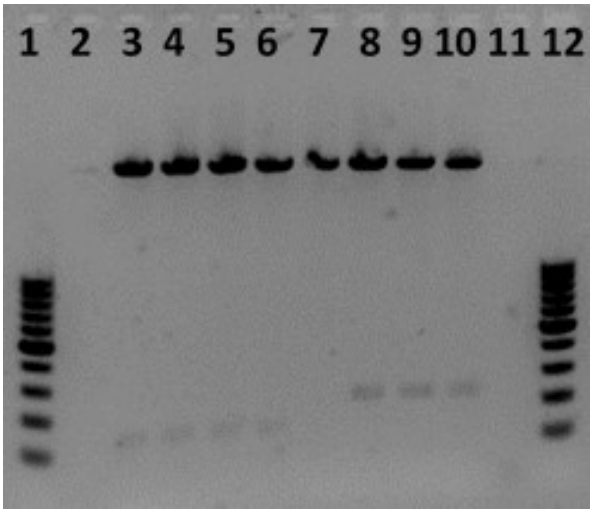

Figure 3.5 An example of the Eco RI restriction digest during plasmid cloning for *vanB* and *intI1*. (1) 100 bp ladder; (2) Blank; (3-6) *vanB* plasmids; (7-10) *intI1* plasmids; (11) Blank; (12) 100 bp ladder.

The PCR gel product was submitted for Sanger sequencing using the M13F and M13R primers for further confirmation and the plasmid sequence inserts are described in Table 3.5. The plasmids for *uidA* and *entero1* were previously developed in the Neumann lab (School of Public Health, University of Alberta) and are therefore not shown.

Table 3.5 Plasmid insert sequences.

Gene Target	Insert Sequences (5' → 3')
***cpn60* (*C. perfringens*)**	AAATGTAACAGCAGGGGCAAATCCTATATTAATAAGAAATGGAATTAA AACTGCAGTTGAAAAAGCTGTAGAGGAAATACAAAAAATTTCTAAGCC TGTAAATGGAAAAGAAGACATAGCTAGAGTTGCTGCAATTTCA
***vanB* (vancomycin)**	ACGGTCAGGTTCGTCCTTTGGCGTAACCAAAGTAAACAGTACGGAAGAA CTAAACGCTGCGATAGAAGC
***intI1* (class 1 integron)**	GCCGAGGTCTTCCGATCTCCTGAAGCCAGGGCAGATCCGTGCACAGCAC CTTGCCGTAGAAGAACAGCA
***tetA* (tetracycline)**	CCTGCCTGGACAACATTGCTTGCAGCGCCGGCATTCCGATGCCACCCGA AGCAAGCAGGACCATGATCGGG

Quantitation of the plasmid was done with the Qubit® 3.0 Fluorometer (Thermo Scientific, USA) and dilutions were made for use as standards in future qPCR runs. Upon dilution, aliquots of 40 µL were stored at -20 °C until use. Ten-fold dilutions of the plasmids were performed to develop a standard calibration curve (50, 000 gene copies/reaction to 0.5 gene copies/reaction) and to determine the limit of detection (LOD_{95}) for each assay. Table 3.6 shows the LOD_{95} calculated for each of the targets that are used for further analysis.

Table 3.6 qPCR limit of detection (LOD_{95}) of each gene target (copies/reaction (5 µL)).

Gene target	LOD_{95}	Lower confidence limit	Upper confidence limit
***uidA* (*E. coli*)**	3.5	1.5	8.5
***entero1* (*Enterococcus* spp.)**	2.1	0.7	6.2
***cpn60* (*C. perfringens*)**	66	38	115
***vanB* (vancomycin)**	6.2	2.3	17
***intI1* (class 1 integron)**	1.4	0.8	2.5
***tetA* (tetracycline)**	2.8	1.2	6.6

3.3 References

Borjesson S, Dienues O, Jarnheimer P-A, Olsen B, Matussek A, Lindgren P-E. 2009. Quantification of genes encoding resistance to aminoglycosides, beta-lactams and tetracyclines in wastewater environments by real-time PCR. Int. J. Environ. Health Res. 19:219–230.

Deer DM, Lampel KA, González-Escalona N. 2010. A versatile internal control for use as DNA in real-time PCR and as RNA in real-time reverse transcription PCR assays. Lett. Appl. Microbiol. 50:366–372.

Dillon B, Thomas L, Mohmand G, Zelynski A, Iredell J. 2005. Multiplex PCR for screening of integrons in bacterial lysates. J. Microbiol. Methods 62:221–232.

Karpowicz E, Novinscak A, Bärlocher F, Filion M. 2010. qPCR quantification and genetic characterization of Clostridium perfringens populations in biosolids composted for 2 years. J. Appl. Microbiol. 108:571–581.

Mirzaei B, Farivar TN, Juhari P, Mehr MA, Babaei R. 2013. Investigation of the prevalence of vanA and vanB genes in vancomycin resistant enterococcus (VRE) by Taq Man real time PCR Assay. J. Microbiol. Infect. Dis. 3:192–198.

Taskin B, Gozen AG, Duran M. 2011. Selective quantification of viable Escherichia coli bacteria in biosolids by quantitative PCR with propidium monoazide modification. Appl. Environ. Microbiol. 77:4329–4335.

U.S. Centers for Disease Control and Prevention. 2013. Antibiotic resistance threats in the United States, 2013.

US. EPA. 2012. Method 1611: enterococci in water by TaqMan® quantitative polymerase chain reaction (qPCR) assay.

Chapter 4 – Technical Paper #1

A version of this chapter has been submitted to Environmental Science & Technology for publication.

Evaluating Microbial and Chemical Hazards in Commercial Struvite Recovered from Wastewater

Rachel A. Yee[1], Mats Leifels[2,3], Candis Scott[2], Nicholas J. Ashbolt[2], Yang Liu[1]

[1]Department of Civil and Environmental Engineering, [2]School of Public Health, University of Alberta, Edmonton, Canada, [3]Centre for Water and Environmental Research (ZWU), University Duisburg-Essen, Essen, Germany

4.1 Abstract

Controlled struvite ($NH_4MgPO_4 \cdot 6H_2O$) precipitation has become a well-known process for nutrient recovery from wastewater treatment systems to alleviate the pressures of diminishing, finite rock phosphate reservoirs. Nonetheless, co-precipitation of potential microbial and chemical hazards, such as metals are poorly understood. On the other hand, antibiotic resistance is a major global public health concern and wastewater is thought to disseminate resistance genes within bacteria. Focusing on struvite produced from pilot and full-scale operations culture and qPCR methods were utilized to identify fecal indicator bacteria, antibiotic resistance genes and human enteric viruses in the final product. Detection of these hazards occurred in both wet and dry struvite samples indicating that there is a potential risk that needs further consideration. While heavy metal concentrations met current fertilizer standards, the presence of K, Na, Ca and Fe ions may impact struvite purity yet provide benefit for agricultural uses. In all, co-precipitation of metals, fecal indicator bacteria, antimicrobial resistance genes and human enteric viruses with struvite is likely and future

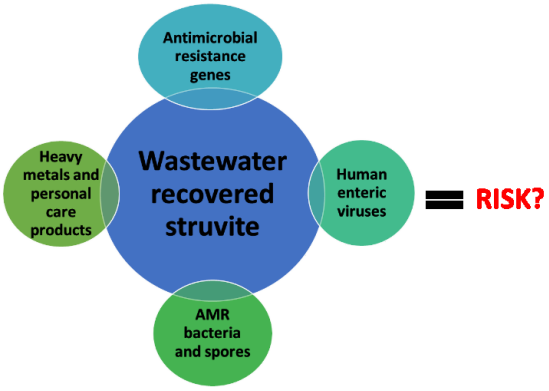

engineered wastewater systems producing struvite may require additional step(s) to manage these newly identified public health risks.

4.2 Introduction

Phosphate rock is the primary but finite source of phosphorus used in agricultural production (Chen et al. 2017). The limited availability results in the need for alternative sources to sustain humanity in the future (Cordell and Neset 2014). Even though industries such as agriculture are becoming limited by phosphorus availability, wastewater treatment plants (WWTPs) are point sources contributing to eutrophication through the release of excess nutrients (phosphorus and nitrogen) within effluent streams (US. EPA 2016). While initial wastewater studies addressed struvite ($NH_4MgPO_4 \cdot 6H_2O$) scale blockages of pipes and fixture (Le Corre et al. 2009), the focus has since shifted to examining methods for maximum struvite precipitation for economic benefits in regards to nutrient recovery (Batstone et al. 2015). Hence, integrating nutrient recovery methods into existing WWTPs has the potential to recover otherwise wasted resources, thus providing a solution to alleviating receiving water nutrient pollution as well as gaining recoverable nitrogen and phosphorus for use in agriculture (Nongqwenga et al. 2017).

Struvite precipitation from wastewater is undertaken by adding magnesium, the limiting ion for struvite formation (Le Corre et al. 2009):

$$NH_4^+ + Mg^{2+} + H_nPO_4^{n-3} + 6H_2O \rightarrow MgNH_4PO_4 \cdot 6H_2O + nH^+ \quad (1)$$

Extensive research has been conducted on struvite precipitation from various waste streams and to date there are several commercial processes operating that focus on utilizing municipal wastewater effluent to recover nutrients. Though each process is optimized to produce struvite, there are many specifics that differ. To highlight a few operational processes, Berliner Wasserbetriebe (in Germany and the Netherlands) utilize their Airplex® Process to produce Berliner Pflanze through a system that aerates with CO_2 stripping and $MgCl_2$ addition (P-Rex 2015). Also, in the Netherlands is the PHOSPAQ™ process operated by Paques® in which an aerated reactor dosed with MgO is used (Paques 2017). Ostara Nutrients Recovery Technologies Inc. operates throughout North America and Western

Europe using the Pearl® Process, with system specifics that follows the Wasstrip® process to produce the product known as Crystal Green™ (Ostara Nutrient Recovery Technologies Inc. 2017). Other notable commercial processes for phosphorus recovery include the Phosnix® Process in Japan (Unitika Ldt.), the Crystalactor® in China (DHV), the NuReSys® Process in Belgium and the Netherlands (Akwadok/NuReSys) and a cone-shaped fluidized bed crystallizer throughout the United States (Multiform Harvest Inc.).

Though the process has been commercialized, limited studies have been conducted that examine the potential co-precipitation occurrence of the recovered products. Wastewater is a reservoir for many potential hazards, such as enteric pathogens, heavy metals and organics of emerging concern that could co-precipitate and pose a threat to public health following the application of struvite fertilizer (Başakçılardan-Kabakcı et al. 2007; Decrey et al. 2011; Abel-Denee et al. 2018). Chemical hazards of potential concern include heavy metals, various endocrine disrupting organics and pharmaceutical residuals. Various macro- and micro-nutrients (including Ca^{2+}, Na^{+}, K^{+}, Fe^{2+}, Zn^{2+} and Mg^{2+}) may also be problematic, as they could interfere with struvite crystallization. In particular, Ca^{2+} has repeatedly been shown to be a competitor with Mg^{2+} in the formation of struvite, resulting in calcium phosphate and carbonate products (Le Corre et al. 2005).

Microbial parameters for effluent discharges include FIB, such as *E. coli* and enterococci (US. EPA 2012a). While *Enterococcus* spp. can be more resilient to environmental stressors than *E. coli* (Byappanahalli et al. 2012), most regulations for wastewater discharge are currently based on coliforms (e.g. not to exceed 200/100 mL) (WHO 2006). Spore-forming FIB, such as *C. perfringens* may also be important due their spore's greater resistance to disinfection/treatment than vegetative FIB cells (Byappanahalli et al. 2012; De Sanctis et al. 2017). WWTPs have also been identified as potential reservoirs for antimicrobial resistant bacteria (ARB) and antimicrobial resistance genes (ARGs) (Karkman et al. 2018) including their FIB (Ranotkar et al. 2014; ECDC EFSA & EMA 2017), which are considered a significant hazard to manage (Pruden et al. 2018). Though naturally found in the environmental microbiota, increasing levels of ARB and ARGs are being detected worldwide in association with engineered water systems (Guo et al. 2017) and thus has topped the WHO concerns list for the decade (WHO 2016). MGEs (such as class 1 integrons)

are important for HGT of ARGs between different bacterial species within the aquatic environment and biofilms (Berendonk et al. 2015; Guo et al. 2017; Karkman et al. 2018). HGT may be more evident within WWTPs as the system provides a means of selective pressures that favour the transfer of ARGs to indigenous bacteria (Szczepanowski et al. 2009; Karkman et al. 2018). However, the lack of antibiotic, ARB and ARG regulations in wastewater effluents results in an unclear view of the target levels required to reduce potential downstream impacts (Larsson et al. 2018). It is only recently that ARB and ARGs within recovered struvite have been examined (Sheets et al. 2015; Chen et al. 2017), where evidence of wastewater-derived struvite can increase the ARG levels in soil, the rhizosphere and phyllosphere following application as fertilizer (Chen et al. 2017). With residual antibiotics, AMR bacteria and ARGs potentially ending up in struvite, it could contribute to the growing issues of AMR via the environment (Sobsey et al. 2015; O'Neill 2016; Wuijts et al. 2017).

Human enteric viruses related to waterborne outbreaks could also be a concern in nutrient recovery from wastewater (Kauppinen and Miettinen 2017; Dunkin et al. 2018). These viruses include noroviruses GI and GII (NoVs) and human adenoviruses (HAdVs), both associated with acute gastrointestinal infections in children and adults via environmental routes (Sales-Ortells et al. 2015; Rames et al. 2016), along with *Enterovirus* members (EV) (Cherkinskii et al. 1978), which can lead to chronic diseases (Bambic et al. 2015). While WWTPs may reduce viral loads to receiving environments, persistent virions (Gall et al. 2015; Leifels et al. 2016; Haramoto et al. 2018), such as noroviruses have been associated with spinach crop outbreaks resulting from irrigation with reclaimed wastewater (Randazzo et al. 2016). Furthermore, analysis of a human virus surrogate (somatic bacteriophage ϕX174) in struvite recovered from urine shows that inactivation and infectivity can be affected by moisture content (Decrey et al. 2011). The study (Decrey et al. 2011) suggested post-processing methods involving drying temperature and storage would help further reduce infectious virions in struvite, although it was based on testing of virus surrogates whose behavior and characteristics in the environment may differ from human enteric viruses (Mackowiak et al. 2018). While likely abundant in the source material, the presence of NoVs, HAdVs and EVs have yet to be reported in struvite. Even though viruses require a

host to reproduce, their high persistence towards disinfection methods and low infectious dose make them a highly relevant hazard group for quantitative microbial risk assessment (QMRA) of residual pathogen risk associated with wastewater-recovered struvite. Hence, to provide initial scoping data to assess potential risks with agricultural use of recovered struvite, the current study focused on yields of plant nutrients and potential metal toxins (Rout and Das 2003) as well as human pathogens and selected AMR genes in precipitated struvite.

4.3 Materials and Methods

4.3.1 Struvite Samples

Commercial struvite samples were obtained from a pilot-scale system utilizing blackwater (toilet flush water) (Sample 1), and from a full-scale system utilizing a side-stream lagoon supernatant from a municipal wastewater source (Sample 2). Commercial struvite Sample 1 was received as a wet, brown slurry sent in a plastic bottle and stored at 4-8 °C, with a subsample stored in 10 % glycerol at -80 °C until analysed. Commercial struvite Sample 2 was received as a dry, white commercial product and was stored in a sterile plastic bag at room temperature until analysed.

Lab-produced struvite (Sample 3) was synthetically prepared in a 1 L sterile glass bottle using 700 mL of sterile distilled H_2O containing 600 mg/L $MgSO_4$ and 550 mg/L $(NH_4)_2HPO_4$ (from 1 M sterile stock solutions) and was adjusted to pH 9 with sterile 1 M NH_4OH. The preparation was mixed with a stir bar at 400 RPM for 15 min at room temperature, then decreased to 200 RPM for 1 h to allow for precipitation. Precipitate was recovered using a 0.45 µm glass fiber filter (Sigma-Aldrich, USA) and dried at 150 °C overnight. The white synthetic struvite recovered was stored in a sterile, air-tight glass vial at room temperature until analysed.

4.3.2 Chemical Composition of Struvite Samples

Samples were analyzed via X-ray diffraction (XRD; Rigaku Ultimate IV, Japan), X-ray photoelectron spectroscopy – for Samples 1 and 2 only (XPS, Kratos AXIS Ultra) and a scanning electron microscope (SEM; Zeiss Sigma 300 VP-FESEM, USA) with energy dispersive X-ray spectroscopy (EDS; Bruker EDS system, USA). The peaks of the XRD figures were compared to the Inorganic Crystal Structure Database (ICSD) for confirmation of struvite using the following cards - PDF #97-006-0626 and PDF #98-000-0419 (http://www2.fiz-karlsruhe.de/icsd_home.html). The CasaXPS program and the Handbook of X-ray Photoelectron Spectroscopy (Moulder et al. 1992) were used as confirmation of the chemical bonds present on the surface of the samples following calibration of peaks in reference to carbon binding energy of 282.4eV. EDS analysis was based on point analysis of the SEM images. Prior to the above analysis, Samples 1 was oven-dried at 150 °C overnight and XPS was not conducted on Sample 3.

The struvite samples were analyzed for metals via induced coupled plasma optical emission spectrometry (ICP-OES; Thermo iCAP 6000 series, Thermo Scientific, USA). Dry samples (0.04-0.07 g) were digested in 5 mL of trace metal grade nitric acid (Thermo Fisher Scientific, USA) following Method 3051A as set by the U.S. EPA (US. EPA 2007). Digested samples were diluted to a volume of 25 mL with distilled water prior to ICP-OES analysis in triplicate.

4.3.3 Faecal Indicator Bacteria, Enteric Viruses and ARG Detection by qPCR

The details of assay development and limits of detection are described in Chapter 3. For bacterial and ARG gene detections, DNA was extraction from 0.25 g of Samples 1 (wet) and 2 (dry) using the PowerSoil DNA extraction kit™ (Qiagen, Germany) following the manufacturer's protocol. Extracted samples were eluted in 100 µL and stored at -20 °C until use. Table 3.4 in Chapter 3 describes the primer/probe information used in the qPCR assays for bacteria and ARGs.

To detect enteric viruses, total nucleic acids from 0.25 g of commercial struvite Sample 1 and 2 were extracted using the DNeasy Blood and Tissue Kit (Qiagen, Germany) according

to manufacturer's recommendation, eluted in 100 µL of inorganic buffer and stored at -20 °C. The kit was chosen due its ability to remove co-concentrated inhibitors as previously described by Hamza et al. (2009, 2011). For EV and NoV GII, extracted RNA was converted to complementary DNA (cDNA) using the High Capacity cDNA Reverse Transcription Kit (Thermo Fischer, USA) according to the manufacturer's protocol. Standards containing DNA and RNA were created according to Hamza et al. (2009), Leifels et al. (2015) and Lowther et al. (2017). LOD_{95} was also determined via serial dilutions for all targets and calculated as five genomic copies (GC) per litre for HAdV, 50 GC for EV and 100 GC for NoV GII (data not shown). Sequences of all enteric virus primers and probes used as well as their amplicon length are listed in Table 4.1. Note that all assays involving virus detection was developed and performed by Mats Leifels, (School of Public Health, University of Alberta).

Table 4.1 List of primer and probe sequences used for qPCR assays for human enteric virus detection.

Target	Primer/Probe	Sequence (5' → 3')	Amplicon size (bp)	Reference
Norovirus GII (NoV GII)	QNIF2	ATG TTC AGR TGG ATG AGR TTC TCW GA	89	(Kageyama et al. 2003; Loisy et al. 2005)
	COG2R	TCG ACG CCA TCT TCA TTC ACA		
	QNIFs	[FAM] AGC ACG TGG GAG GGC GAT CG [TAMRA]		
Human Adenoviruses (HAdV)	AQ1	GCC ACG GTG GGG TTT CTA AAC TT	139	(Heim et al. 2003)
	AQ2	GCC CCA GTG GTC TTA CAT GCA CATC		
	AdVP	[Hex]-TGC ACC AGA CCC GGG CTC AGG TAC TCC GA-[BHQ1]		
Enteroviruses (EV)	EV 444	CCT CCG GCC CCT GAA TG	178	(Hamza et al. 2009)
	EV 621	ACC GGA TGG CCA ATC CAA		
	EV P	[FAM] ACG GAC ACC CAA AGT CGG TTC CG [BHQ1]		

The qPCR reaction for bacterial, virus and ARG detection was performed under sterile conditions using the PrimeTime® Gene Expression Master Mix Kit (IDT, USA) in a 20 µL reaction volume containing 5 µL of DNA or 2 µL of cDNA template. For bacteria and

ARGs, 0.9 µM of both forward and reverse primers and 0.25 µM of specific probes were used, while for viruses, 0.25 µM of both forward and reverse primer and 1 µM of specific probes were used. The internal amplification control was used with the *uidA* assay with a reaction volume of 25 µL. Cycling conditions for bacterial and ARG detection were 95 °C for 3 mins (hold) and 40 cycles of 95 °C for 5 secs and 60 °C for 30 secs. Cycling conditions for enteric virus detection have been previously described as seen in Table 4.1. The Rotorgene 6,000 qRT cycler system (Qiagen, Germany) was used for both amplification and quantification of the targets.

Due to the high complexity of the struvite matrix, both internal and external inhibition controls were utilized to determine the level of signal suppression as advised by Buckwalter et al. (2014). Approximately 500 and 50,000 genome copies of the target virus as well as the above-mentioned amplification controls were spiked to samples under investigation. The results were then compared to the original concentration.

4.3.4 Viability/Infectivity Assays for E. coli, Enterococcus *spp. and Human Enteric Viruses*

Fresh, wet samples (0.3 mL) of Sample 1 were inoculated into Colilert (IDEXX, USA) and Enterolert (IDEXX, USA) media and quantified using Quanti-trays 2000® according to manufacturer's protocols to estimate culturable *E. coli* and *Enterococcus* spp. concentrations, respectively. While most probable number (MPN) counts were used to quantify *E. coli* and *Enterococcus* spp. viability, the plate method using CM0587 Perfringens agar base (TSC & SFP) media (Thermo Scientific, USA) with 85 mg/L 4-methylumbelliferyl phosphate (Invitrogen, USA) was used to quantify *C. perfringens* via colony forming unit (CFU) counts. For plate counts, 1:10 serial dilutions of fresh, wet samples (100 µL) of Sample 1 were conducted. Plates were incubated in an anaerobic box at 37 °C overnight.

For enteric viruses, infectivity was determined based on an adapted capsid-integrity (ci-) PMA-qPCR as described by Randazzo et al. (2018) and Leifels et al. (2016). Furthermore, the culture-based integrated cell culture (ICC) qPCR using buffalo green monkey (BGM)

cells was utilized to assess the infectivity of HAdV and EV according to Hamza et al. (2009). For ci-qPCR, a stock solution of PMA (Biotium Inc, USA) was reconstituted with 20 % dimethyl sulfoxide (DMSO; Sigma-Aldrich, USA) to a final concentration of 10 mM and was stored at -20 °C. A working solution of 1 mM was prepared in aliquots (to avoid freezing and thawing). The PMA pre-treatment was undertaken using a modified protocol (Dinh Thanh et al. 2017) as follows; PMA in the working solution was added to 200 µL of samples up to a final concentration of 0.04 mM per reaction, mixed gently and incubated in the dark for 30 min at room temperature to allow the dye to penetration into virions with permeable capsids. Afterwards, samples were exposed to daylight for 15 min to enable photo-induced crosslinking of the reagent before the tubes were exposed to a 4-Watt LED lamp for 15 min to develop irreversible and polymerase inhibiting azo-dye genome complexes. The efficacy of the treatment was confirmed by adding extracted HAdV whole genome as an internal control which showed qPCR signal reduction between 4-6 $\log_{10}$ for each (RT)-ci-qPCR run (data not shown).

4.4 Results and Discussion

4.4.1 Struvite Sample Morphology

The presence of struvite in Samples 1-3 was confirmed by XRD analysis (Figure 4.1). Utilizing the ICSD, the observed peaks aligned with crystalline struvite as indicated by the red dots in Figure 4.1, however the intensity of the peaks differ. While the peak positions corresponded with the diffraction angles calculated by Bragg's law (Jian and Hejing 2003), the peak intensities differed between the samples, which is likely due to the X-ray absorbance and different sample volumes used in the analysis (Jian and Hejing 2003). Though co-precipitates are indicated by the mineral analyses (described later), these were not detected by XRD, presumably due to relatively low levels and the crystalline structure of struvite. Regardless of the process utilized and the wastewater source, struvite was efficiently recovered and phase identified.

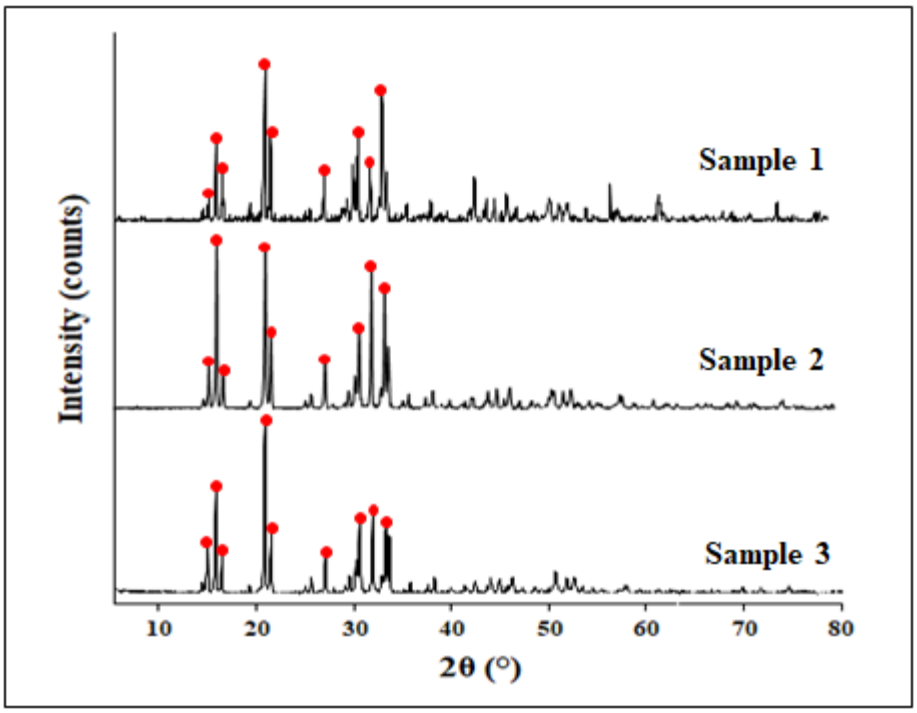

Figure 4.1 XRD analysis of Sample 1, Sample 2 and Sample 3.

SEM images assessed the differences in size and shape of the struvite crystals (Figure 4.2). Sample 1 appeared to be an orthorhombic shaped crystal with an approximate size of 120 µm. However, as seen in the left-hand corner of the Sample 1 image, there also appeared to be an amorphous, non-struvite structure. The large struvite crystalline structure obscured XRD identification of the observed co-precipitate. Sample 2 consisted of larger (spanning a few mm), round compact pebble-like crystals, which were fractured with a mortar and pestle into smaller pieces prior to undertaking SEM analysis. As a result, the images shown have a rougher surface appearance. Sample 3 differed in structure to the commercial struvite products as crystal twinning was observed. This is likely due to equal crystal growth in two directions under the laboratory controlled conditions (Prywer et al. 2012).

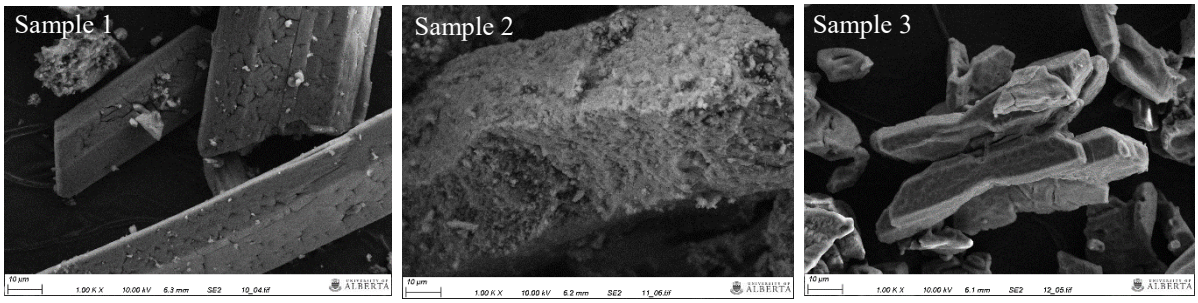

Figure 4.2 SEM images of Sample 1, Sample 2 and Sample 3 at 1000x magnification.

Previous descriptions of crystalline struvite describe dendritic and orthorhombic crystal structures (Mehta and Batstone 2013; Doyle et al. 2000; Wang et al. 2006), with several factors accounting for different crystal morphologies. It has been suggested that mixing speed, mixing time and the presence of a seed can impact crystal growth. The varying processes used for recovery will thus impact nucleation and crystal formation. Hence, the different shaped crystals are not surprising given the different conditions and feeds used to form the three struvite products examined. As a result, chemical hazards could differentially embed during crystallization and/or form separate amorphous co-precipitates.

4.4.2 Metal co-precipitation

XPS analysis was performed for further surface analysis of Mg, P, C, O and N as the likely major elements to be detected in struvite (Figure 4.3). As all elements were not analyzed, co-precipitates could not be directly detected using XPS. The resulting binding energies in comparison to the database confirmed the main N peaks at 399.6 eV (Sample 1) and 400.4 eV (Sample 2) as ammonia, while the P peaks at 132.4 eV (Sample 1) and 133.4 eV (Sample 2) were representative of phosphate (Moulder et al. 1992). The oxygen peaks of both samples overlap with binding energies that match with phosphates, required for struvite formation, as well as carbonates that could account for potential co-precipitation.

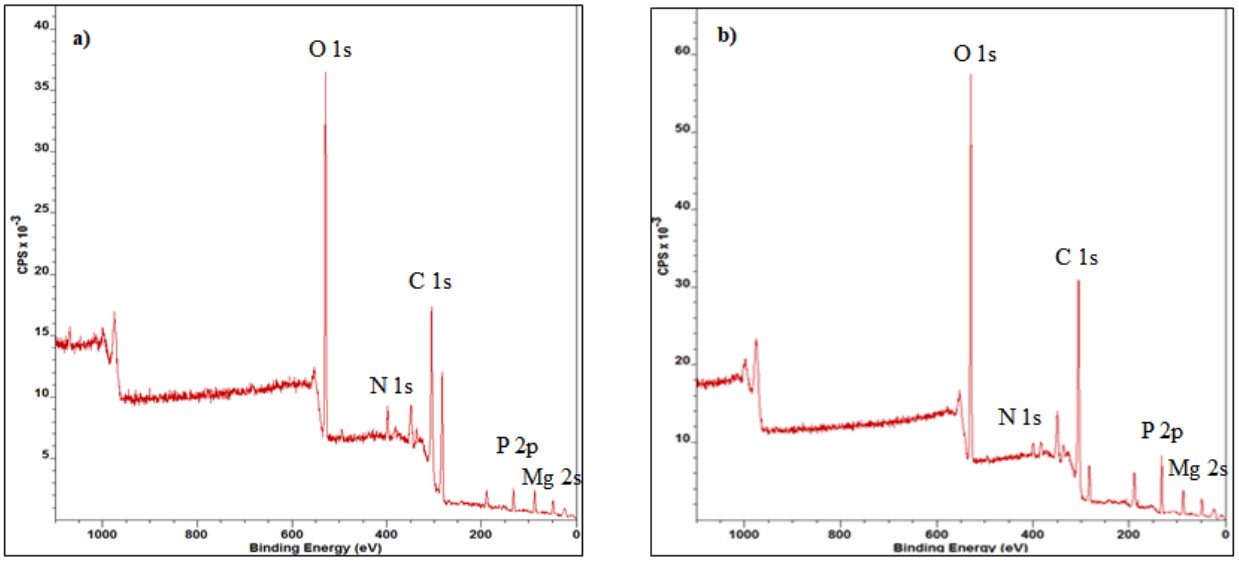

Figure 4.3 XPS analysis of a) Sample 1 and b) Sample 2.

The surface chemical composition of the struvite samples examined by EDS analysis showed that C, O, Mg and P were the predominant elements detected, which is in line with the struvite chemical composition. Specifically, crystals of Sample 1 were composed of: 18.2 % C, 50.5 % O, 15.7 % Mg, 14.8 % P and 0.83 % K, while Sample 2: 28.9 % C, 45.5 % O, 13.3 % Mg and 12.4 % P. Similarly, the lab produced struvite was composed of 14.4 % C, 59.8 % O, 12.3 % Mg and 13.5 % P. The presence of carbon is likely due to carbonates as well as trace amounts of organics. The observed oxygen detection is likely due to the hydrate required for struvite formation. The potassium detected in Sample 1 could be due to very low levels of potassium struvite, where K^+ replaces NH_4^+ in the crystal structure (Xu et al. 2015). EDS analysis of the amorphous structure observed in Sample 1 (Figure 4.4) provides evidence of co-precipitation as the composition consisted of the following: 47.5 % C, 31.6 % O, 12.8 % Mg, 1.23 % P, 1.27 % Ca, 0.71 % K, 1.73 % Na and 2.17 % Cl. EDS cannot solely be used to determine the identity of the co-precipitate as it only highlights the surface chemical composition, though indicates co-precipitation occurred.

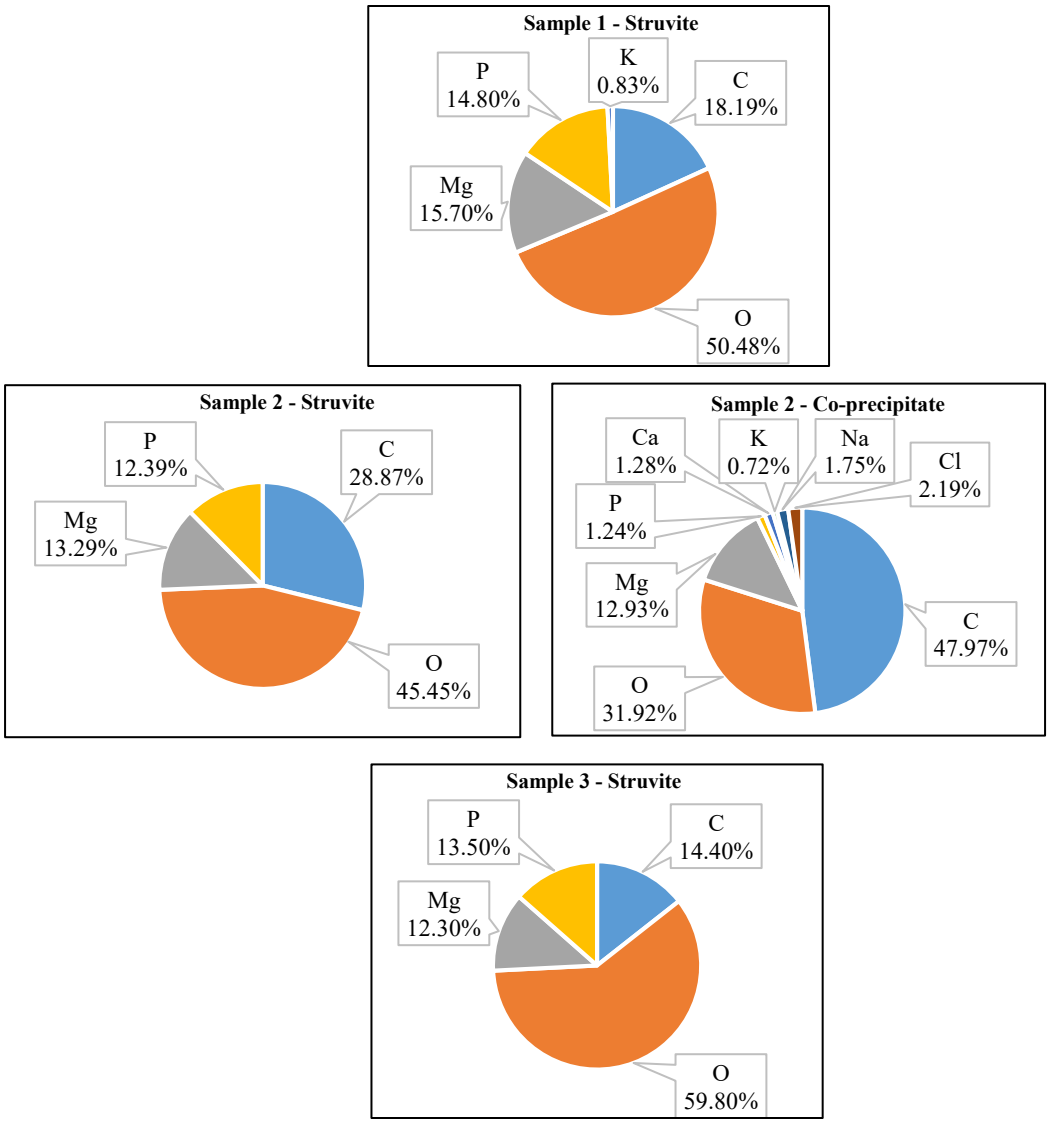

Figure 4.4 EDS results of amorphous and crystal precipitates observed in SEM images of Sample 1-3. Elements not shown are below the detection limit.

Metal detection further into the center of the crystal was investigated using ICP-OES, further confirming that elemental ions other than Mg and P were detected (Figure 4.5). The ratios of P and Mg for each sample were similar, which is expected if struvite is the main product (given its 1:1 molar ratio of Mg:P). The dominant metals observed in the commercial samples included Na, Ca, K and Fe. Other metals that were detected include Zn, Cu, Mn

and Cr, with only trace amounts of As, Cd, Pb and Ni. Higher traces of micro- and macronutrients compared to Samples 2-3 were detected in Sample 1, presumably due to the concentrated blackwater source. Precipitation from a municipal wastewater source, as in Sample 2, versus a blackwater source would result in a large dilution factor that reduces metal concentrations. Sample 3 was produced from sterile stock chemical solutions and therefore the detection for the above mentioned metals were well below the limit of detection (0.001 – 0.019 µg metal/g of struvite), thus not shown in Figure 4.5.

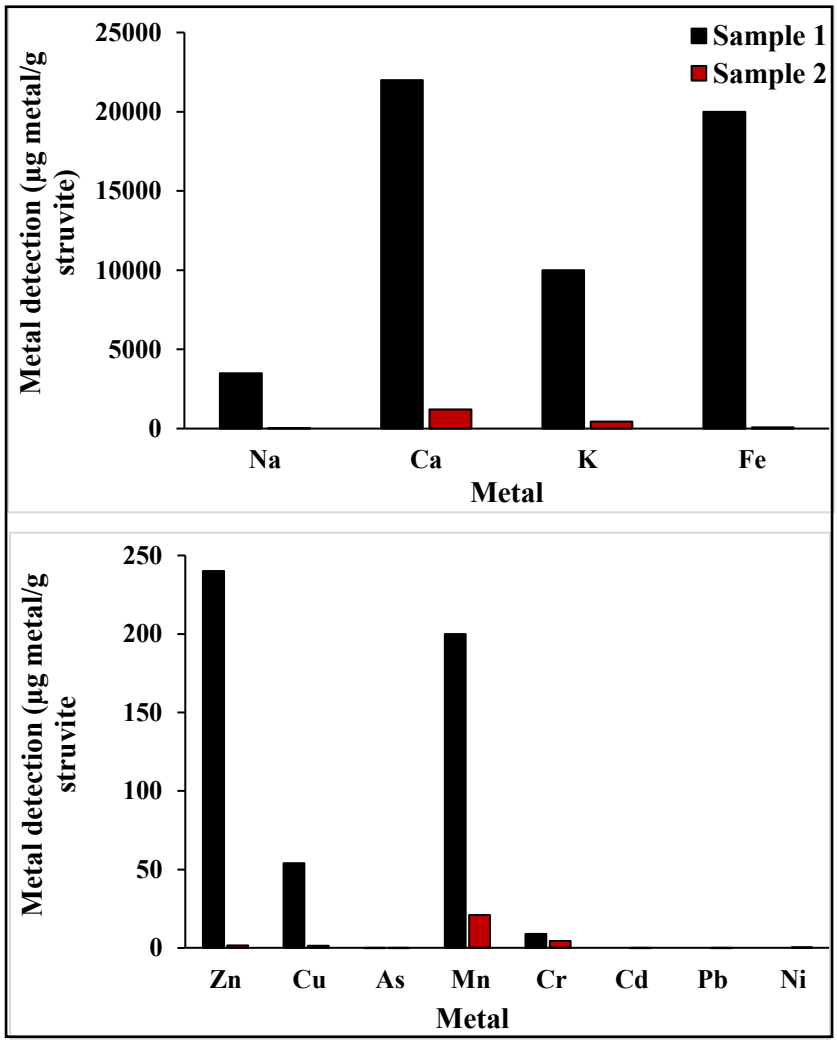

Figure 4.5 ICP-OES results of Sample 1 and Sample 2. The dominant metals are shown in the top graph of the figure (N = 3).

Based on previous reports and surface analysis, the presence of calcium carbonates and phosphates as an amorphous compound is likely to be an observed co-precipitate (Le Corre et al. 2005). The remaining P and Mg not accounted for in struvite can be used with Ca to estimate the residuals $Ca_3(PO_4)_2$ and $CaCO_3$. With Mg as the limiting reagent, residual P could be assumed to form $Ca_3(PO_4)_2$ and equate to approximately 0.06 g/g of struvite and 0.03 g/g of struvite for Sample 1 and 2 respectively.

According to the fertilizers regulations used by the Canadian Food Inspection Agency (CFIA), the metals added to soils must meet fertilizer/supplement standards, which are similar to those used in other countries (US. EPA 1999; Canadian Food Inspection Agency 2017). Several macro- and micronutrients are essential plant growth components at low levels (Kim et al. 2009), which are reflected in the ranges provided in the standards. Based on the annual acceptable metal concentrations, the detected metals in the samples were all within the allowable range despite potentially affecting the purity of the final product. Limits regarding Na, Ca and K levels are not addressed in the CFIA safety guidelines, but higher levels of these nutrients are generally acceptable. Surface metal presence and inclusion could be important to understand the impact on struvite purity and may also indicate metal accumulation and potential toxicity to crops upon downstream application.

4.4.3 Biological Analysis

Addressing gene presence, qPCR was performed to quantify FIB, ARGs and enteric viruses. Most bacterial gene targets were detected in quantities above the LOD_{95} in all samples (Figure 4.6). Of unknown relative significance, Sample 1 (which was sourced from blackwater) had a higher overall presence of ARG copies per gram of struvite than Sample 2, which was sourced from municipal wastewater. The highest target gene detected in each sample was the class 1 integron gene (*intI1*), which is of potential concern given its role in HGT of AMR genes (Gillings 2017). Of the FIB, enterococci was the most numerous in Sample 1, which fits with evolving practice to utilize qPCR targeting the more persistent enterococci as a health-related marker for sewage-contaminated environments and standard

methods for its assay are also well described (Haugland et al. 2014; Korajkic et al. 2014). Given the drying process step expected for commercial struvite fertilizer production (Wen et al. 2009), the samples were also screened for highly resistant spores of *C. perfringens*, though no copies of the *cpn60* gene were detected in Sample 2. For all targets, only a portion of the entire gene is amplified via qPCR, thus the viability status of the host cell and functionality of the ARGs remains unknown, but could still be transferred to soil bacteria (Christou et al. 2017).

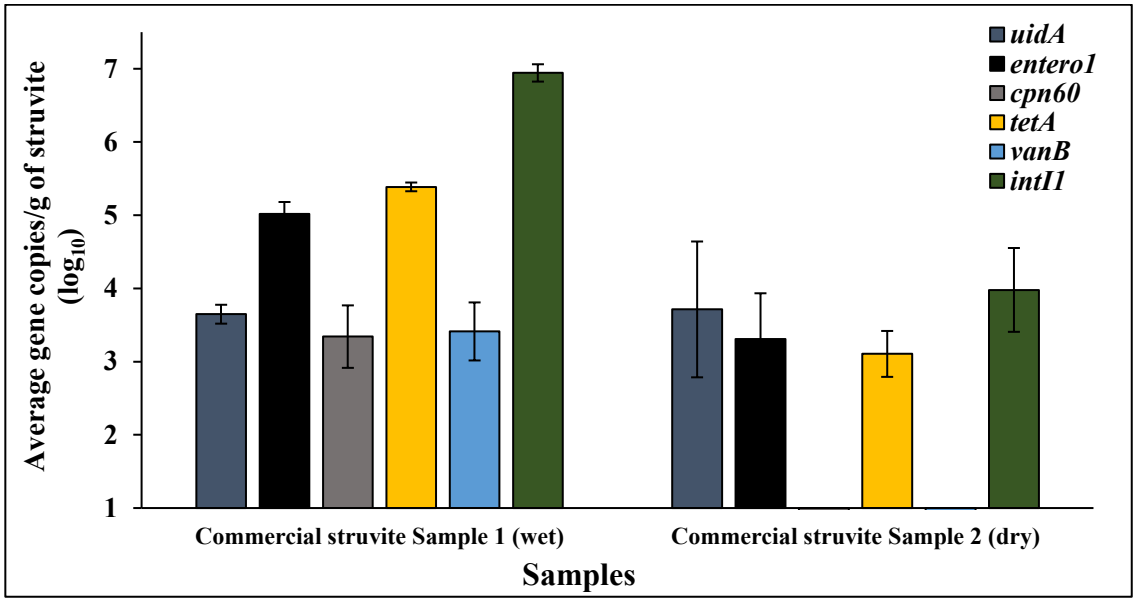

Figure 4.6 qPCR analysis of Sample 1 (wet weight) and Sample 2 (dry weight) shown as average gene copies/g of struvite (N = 3, errors bar indicate standard deviation).

Bacterial viability assays detected enterococci within the wet Sample 1 material, with an estimated quantification of 1.04 x 10^3 MPN.mL^{-1}. In comparison, the MPN of enterococci in the dried Sample 1 material was 215 MPN.g^{-1}. Colilert results were negative indicating that viable *E. coli* cells, if present, were below detection. These results are consistent with previous knowledge that enterococci are generally more resilient to changing environments than *E. coli* (Korajkic et al. 2014). Nonetheless, comparison of results to the CFIA maximum acceptable level of indicator organisms in fertilizers (1.00 x 10^3 MPN.g^{-1} solid) suggests that

Sample 1 following drying was within the acceptable limit (Canadian Food Inspection Agency 2017). Such FIB targets were developed before AMR became a global concern and without consideration of more persistent enteric pathogens. Hence, the presence of viable FIB in conjunction with possible dissemination of ARGs (such as vancomycin resistance in enterococci) could still pose a potential risk that requires further examination. Of increasing concern are the culturable *C. perfringens* spores from the wet Sample 1 material that were estimated at 3.0×10^5 $CFU.mL^{-1}$. Correlation between viability and qPCR results are not clear as not all spores may germinate on culture of *C. perfringens*. Though the dry sample was not tested, post precipitation processing steps will be integral for microbial reduction should spore-formers be considered an important class of AMR hazard. Figure 4.7 provides examples of the Quanti-trays 2000® and agar plates used to quantify the viability of the tested samples.

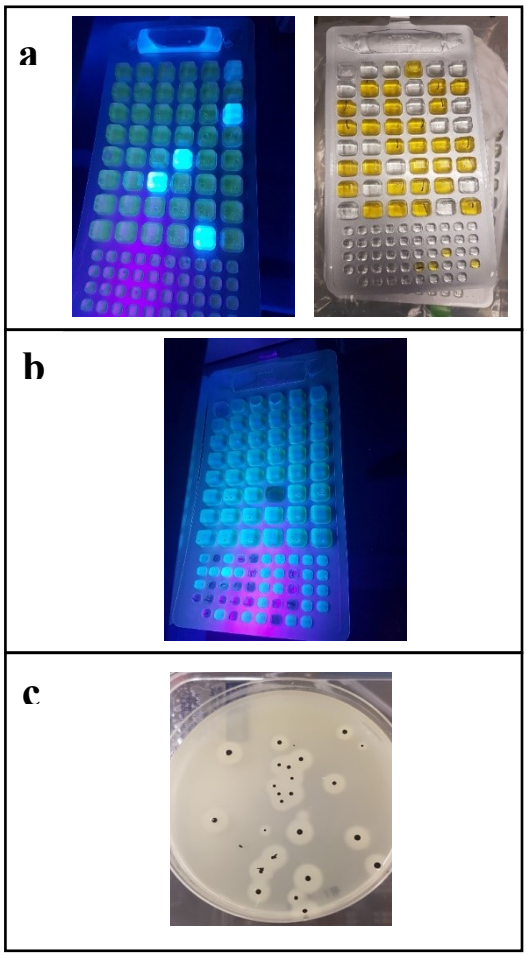

Figure 4.7 Examples of a) Colilert, b) Enterolert and c) *C. perfringens* agar plates. Images are examples of quantification method and not representative of Sample 1 results.

While more than 150 different genera of enteric viruses have been described as waterborne (Clasen et al. 2014), a relatively short list of viruses are considered representative in wastewater for QMRA studies (Soller et al. 2010), hence the focus on EV, HAdV and NoV GII. RT-ci-qPCR only confirmed enterovirus virions with intact capsids (Figure 4.8), indicating infectivity potential. Should struvite fertilizer be utilized in crops eaten raw, such as lettuce or carrots, the infectivity of these enteric viruses is also of potential concern (Li et al. 2015).

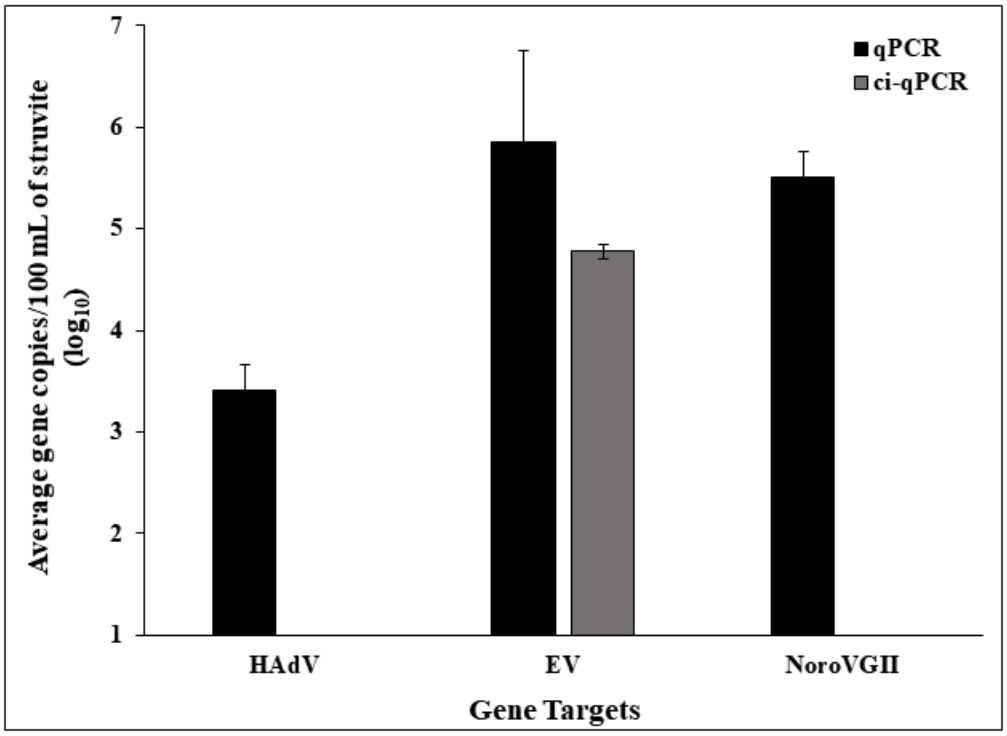

Figure 4.8 (RT)-qPCR and ci-(RT)-qPCR analysis of Sample 1 for EV, HAdV and NoV GII shown as average gene copies/100 mL of struvite (N = 6, error bars indicate standard deviation).

4.5 Conclusion

The process of precipitating struvite and applying it for use in agriculture has economic potential to resourcefully recover nutrients that would otherwise be wasted, and in the long term may be part of sustaining food production. This study showed that despite varying feed and processing conditions, the struvite collected contained metals of interest on crystal surfaces, with higher concentrations likely within or simultaneously co-precipitating separately as amorphous structures contaminating the final product. With microbial hazards in wastewater, our results indicated potential exposure to AMR bacteria and enteric viruses that needs to be further assessed. Viability assays for *E. coli*, *Enterococcus* spp. and *C. perfringens* in a wet struvite sample indicated quantifiable numbers of enterococci and *C. perfringens* present; therefore, post-precipitation processing steps will be necessary for reducing microbial risks. Further qPCR analysis showed genes corresponding to *E. coli*,

*Enterococcu*s spp., *C. perfringens* and ARGs were detected in the samples. Regardless of cell viability, detection of these genes could pose a risk given their ability to be taken up by and transferred between indigenous soil bacteria. Additionally, (RT)-qPCR detected EV, HAdV and NoV GII in at least one struvite sample studied, while a novel molecular assay measuring capsid integrity inferred potentially infectious Enterovirus presence. The results of this study confirm that there is a need to determine the risks associated with using wastewater-recovered nutrients. In addition, as not all potential hazards were assessed in this study, the co-precipitation of other chemical hazards such as pharmaceuticals and personal care products would be useful in further understanding the hazards present in struvite. Along with determining the presence of hazards, the operational conditions and processes that elevate or reduce these risks should also be considered to minimize downstream public health concerns.

4.6 Acknowledgements

The work was supported by research grants provided by the Natural Sciences and Engineering Research Council (NSERC), the City of Edmonton, the NSERC Industrial Research Chair (IRC) Program in Sustainable Urban Water Development (Liu, Y.) and the Canada Research Chair (CRC) in Future Community Water Services (Liu, Y.). The authors wish to also thank Nancy Price (School of Public Health, University of Alberta) for microbiological training and technical support.

4.7 References

Abel-Denee M, Abbott T, Eskicioglu C. 2018. Using mass struvite precipitation to remove recalcitrant nutrients and micropollutants from anaerobic digestion dewatering centrate. Water Res. 132:292–300.

Bambic DG, Kildare-Hann BJ, Rajal VB, Sturm BSM, Minton CB, Schriewer A, Wuertz S. 2015. Spatial and hydrologic variation of Bacteroidales, adenovirus and enterovirus in a semi-arid, wastewater effluent-impacted watershed. Water Res. 75:83–94.

Başakçılardan-Kabakcı S, Thompson A, Cartmell E, Le Corre K. 2007. Adsorption and precipitation of tetracycline with struvite. Water Environ. Res. 79:2551–2556.

Batstone DJ, Hülsen T, Mehta CM, Keller J. 2015. Platforms for energy and nutrient recovery from domestic wastewater: A review. Chemosphere 140:2–11.

Berendonk TU, Manaia CM, Merlin C, Fatta-Kassinos D, Cytryn E, Walsh F, Bürgmann H, Sørum H, Norström M, Pons M-N, et al. 2015. Tackling antibiotic resistance: the environmental framework. Nat. Rev. Microbiol. 13:310–317.

Buckwalter SP, Sloan LM, Cunningham SA, Espy MJ, Uhl JR, Jones MF, Vetter EA, Mandrekar J, Cockerill FR, Pritt BS, et al. 2014. Inhibition controls for qualitative real-time PCR assays: Are they necessary for all specimen matrices? J. Clin. Microbiol. 52:2139–2143.

Byappanahalli MN, Nevers MB, Korajkic A, Staley ZR, Harwood VJ. 2012. Enterococci in the environment. Microbiol. Mol. Biol. Rev. 76:685–706.

Canadian Food Inspection Agency. 2017. T-4-93 - Safety Guidelines for Fertilizers and Supplements.

Chen Q, An X, Zhu Y, Su J, Gillings MR, Ye Z. 2017. Application of struvite alters the antibiotic resistome in soil, rhizosphere, and phyllosphere. Environ. Sci. Technol. 51:8149–8157.

Cherkinskii SN, Gabrilevskaia LN, Klimenkova KM, Kozlova MV. 1978. Substantiation of the standard indices for the chlorine decontamination of afterpurified municipal sewage. Gig. Sanit. 5:25–28.

Christou A, Agüera A, Bayona JM, Cytryn E, Fotopoulos V, Lambropoulou D, Manaia CM, Michael C, Revitt M, Schröder P, et al. 2017. The potential implications of reclaimed wastewater reuse for irrigation on the agricultural environment: the knowns and unknowns of the fate of antibiotics and antibiotic resistant bacteria and resistance genes – A review. Water Res. 123:448–467.

Clasen T, Pruss-Ustun A, Mathers CD, Cumming O, Cairncross S, Colford JM. 2014. Estimating the impact of unsafe water, sanitation and hygiene on the global burden of disease: evolving and alternative methods. Trop. Med. Int. Heal. 19:884–893.

Cordell D, Neset TSS. 2014. Phosphorus vulnerability: A qualitative framework for assessing the vulnerability of national and regional food systems to the multi-dimensional stressors of phosphorus scarcity. Glob. Environ. Chang. 24:108–122.

Decrey L, Udert KM, Tilley E, Pecson BM, Kohn T. 2011. Fate of the pathogen indicators phage ΦX174 and Ascaris suum eggs during the production of struvite fertilizer from source-separated urine. Water Res. 45:4960–4972.

Deer DM, Lampel KA, González-Escalona N. 2010. A versatile internal control for use as DNA in real-time PCR and as RNA in real-time reverse transcription PCR assays. Lett. Appl. Microbiol. 50:366–372.

De Sanctis M, Del Moro G, Chimienti S, Ritelli P, Levantesi C, Di Iaconi C. 2017. Removal of pollutants and pathogens by a simplified treatment scheme for municipal wastewater reuse in agriculture. Sci. Total Environ. 580:17–25.

Dinh Thanh M, Agustí G, Mader A, Appel B, Codony F. 2017. Improved sample treatment protocol for accurate detection of live Salmonella spp. in food samples by viability PCR. PLoS One 12:1–13.

Dunkin N, Weng SC, Coulter CG, Jacangelo JG, Schwab KJ. 2018. Impacts of virus processing on human norovirus GI and GII persistence during disinfection of municipal secondary wastewater effluent. Water Res. 134:1–12.

ECDC EFSA & EMA. 2017. ECDC, EFSA and EMA joint scientific opinion on a list of outcome indicators as regards surveillance of antimicrobial resistance and antimicrobial consumption in humans and food-producing animals. EFSA J. 15.

Gall AM, Mariñas BJ, Lu Y, Shisler JL. 2015. Waterborne viruses: a barrier to safe drinking water. PLoS Pathog. 11:1–8.

Gillings MR. 2017. Class 1 integrons as invasive species. Curr. Opin. Microbiol. 38:10–15.

Guo J, Li J, Chen H, Bond PL, Yuan Z. 2017. Metagenomic analysis reveals wastewater treatment plants as hotspots of antibiotic resistance genes and mobile genetic elements. Water Res. 123:468–478.

Hamza IA, Jurzik L, Stang A, Sure K, Überla K, Wilhelm M. 2009. Detection of human viruses in rivers of a densly-populated area in Germany using a virus adsorption elution method optimized for PCR analyses. Water Res. 43:2657–2668.

Hamza IA, Jurzik L, Überla K, Wilhelm M. 2011. Evaluation of pepper mild mottle virus, human picobirnavirus and Torque teno virus as indicators of fecal contamination in river water. Water Res. 45:1358–1368.

Haramoto E, Kitajima M, Hata A, Torrey JR, Masago Y, Sano D, Katayama H. 2018. A review on recent progress in the detection methods and prevalence of human enteric viruses in water. Water Res. 135:168–186.

Haugland RA, Siefring SD, Varma M, Dufour AP, Brenner KP, Wade TJ, Sams E, Cochran S, Braun S, Sivaganensan M. 2014. Standardization of enterococci density estimates by EPA qPCR methods and comparison of beach action value exceedances in river waters with culture methods. J. Microbiol. Methods 105:59–66.

Heim A, Ebnet C, Harste G, Pring-Åkerblom P. 2003. Rapid and quantitative detection of human adenovirus DNA by real-time PCR. J. Med. Virol. 70:228–239.

Jian Z, Hejing W. 2003. The physical meanings of 5 basic parameters for an x-ray diffraction peak and their application. Chinese J. Geochemistry 22:38–44.

Kageyama T, Kojima S, Shinohara M, Uchida K, Fukushi S, Hoshino FB, Takeda N, Katayama K. 2003. Broadly reactive and highly sensitive assay for Norwalk-like viruses based on real-time quantitative reverse transcription-PCR. J. Clin. Microbiol. 41:1548–1557.

Karkman A, Do TT, Walsh F, Virta MPJ. 2018. Antibiotic resistance genes in waste water. Trends Microbiol. 26:220–228.

Kauppinen A, Miettinen I. 2017. Persistence of norovirus GII genome in drinking water and wastewater at different temperatures. Pathogens 6.

Kim H, Sudduth A, Hummel JW. 2009. Soil macronutrient sensing for precision agriculture. J. Environ. Monit. 11:1810–1824.

Korajkic A, McMinn BR, Shanks OC, Sivaganesan M, Fout GS, Ashbolt NJ. 2014. Biotic interactions and sunlight affect persistence of fecal indicator bacteria and microbial source tracking genetic markers in the upper mississippi river. Appl. Environ. Microbiol. 80:3952–3961.

Larsson DGJ, Andremont A, Bengtsson-Palme J, Brandt KK, de Roda Husman AM, Fagerstedt P, Fick J, Flach C-F, Gaze WH, Kuroda M, et al. 2018. Critical knowledge gaps and research needs related to the environmental dimensions of antibiotic resistance. Environ. Int. 117:132–138.

Le Corre KS, Valsami-jones E, Hobbs P, Parsons SA. 2005. Impact of calcium on struvite crystal size, shape and purity. J. Cryst. Growth 283:514–522.

Le Corre KS, Valsami-Jones E, Hobbs P, Parsons SA. 2009. Phosphorus recovery from wastewater by struvite crystallization: a review. Crit. Rev. Environ. Sci. Technol. 39:433–477.

Leifels M, Hamza IA, Krieger M, Wilhelm M, Mackowiak M, Jurzik L. 2016. From lab to lake - Evaluation of current molecular methods for the detection of infectious enteric viruses in complex water matrices in an urban area. PLoS One 11:1–16.

Leifels M, Jurzik L, Wilhelm M, Hamza IA. 2015. Use of ethidium monoazide and propidium monoazide to determine viral infectivity upon inactivation by heat, UV-exposure and chlorine. Int. J. Hyg. Environ. Health 218:686–693.

Li D, De Keuckelaere A, Uyttendaele M. 2015. Fate of Foodborne Viruses in the "Farm to Fork" Chain of Fresh Produce. Compr. Rev. Food Sci. Food Saf. 14:755–770.

Loisy F, Atmar RL, Guillon P, Le Cann P, Pommepuy M, Le Guyader FS. 2005. Real-time RT-PCR for norovirus screening in shellfish. J. Virol. Methods 123:1–7.

Lowther JA, Bosch A, Butot S, Ollivier J, Mäde D, Rutjes SA, Hardouin G, Lombard B, in't Veld P, Leclercq A. 2017. Validation of ISO method 15216 part 1 – quantification of hepatitis A virus and norovirus in food matrices. Int. J. Food Microbiol.

Mackowiak M, Leifels M, Hamza IA, Jurzik L, Wingender J. 2018. Distribution of Escherichia coli, coliphages and enteric viruses in water, epilithic biofilms and sediments of an urban river in Germany. Sci. Total Environ. 626:650–659.

Mehta CM, Batstone DJ. 2013. Nucleation and growth kinetics of struvite crystallization. Water Res. 47:2890–2900.

Meschke JS, Vilchez S. 2015. Antimicrobial resistance: an emerging water, sanitation and hygiene issue briefing note WHO/FWC/WSH/14.07. World Heal. Organ.

Moulder JF, Stickle WF, Sobol PE, Bomben KD. 1992. Handbook of X-ray photoelectron spectroscopy.

Nongqwenga N, Muchaonyerwa P, Hughes J, Odindo A. 2017. Possible use of struvite as an alternative phosphate fertilizer. 17:581–593.

O'Neill J. 2016. Tackling drug-resistant infections globally: final report and recommendations. Rev. Antimicrob. Resist.:1–84.

Ostara Nutrient Recovery Technologies Inc. 2017. The only nutrient recovery solution that prevents digester struvite build-up. Tech. Factsheet:1–2.

P-Rex. 2015. AirPrex® Struvite crystallization in sludge. Tech. Factsheet:1–2.

Paques. 2017. PHOSPAQ ^{TM} Sustainable phosphorus recovery. Tech. Factsheet:1–4.

Pruden A, Alcalde R, Alvarez P, Ashbolt N, Bischel H, Capiro N, Crossette E, Frigon D, Grimes K, Haas CN, et al. 2018. An environmental science and engineering framework for combating antimicrobial resistance. Environ. Eng. Sci. 35:1–7.

Prywer J, Torzewska A, Plociński T. 2012. Unique surface and internal structure of struvite crystals formed by Proteus mirabilis. Urol. Res. 40:699–707.

Rames E, Roiko A, Stratton H, Macdonald J. 2016. Technical aspects of using human adenovirus as a viral water quality indicator. Water Res. 96:308–326.

Randazzo W, Khezri M, Ollivier J, Le Guyader FS, Rodríguez-Díaz J, Aznar R, Sánchez G. 2018. Optimization of PMAxx pretreatment to distinguish between human norovirus with intact and altered capsids in shellfish and sewage samples. Int. J. Food Microbiol. 266:1–7.

Randazzo W, López-Gálvez F, Allende A, Aznar R, Sánchez G. 2016. Evaluation of viability PCR performance for assessing norovirus infectivity in fresh-cut vegetables and irrigation water. Int. J. Food Microbiol. 229:1–6.

Ranotkar S, Kumar P, Zutshi S, Prashanth KS, Bezbaruah B, Anand J, Lahkar M. 2014. Vancomycin-resistant enterococci: troublemaker of the 21st century. J. Glob. Antimicrob. Resist. 2:205–212.

Rout GR, Das P. 2003. Effect of metal toxicity on plant growth and metabolism: I. Zinc. Argonomic 23:3–11.

Sales-Ortells H, Fernandez-Cassi X, Timoneda N, Dürig W, Girones R, Medema G. 2015.

Health risks derived from consumption of lettuces irrigated with tertiary effluent containing norovirus. Food Res. Int. 68:70–77.

Sheets JP, Yang L, Ge X, Wang Z, Li Y. 2015. Beyond land application : Emerging technologies for the treatment and reuse of anaerobically digested agricultural and food waste. Waste Manag. 44:94–115.

Sobsey MD, Abebe L, Andremont A, Ashbolt NJ, de Roda Husman AM, Gin KY-H, Hunter PR,

Soller JA, Bartrand T, Ashbolt NJ, Ravenscroft J, Wade TJ. 2010. Estimating the primary etiologic agents in recreational freshwaters impacted by human sources of faecal contamination. Water Res. 44:4736–4747.

Szczepanowski R, Linke B, Krahn I, Gartemann KH, Gützkow T, Eichler W, Pühler A, Schlüter A. 2009. Detection of 140 clinically relevant antibiotic-resistance genes in the plasmid metagenome of wastewater treatment plant bacteria showing reduced susceptibility to selected antibiotics. Microbiology 155:2306–2319.

Taskin B, Gozen AG, Duran M. 2011. Selective quantification of viable Escherichia coli bacteria in biosolids by quantitative PCR with propidium monoazide modification. Appl. Environ. Microbiol. 77:4329–4335.

US. EPA. 1999. Estimating Risk from Contaminants Contained in Agricultural Fertilizers Draft Report.

US. EPA. 2007. Method 3051A - Microwave assisted acid digestion of sediments, sludges, soils and oils.

US. EPA. 2012a. 2012 Recreational Water Quality Criteria.

US. EPA. 2012b. Method 1611: enterococci in water by TaqMan® quantitative polymerase chain reaction (qPCR) assay.

US. EPA. 2016. National rivers and streams assessment 2008-2009: a collaborative survey (EPA/841/R-16/007). Washington, DC.

Wen Q, Tutuka C, Keegan A, Jin B. 2009. Fate of pathogenic microorganisms and indicators in secondary activated sludge wastewater treatment plants. J. Environ. Manage. 90:1442–1447.

WHO. 2006. Guidelines for the safe use of wastewater, excreta and greywater. Geneva.

WHO. 2016. Global priority list of antibiotic-resistant bacteria to guide research, discovery, and development of new antibiotics.

Wuijts S, van den Berg HHJL, Miller J, Abebe L, Sobsey M, Andremont A, Medlicott KO, van Passel MWJ, de Roda Husman AM. 2017. Towards a research agenda for water, sanitation and antimicrobial resistance. J. Water Health 15:175–184.

Xu K, Li J, Zheng M, Zhang C, Xie T, Wang C. 2015. The precipitation of magnesium potassium phosphate hexahydrate for P and K recovery from synthetic urine. Water Res. 80:71–79.

Chapter 5 - Technical Paper #2

A version of this chapter has been submitted for publication in the Journal of Hazardous Materials.

Nutrient Recovery from Source-Diverted Blackwater: Optimization for Enhanced Phosphorus Recovery and Reduced Co-Precipitation

Rachel A. Yee [1], Daniel S. Alessi [2], Nicholas J. Ashbolt [3], Weiduo Hao [2],
Kurt Konhauser [2], Yang Liu [1]

[1] Department of Civil and Environmental Engineering, [2] Department of Earth and Atmospheric Sciences, [3] School of Public Health, University of Alberta, Edmonton, Canada

5.1 Abstract

High residual phosphorus in anaerobically digested source-diverted blackwater allows for increased phosphorus recovery through struvite ($NH_4MgPO_4 \cdot 6H_2O$) precipitation. Due to the complex matrix of blackwater, recovered products inevitably contain co-precipitates of other wastewater components that have not been well characterized. The potential hazards present include pathogens, antimicrobial resistance genes (ARGs), organic and inorganic compounds. In this study, several important struvite precipitation conditions (pH, Mg^{2+}:PO_4^{3-} molar ratio and $MgCl_2$ dosing rate) were tested to determine their impact on phosphorus recovery, while taking into account the co-precipitation of enteric bacteria, ARGs and micro- and macronutrients. Results demonstrate that phosphorus recovery efficiency does not correlate to the degree of metal/microbial co-precipitation. Both PO_4^{3-} recovery and co-precipitates were affected by the operation conditions examined, and the optimal condition for nutrient recovery from blackwater was at pH 9, a 1.5:1 Mg^{2+}:PO_4^{3-} molar ratio, and a dosing rate of 24 $mM \cdot min^{-1}$. In all, examination of struvite precipitation conditions on enhanced phosphorus recovery, along with co-precipitates, is necessary when considering the public health risk associated with efficiently recovering residual nutrients.

5.2 Introduction

WWTPs are often faced with scaling deposits of struvite ($NH_4MgPO_4 \cdot 6H_2O$) that can reduce treatment efficiency. Early methods investigated to control struvite scaling included chemical addition of alum and ferric chloride for phosphorus removal (Mamais et al. 1994) and changes to pipe materials (Parsons and Doyle 2002). However, with the need for new phosphorus sources to maintain agricultural practices, an increased number of investigations have directed the focus to wastewater phosphorus recovery instead of control and elimination. Struvite can be recovered applied as a slow release fertilizer (Le Corre et al. 2009), which utilizes existing scaling deposits, reduces phosphorus release into receiving environments, and provides a source of phosphorous to maintain current agricultural practices.

Successful struvite precipitation from several types of wastewater streams have been demonstrated where many factors, including pH, the presence of Mg^{2+} ions, temperature and mixing have been identified for optimized struvite precipitation (Wang et al. 2005; Le Corre et al. 2007a; Li et al. 2012). Supplementing the process with Mg^{2+} has been defined as a requirement for all waste streams (Alp et al. 2008). Although, there is a general consensus on the conditions that most effectively promote precipitation, consideration of the water chemistry of the specific feed source and practical issues must also be taken into account for any particular system. Literature focusing on source-diverted blackwater (toilet water, with or without kitchen sink wastewater) is limited with respect to struvite recovery conditions. In comparison to greywater (shower and laundry water) and municipal wastewater (centralized wastewater collection), blackwater has a considerably higher amount of carbon and nutrients that can be recovered (Alp et al. 2008; de Graaff et al. 2011). Anaerobic treatment of blackwater is effective for energy recovery, but a high residual nutrient concentration remaining in the effluent needs to be managed (de Graaff et al. 2011; Gao et al.), which can be a good source for phosphorus recovery through struvite precipitation. One of the few reported studies on struvite recovery from raw blackwater demonstrated that the highest phosphorus removal occurs at a pH of 9.5 and a Mg^{2+}:PO_4^{3-} molar ratio of 1.3:1 (Alp et al. 2008). However, no study has been reported on the process optimization of

anaerobically treated blackwater phosphorus and nitrogen recovery through struvite precipitation.

In addition to process optimization, there are several caveats that need to be further examined to identify the risks that could be involved in the use of recovered struvite. Hazards such as heavy metals, pharmaceuticals and pathogens are present in blackwater (Gell et al. 2011) and thus products derived for reuse could pose a public health concern. Evaluation of chemical and microbial co-precipitates in commercial struvite samples from wastewater indicates that co-precipitation is likely to occur (Yee et al. 2018), however, no study has specifically linked the operational conditions with co-precipitation processes. The few reported studies have demonstrated the co-precipitation of metals, e.g., K, Ca, S, Na and Fe in struvite (Gell et al. 2011; Yee et al. 2018). Furthermore, calcium phosphate and carbonate co-precipitates have been identified, as Ca^{2+} is a known competitor of Mg^{2+} in struvite formation (Le Corre et al. 2005). Low levels of trace elements and nutrients could be beneficial from an agricultural perspective, thus adding value to the final product. The recovery of struvite in the form of potassium struvite ($MgKPO_4 \bullet H_2O$) could also be an attractive co-precipitate, as K^+ serves as an important macronutrient in agriculture (Mayer et al. 2016). On the other hand, trace heavy metal co-precipitation exceeding the standards could be problematic as plant toxicity could be induced (Nagajyoti et al. 2010).

As for the microbial risks associated with struvite co-precipitation, AMR and their associated ARGs should be considered with their rising public health concern (WHO 2016). While faecal indicator organisms such as *E. coli* and *Enterococcus* spp. are current regulatory indicators for wastewater effluents, spore-forming bacteria, such as *C. perfringens* could be a better indicator of persistent enteric viral and protozoan pathogens due to the increased resistance of their spores to disinfection treatment processes (De Sanctis et al. 2017). Furthermore, the threat of AMR on public health from wastewater sources and the potential genes that could be detected and persistent through treatment are not clearly defined, despite knowledge that WWTPs act as reservoirs (Guo et al. 2017). A recent study examining the application of struvite on the soil profile showed that there was an increase in ARG presence following application (Chen et al. 2017), which underlines the need to evaluate the co-

precipitation that occurs during the formation process. However, previous studies evaluating struvite recovery from wastewater have not addressed the potential pathogen or ARG level associated with the precipitation process.

With blackwater as the source of recovery, it is critical for sustainable application that potential hazards present are considered in the precipitation process as a first step to considering controls for the final struvite product. Hence, the goal of this study was to identify co-precipitates from anaerobically treated blackwater under conditions optimized for enhanced phosphorus recovery. Here results are present on the effects of varying water chemistry conditions (pH, Mg^{2+}:PO_4^{3-} molar ratio and $MgCl_2$ dosing rate) on struvite precipitation and co-associated metals, enteric bacteria and related ARGs within recovered struvite precipitates.

5.3 Materials and Methods

5.3.1 Struvite Precipitation Experiments

Struvite precipitation experiments were conducted using a standard coagulant jar test apparatus (ESICO International, India) and titration instrument (Metrohm, Switzerland) with 1 L beakers as shown in Figure 5.1.

Figure 5.1 Jar test apparatus and titrator instrument used for experiments.

Preliminary experiments to examine the effects of PO_4^{3-} recovery with and without a seed were done to confirm previous literature and determine whether a seed will be used in further experiments. Jar test experiments were conducted in 1 L beakers with 500 mL of 0.45 µm filtered lagoon supernatant obtained from Alberta Capital Region Wastewater Commission and 100 mg of dried struvite (identified as Sample 1 in Chapter 4). The contents of each were adjusted to a pH of 7, 9 or 11 with sterile 1 M NaOH solution. Flash mixing at 200 RPM occurred for 15 mins, followed by slow mixing at 100 RPM for 45 mins. Following the mixing stage, the contents of the jars were allowed to settle for a minimum of 30 mins in the beaker that the experiment was carried out in. The precipitate was collected via centrifugation.

For further jar test experiments, a controllable system was required to allow for appropriate quantification of potential hazard co-precipitation in the varying conditions. Thus, synthetic wastewater mimicking the conditions of anaerobically digested blackwater (Table 5.1) was used as the feed for all further batch experiments.

Table 5.1 Synthetic wastewater recipe (modified from Seib et al. 2016).

	Components	Concentration (mg/L)
Organic	Non-fat dry milk	250
	Soluble potato starch	100
	Yeast extract	200
	Casein peptone	200
	Sodium acetate	1000
	Cysteine	5
Inorganic	Na_2CO_3	100
	$CaCl_2 \cdot 2H_2O$	100
	NaCl	100
	NH_4Cl	800
	KCl	100
	$MgHPO_4 \cdot 3H_2O$	100
	$(NH_4)_2HPO_4$	100
	$FeCl_3$	6.75
	$MnCl_2$	1
	$ZnCl_2$	0.7
	$CoCl_2$	0.25
	$NiCl_2$	0.25

In each beaker, 600 mL of synthetic anaerobically digested blackwater was seeded with 100 mg of lab produced struvite (identified as Sample 3 in Chapter 4). To evaluate the co-precipitation of enteric bacterial indicators potentially reflective of the behaviour of AMR bacterial pathogens, test reactors were also spiked with *E. coli* and *C. perfringens* wastewater isolates and *E. faecalis* ATCC 51299, which carried specific gene markers (*uidA*, *entero1*, *cpn60*, *tetA*, *vanB* and *intI1*; Table 5.2). Pure cultures of the bacterial isolates were grown overnight in TSB at 37 °C and washed thrice with 1x PBS. Two sets of experiments were conducted with different concentrations of spiked bacteria into the synthetic anaerobically digested blackwater. For the first set of experiments (A), a total cell concentration of $4x10^4$ cells/mL consisting of *E. coli* wastewater isolate #1 and *E. faecalis* ATCC 51299 were spiked in. For the second set of experiments (B), a total cell concentration of $8x10^4$ cells/mL of all four isolates (*E. coli* wastewater isolate #1 and #2, *C. perfringens* wastewater isolate #1 and *E. faecalis* ATCC 51299) were spiked in.

Table 5.2 Spiked bacterial isolates used to target genes and organisms of interest.

Target	Bacterial Isolate	Gene Target
E. coli	*E. coli wastewater isolate #1 and #2*	*uidA*
***Enterococcus* spp.**	*E. faecalis ATCC 51299*	*entero1*
C. perfringens	*C. perfringens wastewater isolate #1*	*cpn60*
Tetracycline	*E. coli wastewater isolate #1*	*tetA*
Vancomycin	*E. faecalis ATCC 51299*	*vanB*
Class 1 Integron	*E. coli wastewater isolate #2*	*intI1*

To examine the impact of reactor operation conditions on phosphorus recovery and co-precipitation, the parameters tested included reaction pH (7, 9 and 11), Mg^{2+}:PO_4^{3-} molar ratio (1:1, 1.5:1 and 2:1) and the $MgCl_2$ dosing rate (0.1, 1, 10 and 24 $mM \cdot min^{-1}$). Sterile 1 M NaOH was used to adjust the pH to the appropriate level. The addition of magnesium required to meet the Mg^{2+}:PO_4^{3-} molar ratio was calculated based on the addition of sterile 1 M $MgCl_2$ and all chemicals were added during the flash mixing stage. $MgCl_2$ dosing rates were controlled by using the Tiamo (Metrohm, Switzerland) software that was used in conjunction with the titrator.

To facilitate struvite precipitation, flash mixing at 200 rpm occurred for 15 mins, followed by slow mixing at 100 rpm for 45 mins. Following the mixing stage, the contents of the jars were allowed to settle for a minimum of 30 mins in the beaker that the experiment was carried out in. The synthetic anaerobically digested blackwater was centrifuged in sterile tubes at 5000 rpm for struvite collection. Overnight drying of the precipitate only occurred for the chemical analysis, while immediate DNA extractions occurred for qPCR and viability analysis as described below.

5.3.2 Chemical and Physical Analysis

Hach phosphorus (TNT844, Hach, USA) and ammonia (TNT832, Hach, USA) kits were used to determine PO_4^{3-} and NH_4^+ concentrations before and after precipitation (Standard Methods Committee 1997). Several techniques were employed to assist with characterization of the struvite samples under varying conditions. The struvite composition was analyzed via X-ray diffraction (XRD; Rigaku Ultimate IV, Japan) with copper radiation and peak comparison to the ICSD using the reference struvite cards – PDF #97-006-0626 and PDF #98-000-0419 (http://www2.fiz-karlsruhe.de/icsd_home.html). The struvite morphology was examined via scanning electron microscopy (SEM; Zeiss Sigma 300 VP-FESEM, USA) and energy dispersive x-ray spectroscopy (EDS; Bruker EDS System, USA). The struvite samples were also analyzed for metals composition and concentration via induced coupled plasma optical emission spectrometry (ICP-OES; Thermo iCAP 6000 series, Thermo Scientific, USA). Dry samples (0.04-0.07 g) were digested in 5 mL of trace metal grade nitric acid (Thermo Fisher Scientific, USA) following Method 3051A as set by the U.S. EPA (US. EPA 2007) Digested samples were diluted to a volume of 25 mL with distilled water prior to ICP-OES analysis in triplicate. All chemical and physical analysis was only conducted on experimental set B.

5.3.3 qPCR Analysis

DNA extractions were undertaken on wet struvite samples (0.15-0.2 g w/w) with the PowerSoil DNA extraction kit™ (Qiagen, Germany) as per manufacturer's protocol. DNA

extractions using 500 µL supernatant samples were done by placing tubes on a heat block at 95 °C for 15 mins. Primer and probe sets for all genes of interest were previously developed and described in Chapter 3. An internal amplification control (Deer et al. 2010), also listed in Table 3.4 (Chapter 3), was used with the *uidA* assay to ensure that inhibition of the samples was not occurring during the qPCR reaction. Cycling conditions and reaction specifics have been previously described in Chapter 4.

5.3.4 Viability Analysis

Colilert and Enterolert (IDEXX, USA) were utilized to estimate culturable spiked bacterial *E. coli* and *E. faecalis* cells in recovered struvite as MPN counts as per manufacturer's recommendations. Whereas *C. perfringens* spores were estimated as CFUs using CM0587 Perfringens agar base (TSC & SFP) media (Oxoid, USA) with 85 mg/L 4-methylumbelliferyl phosphate (Invitrogen, USA) to identify colonies by fluorescence under UV light (Davies et al. 1995). Wet samples of struvite (0.1-0.2 g) were washed twice with sterile 1x PBS and centrifuged (0.1-0.2 g), and washed samples were re-suspended in 1 mL of sterile 1x PBS. Following re-suspension, 1:10 serial dilutions were performed and 100 µL samples of the dilutions were used for quantification. Quanti-trays 2000® (IDEXX, USA) were incubated overnight according to the manufacturer's protocol and agar plates at 35 °C for up to 48 h.

5.3.5 Zeta Potential Analysis

Overnight cultures of the bacterial isolates were centrifuged and washed thrice with 1x PBS and separately spiked into synthetic wastewater that was adjusted to a pH of 7, 9 or 11 with sterile 1 M NaOH. Following the pH adjustment, the zeta potential was measured in folded capillary zeta cells (Zetasizer nano series, Malvern, UK). Triplicate values were obtained and based on 20 measurements of the sample.

5.3.6 Microbial Hydrophobicity Analysis

The hydrophobicity of bacterial isolates was determined with the microbial adhesion to hydrocarbons (MATH) assay via simultaneously measuring the change in absorbance as well as by counting CFUs on a trypticase soy agar (TSA) plate (Qiao et al. 2012). Overnight cultures of *E. coli*, *E. faecalis* and *C. perfringens* isolates were centrifuged and washed thrice with 1x PBS. The cultures were adjusted to an optical density of 1.0 measured at an absorbance of 600 nm. 300 µL of filter sterile hexadecane was added to 5 mL of cells and vortexed for 2 mins. The tubes were allowed to rest for a minimum of 15 mins for separation to occur and the final absorbance at 600 nm was measured. Serial dilutions were performed with the measured cells before and after hexadecane addition and 100 µL was plated on TSA plates for colony growth. The following formula was used to determine the fraction partitioned to the hydrocarbon phase (% Adh) based on the absorbance readings or CFU counts, represented as C:

$$\% \text{ Adh} = [1\text{-}C_{\text{aqueous phase}}/C_{\text{original bacteria suspension}}] \text{ x } 100$$

% Adh corresponds to high (≥ 70%), moderate (50-70 %) and low hydrophobicity (< 50 %). All tests were conducted in triplicate for each isolate.

5.4 Results and Discussion

5.4.1 Preliminary PO_4^{3-} Recovery Examining Addition of Seed

Preliminary results with lagoon supernatant comparing the PO_4^{3-} recovery (%) with and without a seed shows that the addition of the seed can increase the recovery (Figure 5.2). The addition of the seed increased recovery from 39-46 % to 68-71 %. Only one replicate was performed as the experiments were performed to determine whether a seed would be useful for further experiments. The results were consistent with literature as the seed acts as a nucleus for crystal formation, thus only one replicate was performed as a quick test for confirmation.

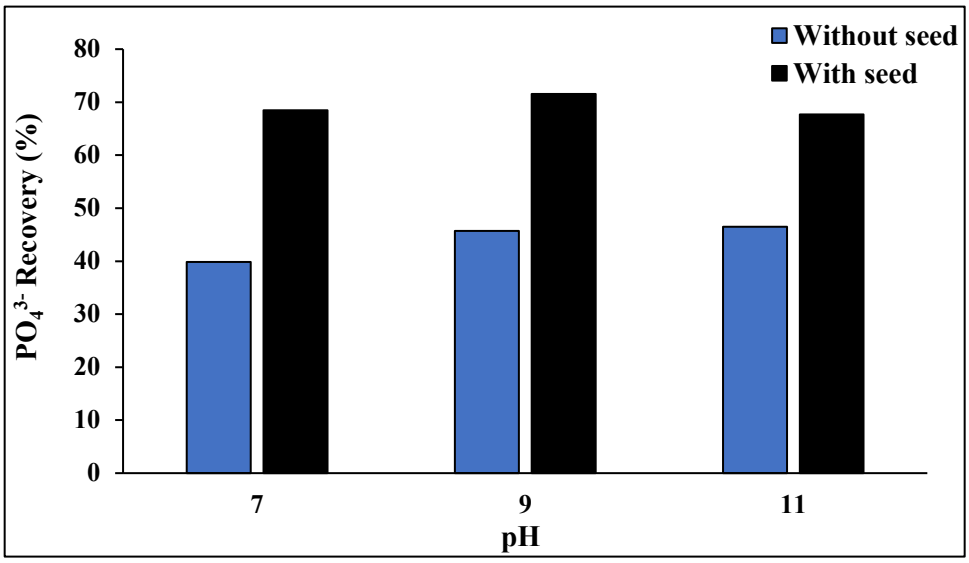

Figure 5.2 PO_4^{3-} recovery (%) with and without a seed addition at pH 7, 9 and 11 (N = 1).

5.4.1 Chemical and Physical Analysis

The chemical and physical analyses were only performed on experimental set B, with a higher bacterial concentration spiked in. As shown in Figure 5.3, XRD provided phase identification that the samples at all tested conditions (pH ranges from 7-11, Mg^{2+}:PO_4^{3-} molar ratio ranges from 1:1-2:1 and $MgCl_2$ dosing rates from 0.1 to 24 $mM \cdot min^{-1}$) were crystalline struvite by comparison with the ICSD. The diffraction angle as determined by Bragg's law is shown by the peak position, where the peaks of the struvite samples show up in the same position (Jian and Hejing 2003). Minor differences in observed peak heights are probably due to the organization of the sample on the mount during the analysis process where x-ray absorption and the sample volume affects scattering (Jian and Hejing 2003). There were no significant peaks that appeared on the profiles that would represent additional compounds that co-precipitated in the sample and the profile of the peak positioning was consistent between all tested samples. Additionally, the low level of background noise indicates that the samples are of a crystalline nature rather than amorphous, thus co-precipitates cannot be detected with this analysis method.

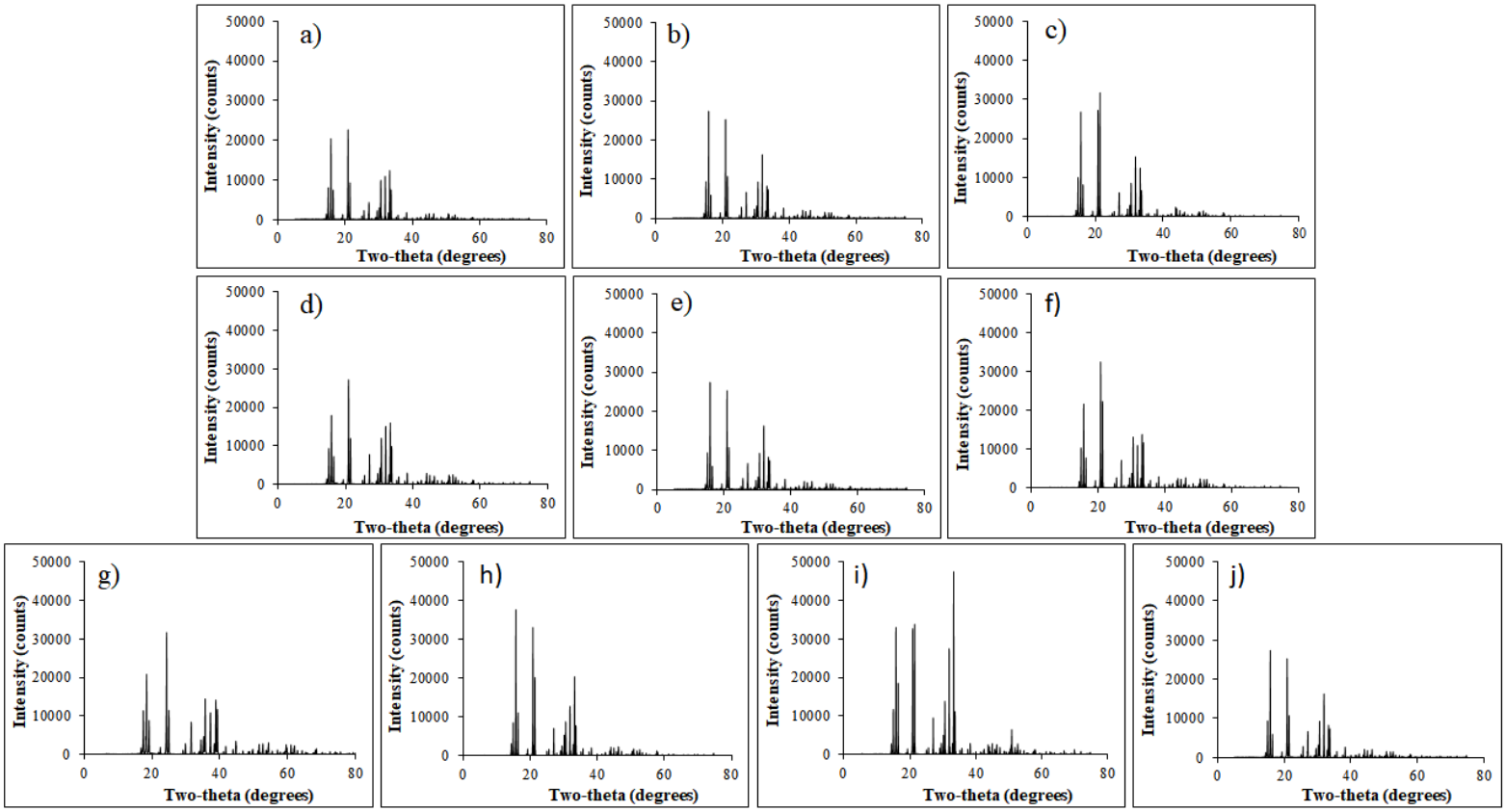

Figure 5.3 XRD diffractogram of struvite samples from varying water chemistry parameters. a) pH 7; b) pH 9; c) pH 11; d) 1:1 Mg^{2+}:PO_4^{3-}; e) 1.5:1 Mg^{2+}:PO_4^{3-}; f) 2:1 Mg^{2+}:PO_4^{3-}; g) 0.1 mM·min^{-1} $MgCl_2$ dosing; h) 1 mM·min^{-1} $MgCl_2$ dosing; i) 10 mM·min^{-1} $MgCl_2$ dosing; j) 24 mM·min^{-1} $MgCl_2$ dosing.

Initial understanding of the potential co-precipitation that occurred with struvite formed under different struvite precipitation conditions was provided by SEM-EDS analyses. Figure 5.4-5.6 shows two magnification views (250x and 1000x) for the samples collected at each condition and all samples appeared to contain two different morphologies – crystal-like structures and rounded particles. Following a 60 min reaction time, both rod-shaped crystals and irregular crystals (20-40 μm) with growth in multiple directions appeared. Growth for larger crystals (up to 3 mm) could occur given a longer reaction time, though it has been shown that increased reaction time may not increase nutrient recovery (Huang et al. 2011). As morphology is dependent on the mixing time and conditions, altering the mixing protocol would likely result in a different morphology.

At a dosing rate of 24 $mM \cdot min^{-1}$, crystal-like structure growth appeared to occur in multiple directions making it more difficult to morphologically define. The images from the $MgCl_2$ dosing rate (0.1 to 10 $mM \cdot min^{-1}$) experiments produced crystals that were more rectangular shaped and elongated indicating that a faster dosing rate, such as 24 $mM \cdot min^{-1}$ results in irregular growth. Crystal formation can also be affected by the inability for ions to access sites required for crystal growth (Le Corre et al. 2005). A crystal that cannot be easily defined morphologically due to crystal growth in multiple directions could contain some level of co-precipitation interfering with proper crystal growth. Subsequently, a slower dosing rate could be an important factor in controlling proper crystal growth.

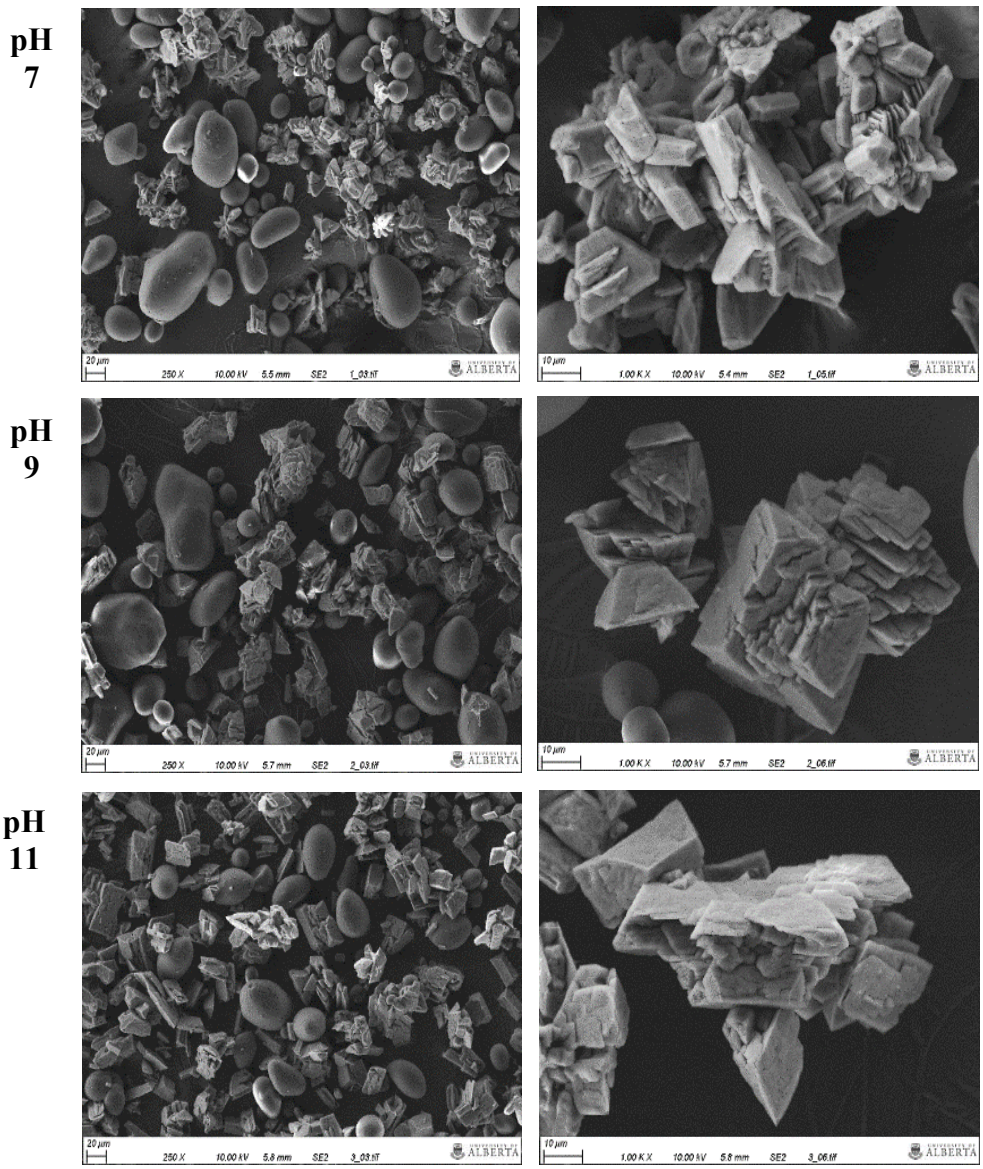

Figure 5.4 SEM images of a struvite sample from blackwater after precipitation at pH 7, 9 and 11 (left = 250x magnification, right = 1000x magnification).

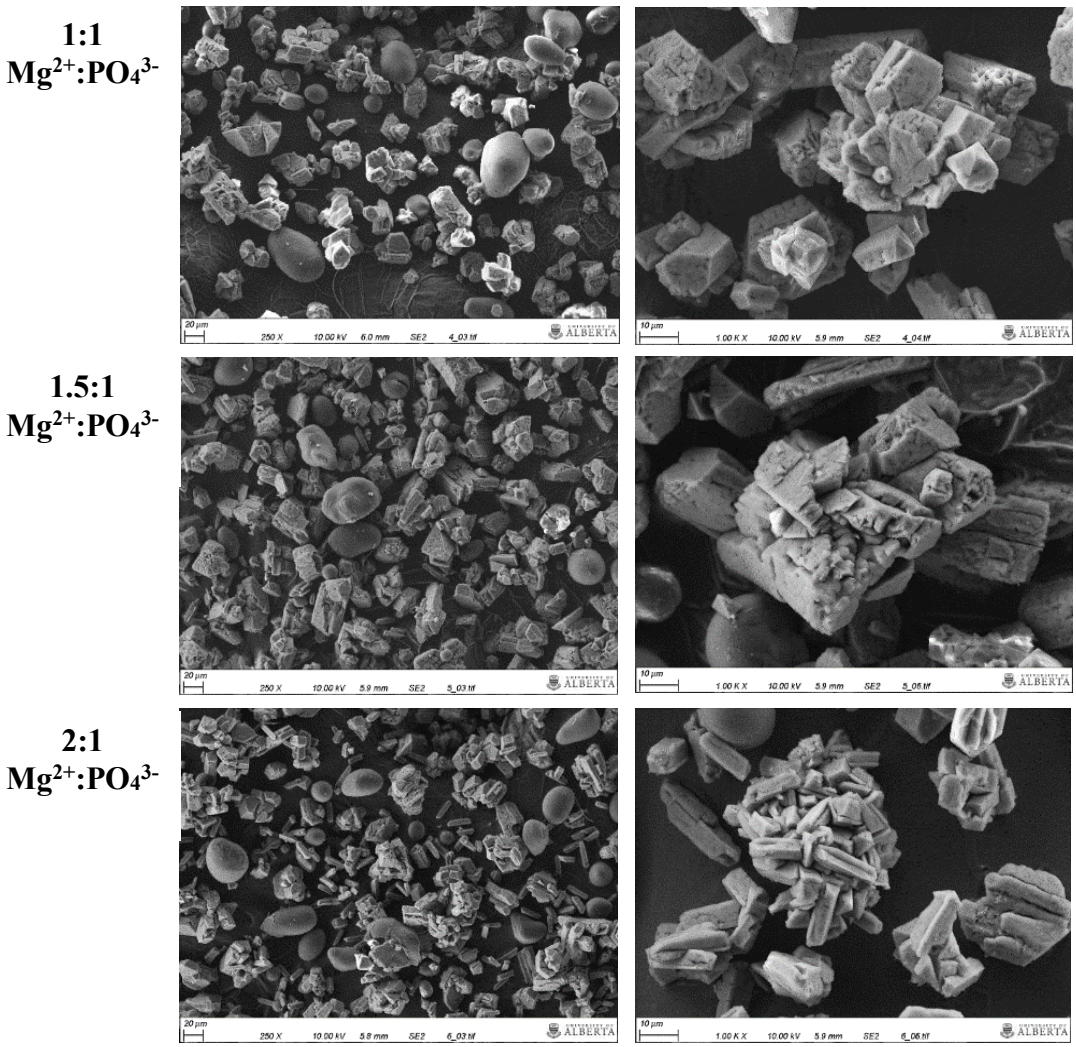

Figure 5.5 SEM images of a struvite sample from blackwater after precipitation at 1:1, 1.5:1 and 2:1 Mg^{2+}:PO_4^{3-} (left = 250x magnification, right = 1000x magnification).

0.1 mM·min^{-1} $MgCl_2$ Dosing Rate

1 mM·min^{-1} $MgCl_2$ Dosing Rate

10 mM·min^{-1} $MgCl_2$ Dosing Rate

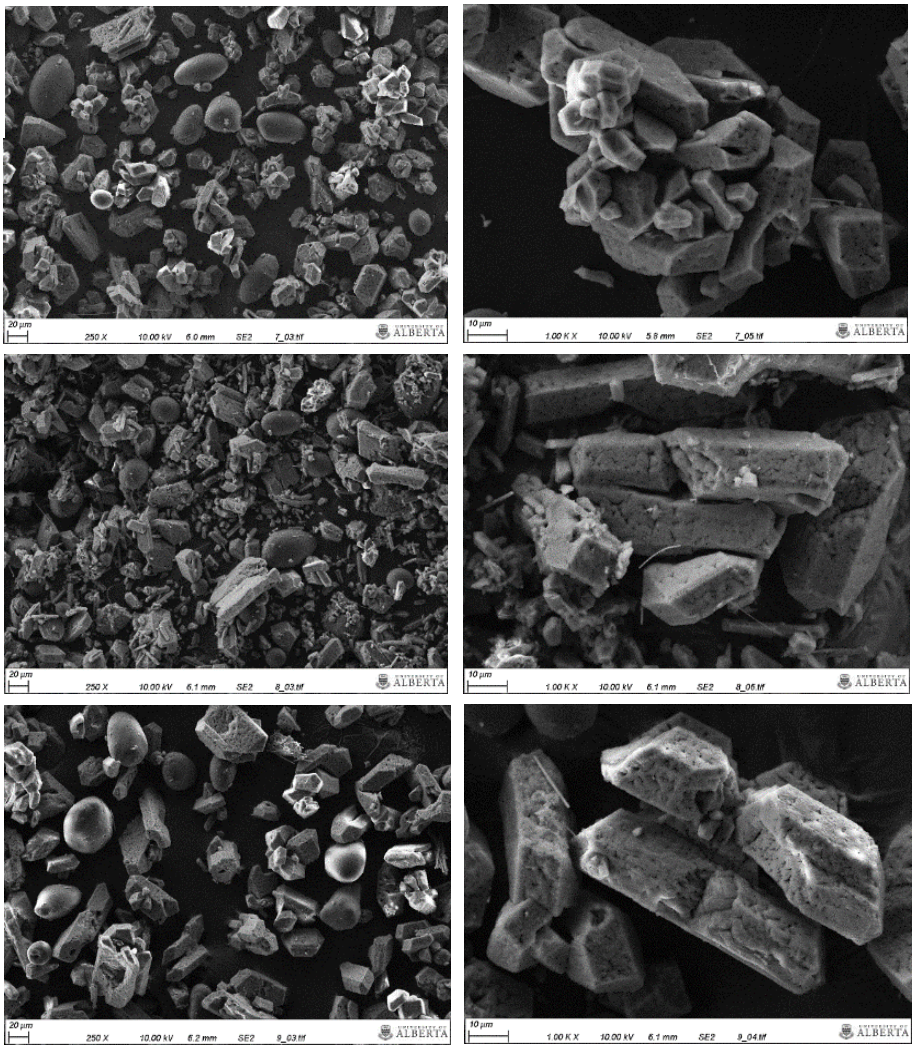

Figure 5.6 SEM images of a struvite sample from blackwater after precipitation at 0.1 mM·min^{-1}, 1 mM·min^{-1} and 10 mM·min^{-1} $MgCl_2$ (left = 250x magnification, right = 1000x magnification).

The round shaped particles, which present a non-crystal-like shape appear to be a co-precipitate that formed in parallel to struvite from the blackwater matrix. Using a qualitative approach, an estimation of the relative percentage between the crystals and the co-precipitate can be made by counting. As observed in Figure 5.7, the struvite crystals dominate in the

SEM images. As pH increased from 7 to 11 there was reduced struvite co-precipitation, while increasing the $MgCl_2$ dosing rate above 10 $mM \cdot min^{-1}$ increased co-precipitation.

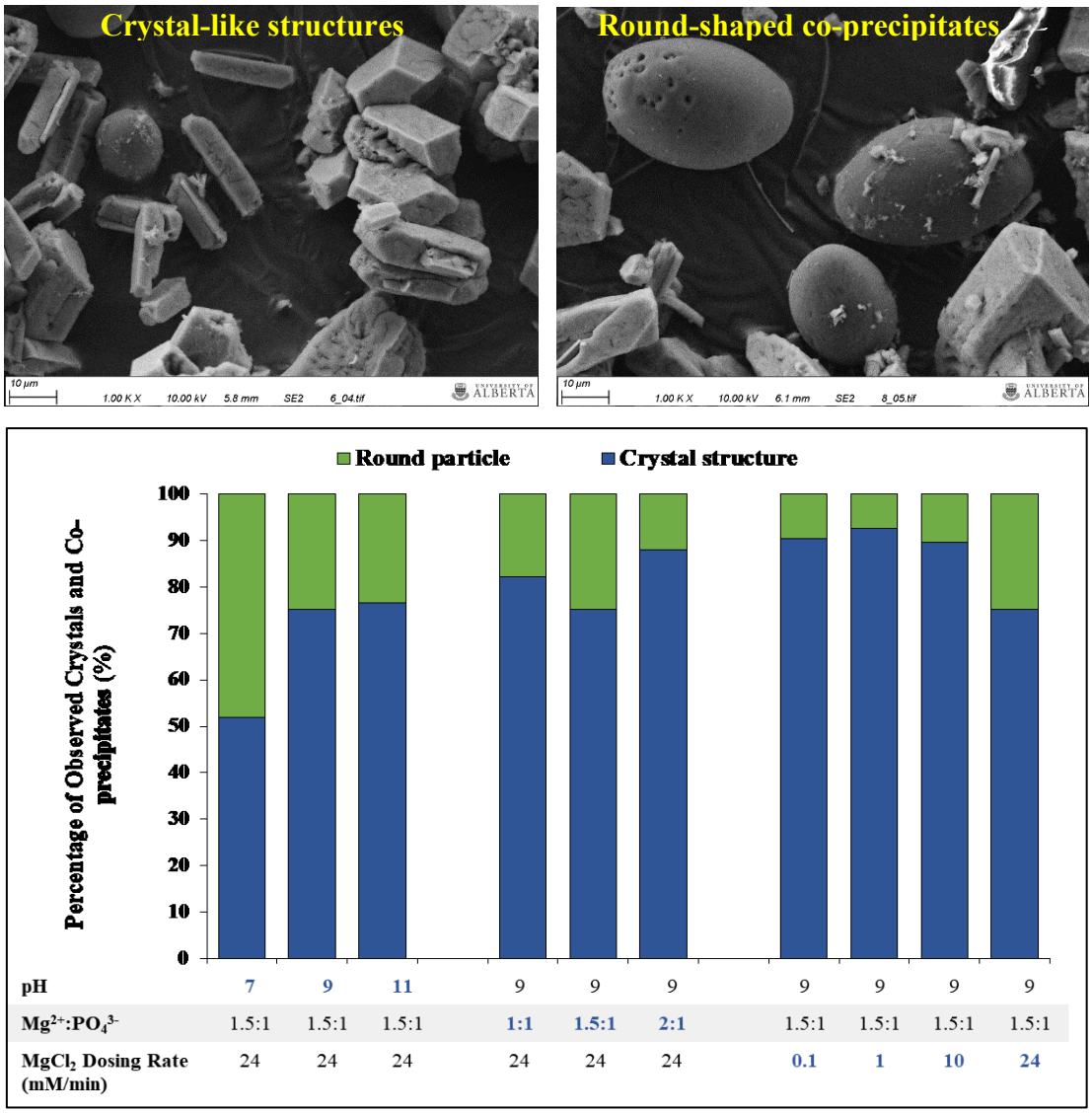

Figure 5.7 Qualitative analysis of crystal structures and round co-precipitates observed. Top images represent SEM images (1000x magnification) of crystal structures (left) and round particles (right). Bottom graph represents estimated percentage of crystals and round particles in images (N = 9 fields of view).

The EDS results further supports that the crystal-like structures are struvite crystals as the results correspond with the expected presence of Mg and P at almost a 1:1 ratio. The main elements detected were P, Mg, C, O and Ca. Detection for Na, K and Cl as potential co-precipitates were below the detection limit. Based on EDS data (Figure 5.8-5.10), it is likely the round co-precipitates are likely to be carbonate compounds, such as calcium and magnesium carbonates or calcium phosphate that simultaneously co-precipitated. In all cases, C and O dominate the composition of the surface with very low levels of Mg, P and Ca. Additionally, the relative percentages of elements appear to be similar to one another, indicating that the surface composition does not significantly differ between conditions. However, since EDS provides an analysis of the surface composition, it is not representative of all potential co-precipitation and is limited to points on the surface.

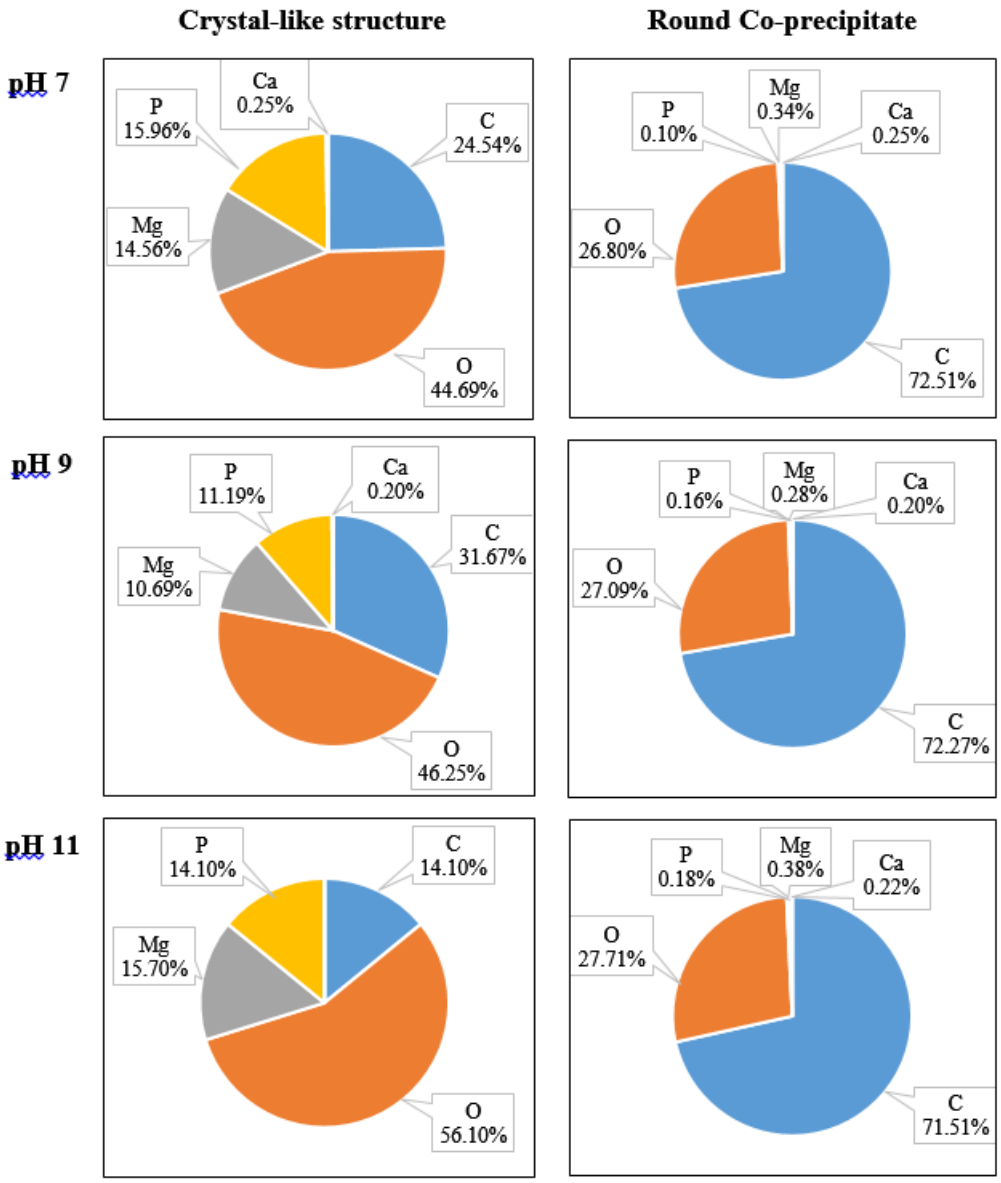

Figure 5.8 EDS analysis of crystal-like structure and round co-precipitate as observed in SEM images of samples collected from blackwater experiments at pH 7, 9 and 11. Based on point analysis.

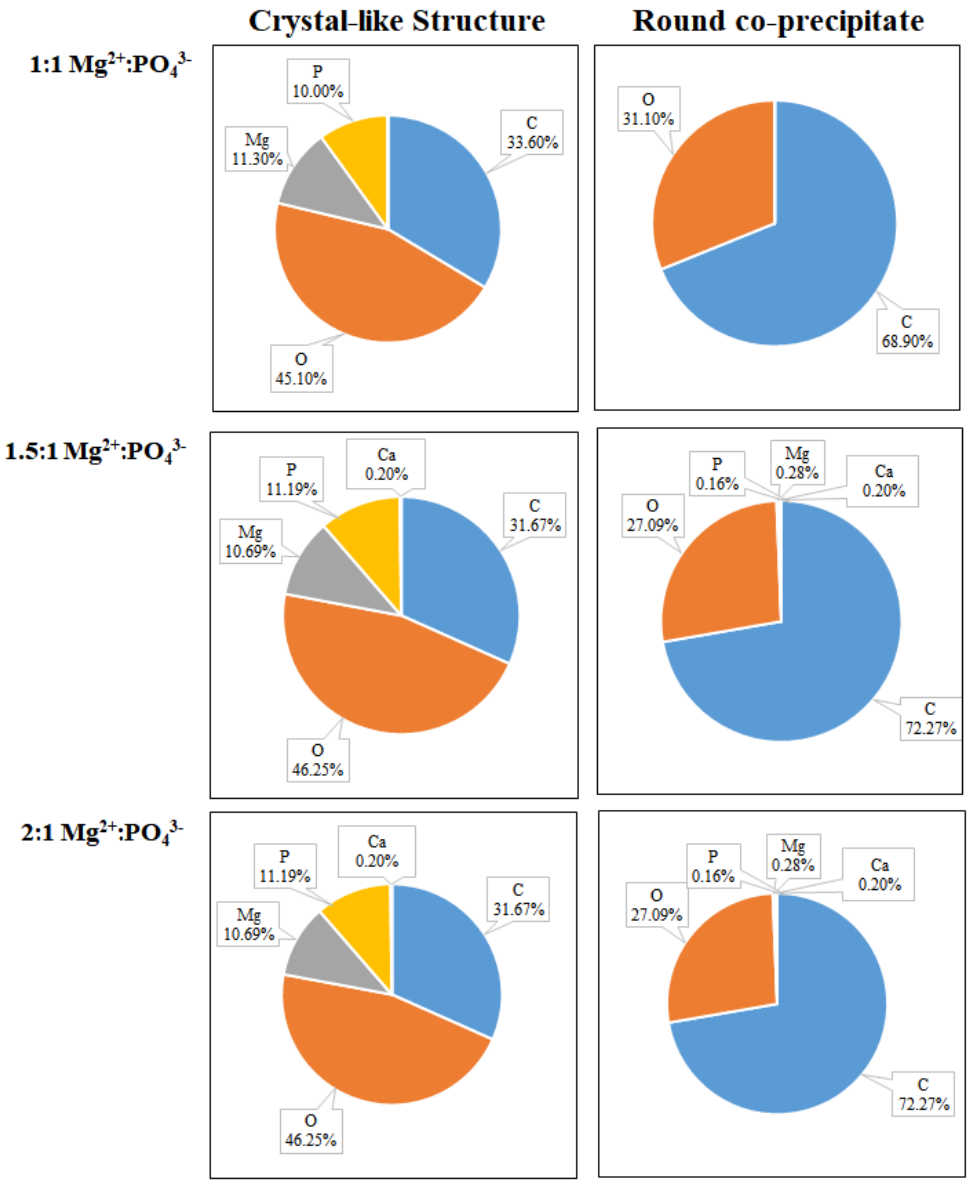

Figure 5.9 EDS analysis of crystal-like structure and round co-precipitate as observed in SEM images of samples collected from blackwater experiments at 1:1, 1.5:1 and 2:1 Mg^{2+}:PO_4^{3-} molar ratio. Based on point analysis.

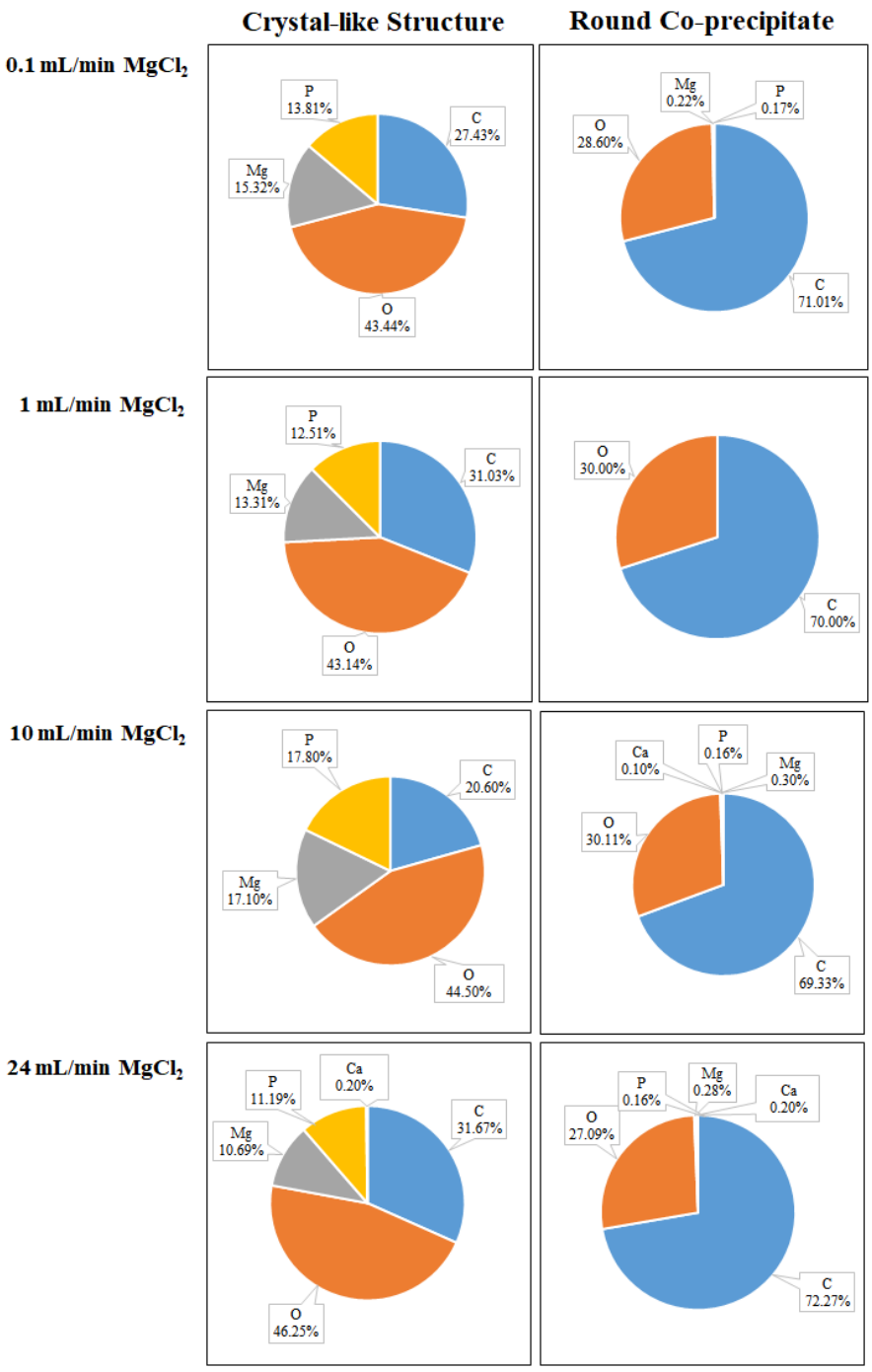

Figure 5.10 EDS analysis of crystal-like structure and round co-precipitate as observed in SEM images of samples collected from blackwater experiments at $MgCl_2$ dosing rate ($mM \cdot min^{-1}$) 0.1, 1, 10 and 24 mL/min. Based on point analysis.

5.4.2 Phosphorus Recovery and Co-preciptiates

Comparison of PO_4^{3-}-P recovery between experimental set A and B shows that the bacteria concentration does not play a large effect on PO_4^{3-}-P recovery (Figure 5.11-5.12). Increasing the pH of the synthetic wastewater results in an upward trend of PO_4^{3-}-P recovery. In experimental set A, PO_4^{3-}-P recovery greater than 71 % was achieved under pH 9 and 11 ($p < 0.05$), while recovery over 83 % was achived in experimental set B ($p < 0.05$). Irregardless of the actual value, the results show that a pH of 9 or over will increase PO_4^{3-}-P recovery. Similar results have been reported for other waste streams with struvite predominately forming when the pH is above 9 (Mehta and Batstone 2013; Tang 2016; Shih et al. 2017).

The effect of limited Mg^{2+} ions is seen in the manipulation of the Mg^{2+}:PO_4^{3-} molar ratio from 1:1 to 2:1 where more Mg^{2+} present increases PO_4^{3-}-P recovery from 48 % to 67 % for experimental set A ($p < 0.05$), and 46 % to 69 % in experimental set B ($p < 0.05$). These results are also consistent with previous studies on other waste streams, which have shown that exceeding a 1:1 molar ratio is beneficial to improve recovery, but exceeding that, such as a 2:1 molar ratio did not grealy improve PO_4^{3-}-P recovery relation to ammonia and COD removal (Kim et al. 2017).

Lastly, recovery when the $MgCl_2$ dosing rate was altered from 0.1 – 24 $mM \cdot min^{-1}$, the recovery efficiency was not significant ($p > 0.05$). Though the p-values do not demonstrate significance, likely due to limited replicates, Figure 5.12 shows that a dosing rate of 24 mL/min could increase recovery in comparison to a slower dosing rate. This is likely due to the rapid preciptaiton that occurs. It appears that a pH of 9 with a 1.5:1 Mg^{2+}:PO_4^{3-} molar ratio is the most effective for recovery. Struvite kinetics, such as pH and Mg^{2+} will control struvite formation and thus play a role in co-precipitation (Le Corre et al. 2007b).

As the synthetic wastewater represents a complex wastewater feed, it is expected that the recovered struvite will contain impurities that co-precipitate. Chemical analysis as described above provides some evidence that co-preciptiation occurs, but it is not clear the extent the conditions play on the co-precipitation level. Based on experimental values, the theortical

amount of struvite in the collected samples were calculated and used to determine the co-precipitation of other PO_4^{3-}-P salts. The results of experimental set A (Figure 5.11) at all tested conditions show that there is not a significant difference observed ($p > 0.05$), however, the significance could be altered given more experiments were performed to decrease the error.

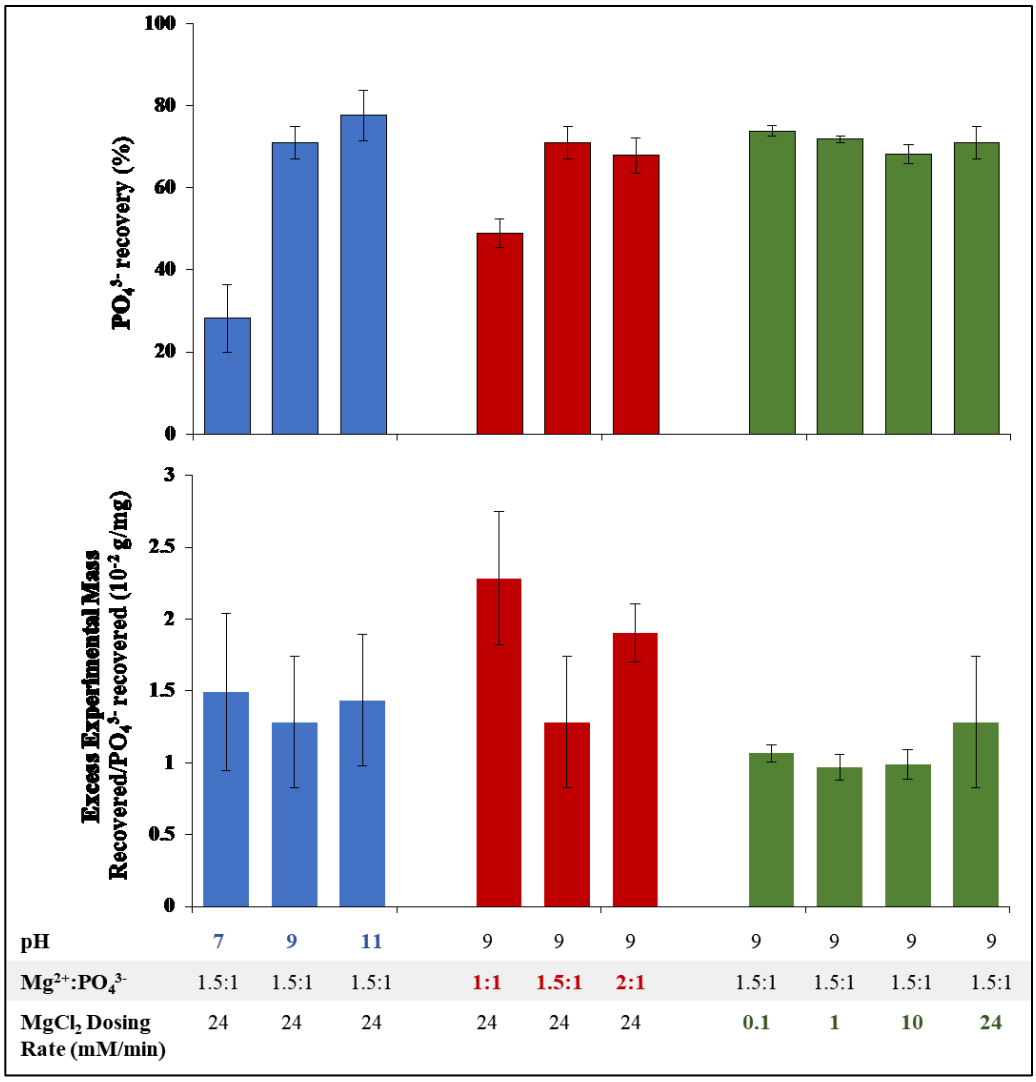

Figure 5.11 PO_4^{3-} recovery (%) and excess experimental mass recovered per PO_4^{3-} recovered (10^{-2} g/mg) of tested conditions from experimental set A from blackwater (N = 3, error bars indicate standard deviation).

The co-precipitation calculated from experimental set B (Figure 5.12) provides differing results from experimental set A as a difference can be observed. As shown in Figure 5.12, the trend of the excess mass collected per gram of PO_4^{3-}-P recovered differs from expected struvite PO_4^{3-}-P recovery. At pH 7, a lower percentage of PO_4^{3-}-P recovery occurred compared to higher pH conditions , hence a large amount of the mass collected cannot be attributed to struvite. A low Mg^{2+}:PO_4^{3-} molar ratio of 1:1 presents a higher excess mass recovered per PO_4^{3-}-P removed, also with a low PO_4^{3-}-P recovery percentage. This is no surprise, as a lower availability of Mg^{2+} would allow for other ions, such as Ca^{2+} that is a competitor of Mg^{2+} in the formation of phosphate preciptiates (Le Corre et al. 2005). The metal analysis, as discussed below, is also consisten with the low excess mass observed when the molar ratio exceeded 1:1 ($p < 0.05$). Further, a higher dosing rate may result in increased co-precipitation as a more rapid addition of Mg^{2+} into the system may induce rapid struvite preciptiation that would entrap ions and microbes during crystal formation (Le Corre et al. 2007b). On the other hand, high dosing rates can also enhance the rate of PO_4^{3-}-P recovery with no significant difference in excess mass ($p > 0.05$). Figure 5.12 shows that under the highest dosing rate condition tested with a pH of 9 and a 1.5:1 Mg^{2+}:PO_4^{3-} molar ratio, high PO_4^{3-}-P recovery and relatively low co-precipitation was observed, so representing the optimal condition tested in the current study.

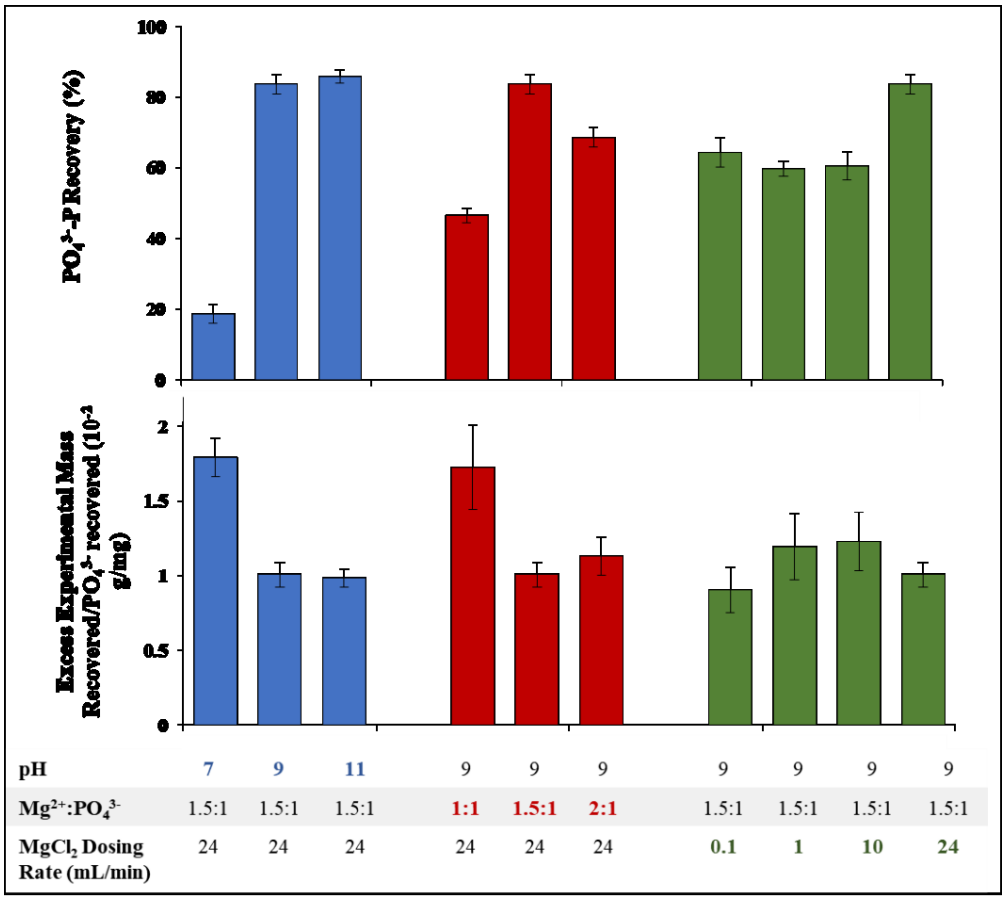

Figure 5.12 PO_4^{3-} recovery (%) and excess experimental mass recovered per PO_4^{3-} recovered (10^{-2} g/mg) of tested conditions from experimental set B from blackwater (N = 3, error bars indicate standard deviation).

It should also be noted that ammonium concentrations before and after struvite precipitation were also measured, but the data is not shown as the results do not present any notable trends. This is most likely due to the open system of the batch experiments. The high pH likely forced remaining NH_4^+ to form NH_3, thus becoming a gas that cannot be accounted for in the system. Based on effluent concentrations, NH_4^+ is typically present in excess and therefore the shift in chemical equilibrium does not significantly impact struvite precipitation from a feed with limited residual phosphorus.

5.4.3 Metal Co-precipitation

Figure 5.13-5.14 depicts the ICP-OES analysis of the major metals that co-preciptiate with struvite at the varying conditions tested in experimental set A and B. Though there are varying levels detected, the general trend of detection at each condition between experimental set A and B remains comparable. Therefore, in addition to presenting no obvious trend in PO_4^{3-} recovery, increased concentrations of bacteria also do not appear to play a large effect on metal co-precipitation.

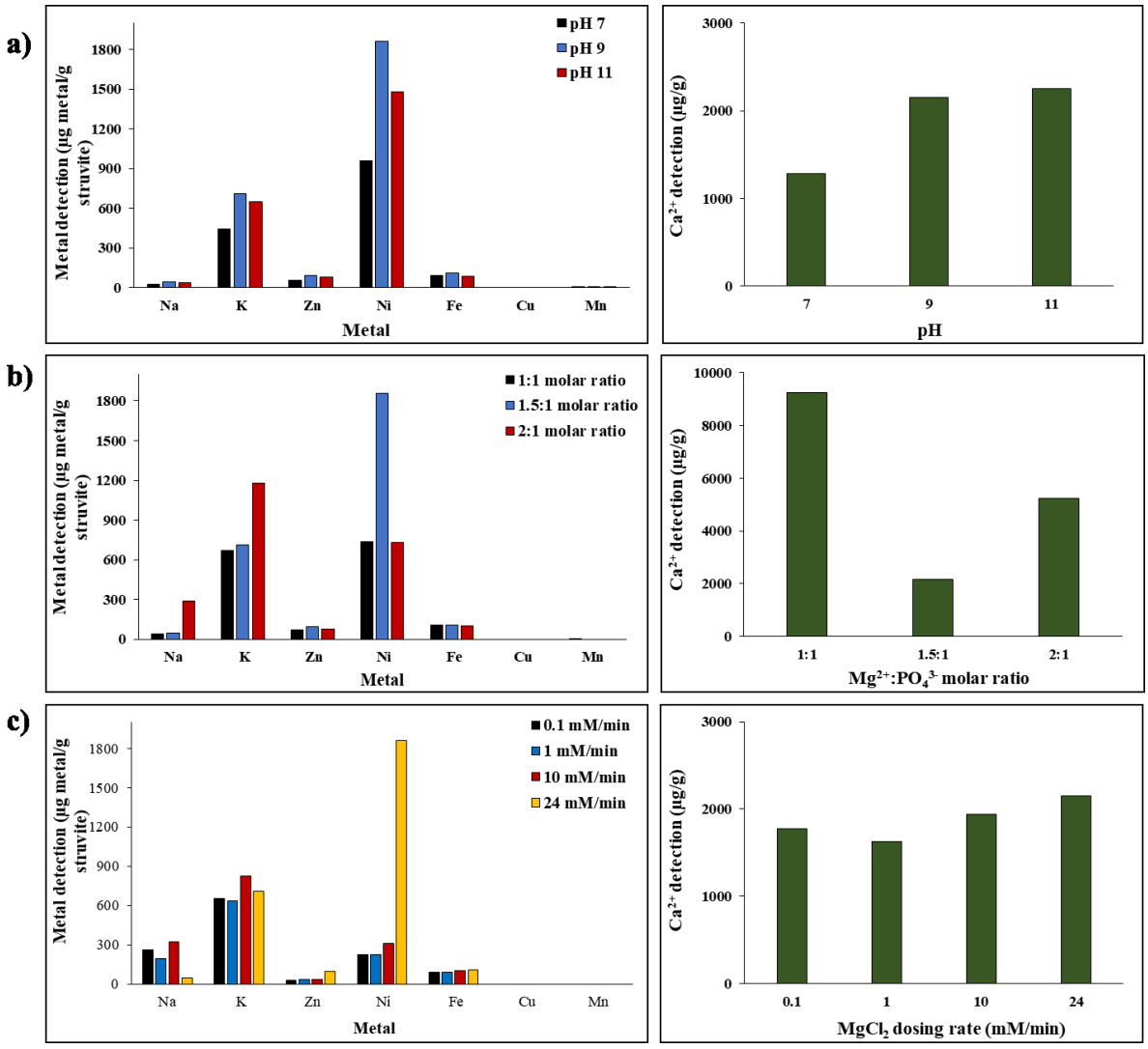

Figure 5.13 ICP-OES analysis of dominant metal co-precipitates in struvite samples of tested conditions in experimental set A from blackwater (N = 3).

Due to the similarity in trends, only the results of experimental set B will be further discussed below. In all tested conditions, besides Mg^{2+} and P, Ca^{2+} dominated in detection, which is expected as Ca^{2+} concentrations in the synthetic wastewater recipe are higher than the other inorganic elements, and Ca^{2+} is a known competitor of Mg^{2+} in the struvite formation process (Le Corre et al. 2005). Though Ca^{2+} dominates of the metals in the mixture, the level of Ca^{2+} is dependent on the specific conditions utilized for precipitation.

In general, an increased pH and $MgCl_2$ dosing rate and a low Mg^{2+}:PO_4^{3-} molar ratio increased metal co-preciptaition. When pH levels were increased, there was a risk that other compounds could form in conjunction with struvite, according to pre-established solubility tables, thus resulting in increased metal detection. The formation of potassium struvite ($MgKPO_4 \bullet 6H_2O$) has also been linked with increased pH levels, which was also observed in the current study at or above pH 9 as more K^+ was detected. Increased levels of K^+ were also detected at a higher Mg^{2+}:PO_4^{3-} molar ratio. As supersaturation helps dictate precipitation and potassium struvite is less soluble than ammonium struvite , the increased Mg^{2+} would also drive the reaction to favour potassium struvite (Bennett et al. 2017). This would not affect PO_4^{3-} recovery as a 1:1:1 molar ratio is still required. Addtionally, higher detection of Ca^{2+} and Ni^{2+} was observed when there was less Mg^{2+} in the system as those ions can replace Mg^{2+} in the formation process (Le Corre et al. 2005).

Comparison of metal detection to calculated co-precipitation in Figure 5.12 shows that the results of the pH tests are not consistent. Based on the ICP-OES analysis, it would be expected that the greater excess mass per PO_4^{3-} recovered calculated for a pH of 7 could be due to other metal and/or organic precipitates. The later is discussed next with regard to recovered bacteria.

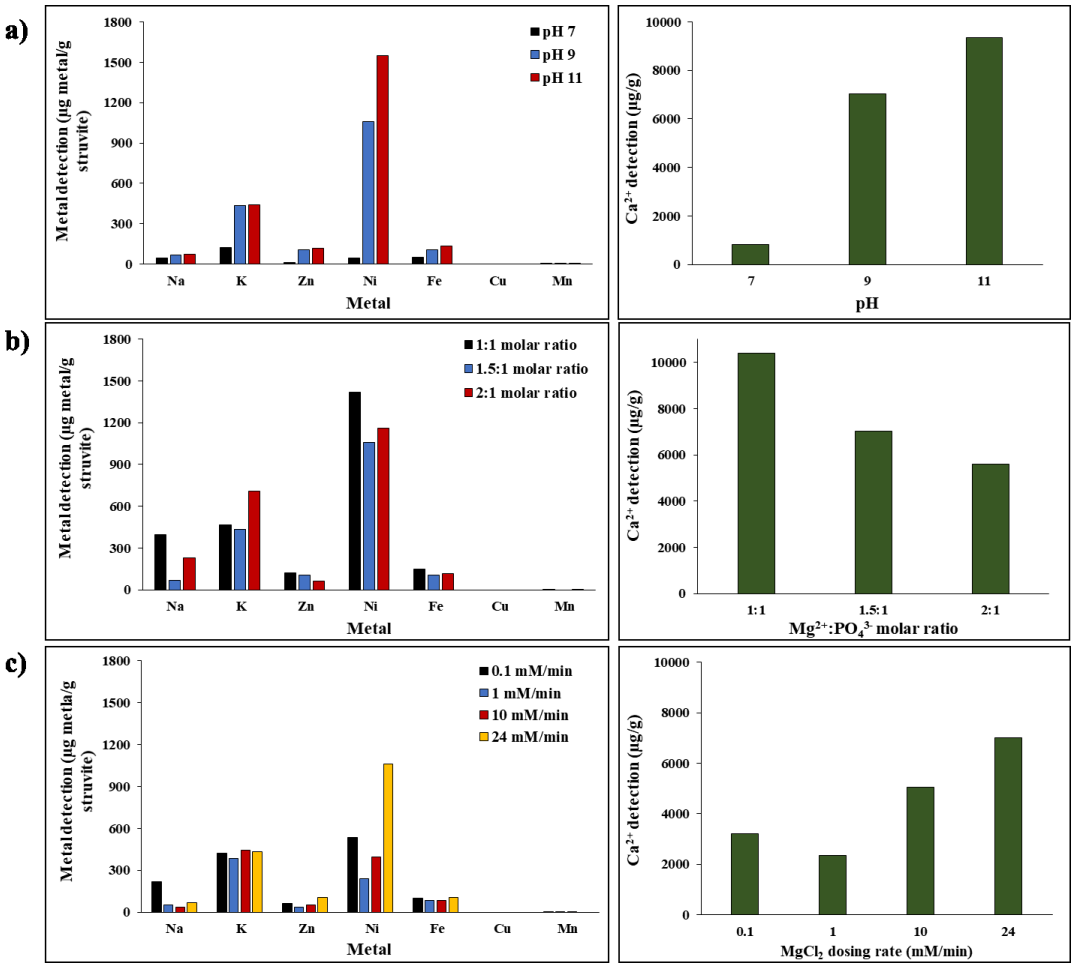

Figure 5.14 ICP-OES analysis of dominant metal co-precipitates in struvite samples of tested conditions of experimental set B from blackwater (N = 3).

5.4.4 Gene Detection and Bacterial Viability

qPCR analysis shows that all gene targets can be detected in the struvite samples of experimental set A and B (Figure 5.15-5.16). Though the experiments do not show an obvious gene precipitation trend nor can confirm gene activity, detection of the gene targets show that a potential risk, particularly with AMR could exist in wastewater recovered struvite. The similar percentages observed between the genes that identify specific bacteria and their associated ARGs supports co-precipitation of spiked strains rather than external contamination effects. The ARG targets were selected based on their likely presence in wastewater, and though the detection of these targets in struvite cannot be used to predict the potential spread of AMR, it is important to consider that co-precipitation of microbes could be a risk that is currently not evaluated, but needs to be.

In experimental set A (Figure 5.15), where a lower concentration and diversity of bacteria were spiked in, the gene detection did not appear significantly different between *uidA* (*E. coli*) and *entero1* (*Enterococcus* spp.). However, when spiking in a greater consortment and at a greater concentration as in experimental set B (Figure 5.16), *uidA* (*E. coli*) detection was observed to be greater than *entero1* (*Enterococcus* spp.) and *cpn60* (*C. perfringens*). Though two *E. coli* isolates were spiked in at equal concentrations to the other bacteria, this set of experiments showed that higher concentrations and bacterial properties may play a role in promoting their co-precipitation. The overall number of genes of *E. coli* surpassed the number of genes that represented *Enterococcus* spp. and *C. perfringens*. The results also indicated that regardless of the condition, a large percentage of bacteria will partition from the liquid to solid phase. Though the gene copies were not shown, the importance of washing and drying methods following prceciptiation to reduce the microbial risk can be emphasized.

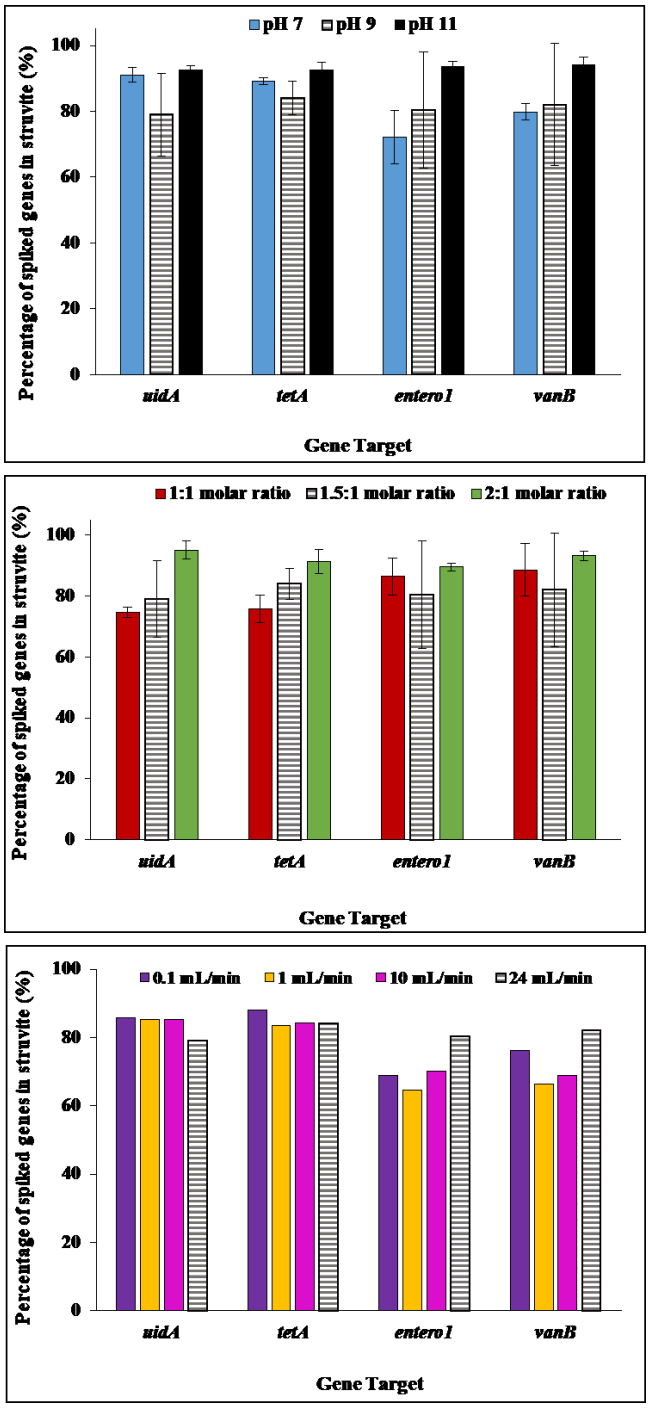

Figure 5.15 Relative percentage of spiked bacteria in struvite from experimental set A from blackwater as determined by qPCR (pH and Mg^{2+}:PO_4^{3-} (N = 2); $MgCl_2$ dosing rate (N = 1)). Error bars indicate standard deviation.

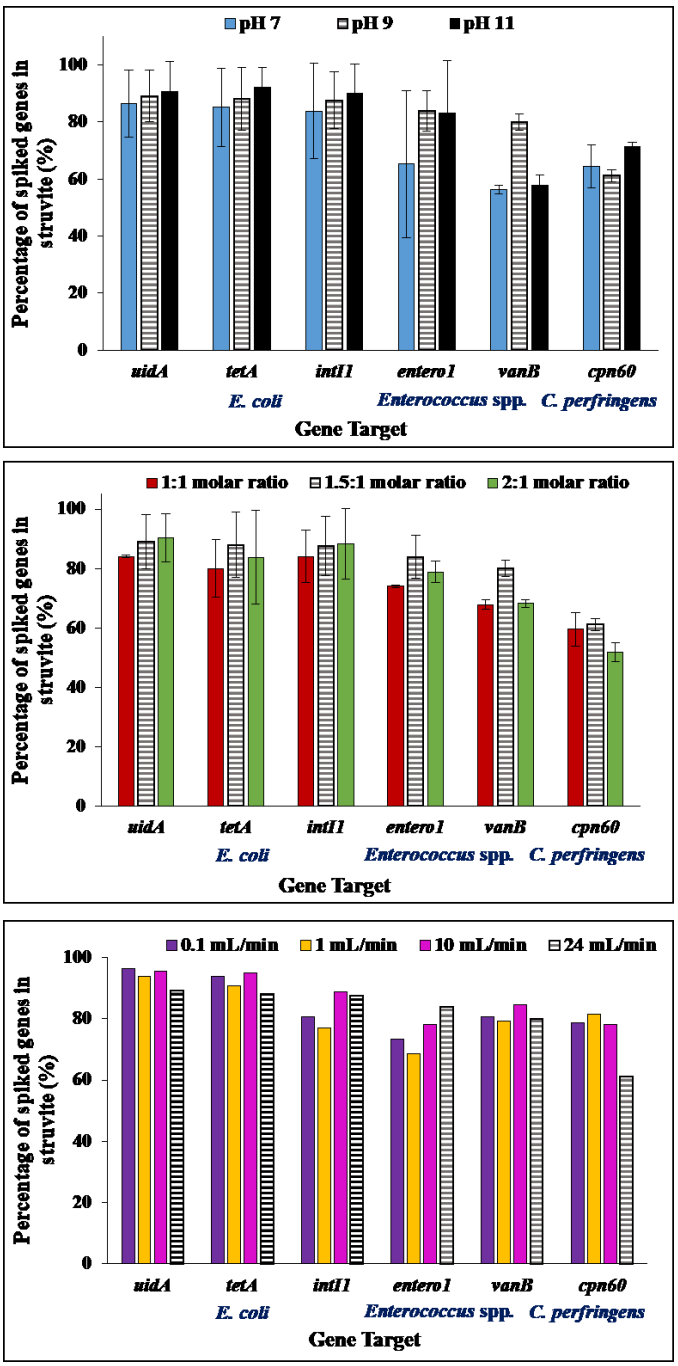

Figure 5.16 Relative percentage of spiked bacteria in struvite from experimental set B from blackwater as determined by qPCR (pH and Mg^{2+}:PO_4^{3-} (N = 2); $MgCl_2$ dosing rate (N = 1)). Error bars indicate standard deviation.

The detection of bacteria and AMR gene targets confirmed that bacterial precipitation occurs regardless of the condition. The activity and functionality of the genes and the host cell cannot be determined with qPCR. Thus, the viabilty of *E. coli*, *E. faecalis* and *C. perfringens* were assessed to determine if the spiked cells were still culturable following exposure to the water chemistry of the synthetic wastewater and the precipitation process. The viability tests were only conducted on samples collected from experimental set B. As expected, the viability of the *E. coli* cells decreased at pH 11, while *E. faecalis* and *C. perfringens* spore viability remained unchanged across all pH conditions tested (Korajkic et al. 2014). Though it would be predicted that at a pH of 9 would also reduce *E. coli* viability (Parhad and Rao 1974), the results indicated the resilence of environmental isolates over culture collection lab strains. Of the other molar ratio and dosing rate conditions tested, the fraction of viable cells did not differ ($p > 0.05$), indicating that Mg^{2+} concentration and rate of $MgCl_2$ addition appear to play a larger role in metal co-preciptiation than on cell viability. Thus, post-precipitation methods would be critical for reducing viable bacteria as the precipitation itself did not drastically affect viability.

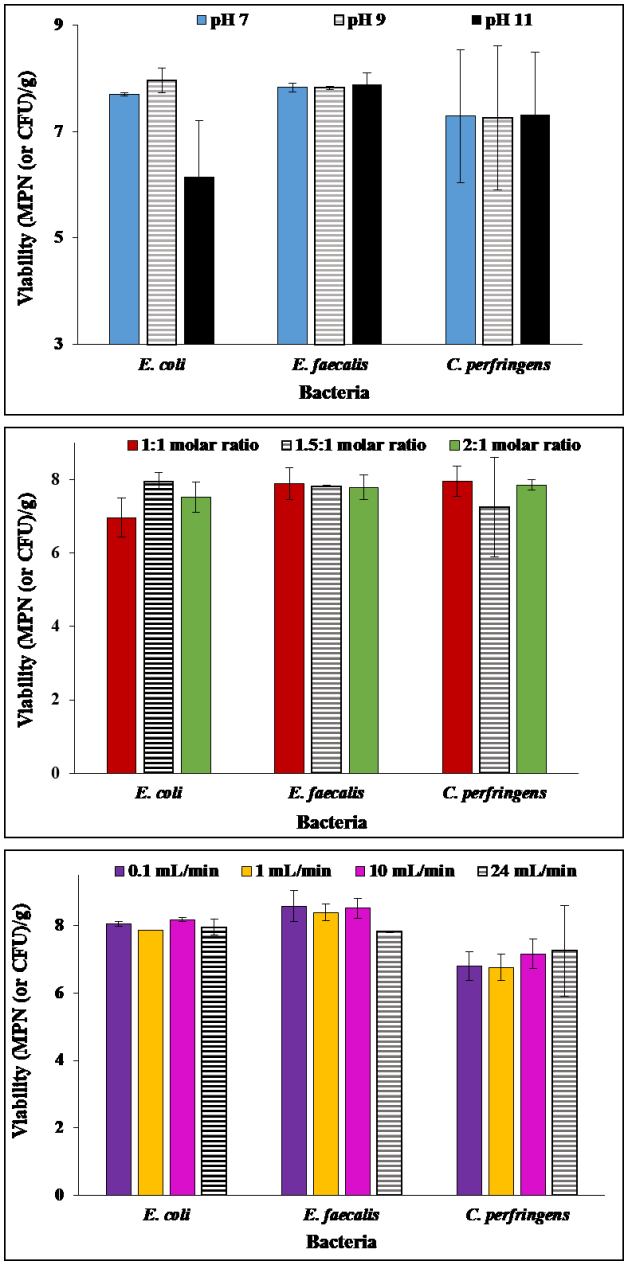

Figure 5.17 Viable cell estimates from struvite produced at varying tested conditions of experimental set B from blackwater (N = 2, error bars indicate standard deviation).

5.4.5 Characterization of Surface Properties of Spiked Bacteria

The zeta potential of pure cultures re-suspended in synthetic wastewater was measured to test the effect of pH on the surface charges of the cells. The *E. coli* and *E. faecalis* strains presented negative zeta potentials (-14 to -28 mV) when exposed to varying pH levels of synthetic wastewater (Figure 5.18). On the other hand, the *C. perfringens* isolate resulted in a positive zeta potential close to zero (0 to 3 mV). The zeta potential can be used to determine the stability of colloidal particles in a system and in this case, the potential for aggregation of bacterial cells can be predicted. Due to the low zeta potential of *C. perfringens* at all tested pH levels, it can be predicted that aggregation of the cells will occur. Co-aggregation can occur, which is dependent on the interactions between specific cell surface properties, such as composition that are not discussed in this study (Krasowska and Sigler 2014).

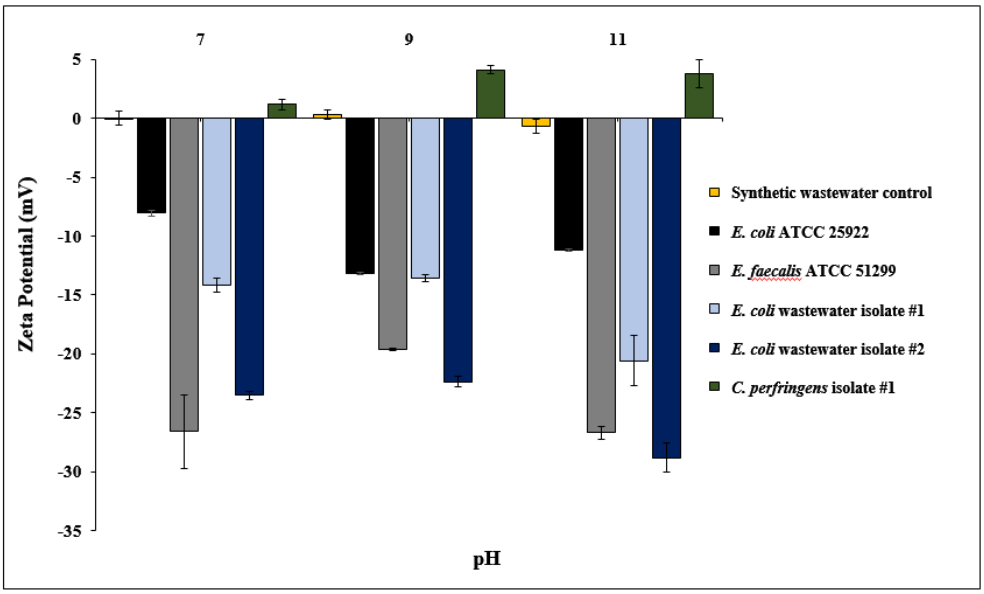

Figure 5.18 Zeta potential measurements of bacterial isolates exposed to synthetic wastewater at varying pH (7, 9, 11) levels (N = 3, error bars indicate standard deviation).

In addition to measuring the zeta potential, the hydrophobicity of the cell surface can also be characterized. Hydrophobicity results show that there was indeed a difference in the percent of cells that adhere to hexadecane following addition (Table 5.3). Though the percent values differed, the range in which the values lie resulted in the same characterization and these tests provided a qualitative assessment of the hydrophobicity. In these assays, *C. perfringens* resulted in a more hydrophobic surface than the vegetative cells of the *E. coli* and *E. faecalis* isolates used (Wiencek et al. 1990). The hydrophilic nature of *C. perfringens* and the ability of its cells to aggregate could indicate that they would be more likely to interact with molecules during the precipitation process. Further studies into the effect of microbe surface properties would help further explain their co-precipitation with struvite. Ultimately, post precipitation treatment processes, such as drying will be essential in reducing the viability of pathogens of potential concern.

Table 5.3 Hydrophobicity measurement of bacterial isolates using absorbance and culture method (N = 3).

Bacterial isolate	Method	% Partitioning	Hydrophobicity characterization
***E. coli* ATCC 25922**	Absorbance	10.1	Low
	Culture	7.08	Low
***E. coli* wastewater isolate #1**	Absorbance	0.89	Low
	Culture	32.6	Low
***E. coli* wastewater isolate #2**	Absorbance	2.17	Low
	Culture	29.7	Low
***E. faecalis* ATCC 51299**	Absorbance	7.80	Low
	Culture	12.0	Low
***C. perfringens* isolate #1**	Absorbance	52.9	Moderate
	Culture	46.2	Moderate

Though the microbial detection does not present an obvious trend, characterization of the cell surface through zeta potential and hydrophobicity measurements can allow for an initial understanding of the microbial interactions in co-precipitation. The hydrophobic nature of *C. perfringens* and its preference for cell aggregation could indicate that they would be less

likely to interact with struvite. Further studies into the effect of microbial surface properties would help further explain their co-precipitation with struvite.

5.5 Conclusion

Given the results presented, it is clear that a degree of metal and microorganism co-precipitation is likely to occur when recovering phosphate and ammonium nutrients by struvite precipitation. The degree of co-precipitation does not correlate to the phosphorus recovery efficiency, and is highly dependent on the nature of the feed and precipitation conditions, as interactions between matrix ions and microbes will dictate the precipitation process. In summary, the optimal conditions demonstrated for enhanced PO_4^{3-}-P recovery with minimized co-precipitation from blackwater are a pH of 9, 1.5:1 Mg^{2+}:PO_4^{3-} molar ratio and a 24 $mM \cdot min^{-1}$ $MgCl_2$ dosing rate. Metal co-precipitation appeared inevitably under all conditions and the presence of some micro- and macro-nutrients could be beneficial for agriculture. Optimization options have yet to be examined to reduce the microbial issues that exist following the precipitation process, but could include struvite heat-drying.

5.6 Acknowledgements

The work was financially supported by Natural Sciences and Engineering Research Council – Collaborative Research and Development (NSERC-CRD) and EPCOR Drainage Services. The authors wish to thank Candis Scott and Nancy Price (School of Public Health, University of Alberta) for molecular/microbiological training and technical support as well as Johnathon Shim (Department of Civil and Environmental Engineering, University of Alberta) for lab assistance.

5.7 References

Alp Ö, Yazgan B, Söhmen U, Gulyas H, Otterpohl R. 2008. Recovery of phosphorus as struvite from source-separated blackwater.

Bennett AM, Lobanov S, Koch FA, Mavinic DS. 2017. Improving potassium recovery with new solubility product values for K-struvite. J. Environ. Eng. Sci. 12:93–103.

Chen Q, An X, Zhu Y, Su J, Gillings MR, Ye Z. 2017. Application of struvite alters the antibiotic resistome in soil, rhizosphere, and phyllosphere. Environ. Sci. Technol. 51:8149–8157.

Davies CM, Long, JAH, Donald, M, Ashbolt, NJ. 1995. Survival of fecal microorganisms in marine and freshwater sediments. Appl. Environ. Microbiol. 61: 1888-1896.

Deer DM, Lampel KA, González-Escalona N. 2010. A versatile internal control for use as DNA in real-time PCR and as RNA in real-time reverse transcription PCR assays. Lett. Appl. Microbiol. 50:366–372.

de Graaff MS, Temmink H, Zeeman G, Buisman CJN. 2011. Energy and phosphorus recovery from black water. Water Sci. Technol. 63:2759–2765.

Gao M, Zhang L, Florentino AP, Liu Y. Anaerobic treatment of blackwater collected from different toliet flushing systems: can we achieve both energy recovery and water conservation? In progres.

Gell K, Ruijter FJ d., Kuntke P, Graaff M De, Smit AL. 2011. Safety and effectiveness of struvite from black water and urine as a phosphorus fertilizer. J. Agric. Sci. 3:67–80.

Guo J, Li J, Chen H, Bond PL, Yuan Z. 2017. Metagenomic analysis reveals wastewater treatment plants as hotspots of antibiotic resistance genes and mobile genetic elements. Water Res. 123:468–478.

Huang HM, Song QW, Xu CL. 2011. The mechanism and influence factors of struvite precipitation for the removal of ammonium nitrogen. Adv. Mater. Res. 189–193:2613–2620.

Jian Z, Hejing W. 2003. The physical meanings of 5 basic parameters for an x-ray diffraction peak and their application. Chinese J. Geochemistry 22:38–44.

Kim D, Min KJ, Lee K, Yu MS, Park KY. 2017. Effects of pH, molar ratios and pre-treatment on phosphorus recovery through struvite crystallization from effluent of anaerobically digested swine wastewater. Environ. Eng. Res. 22:12–18.

Korajkic A, McMinn BR, Shanks OC, Sivaganesan M, Fout GS, Ashbolt NJ. 2014. Biotic interactions and sunlight affect persistence of fecal indicator bacteria and microbial source tracking genetic markers in the upper Mississippi river. Appl. Environ. Microbiol. 80:3952–3961.

Krasowska A, Sigler K. 2014. How microorganisms use hydrophobicity and what does this mean for human needs? Front. Cell. Infect. Microbiol. 4:1–7.

Le Corre KS, Valsami-jones E, Hobbs P, Parsons SA. 2005. Impact of calcium on struvite

crystal size, shape and purity. J. Cryst. Growth 283:514–522.

Le Corre KS, Valsami-Jones E, Hobbs P, Parsons SA. 2007a. Impact of reactor operation on success of struvite precipitation from synthetic liquors. Environ. Technol. 28:1245–56.

Le Corre KS, Valsami-Jones E, Hobbs P, Parsons SA. 2007b. Kinetics of struvite precipitation: effect of the magnesium dose on induction times and precipitation rates. Environ. Technol. 28:1317–1324.

Le Corre KS, Valsami-Jones E, Hobbs P, Parsons SA. 2009. Phosphorus recovery from wastewater by struvite crystallization: a review. Crit. Rev. Environ. Sci. Technol. 39:433–477.

Li Z, Ren X, Zuo J, Liu Y, Duan E, Yang J, Chen P, Wang Y. 2012. Struvite precipitation for ammonia nitrogen removal in 7-aminocephalosporanic acid wastewater. Molecules 17:2126–2139.

Mamais D, Pitt PA, Cheng YW, Loiacono J, Jenkins D, Wen Y. 1994. Digesters determination to control in anaerobic of ferric chloride precipitation digesters dose struvite sludge. Water Environ. Res. 66:912–918.

Mayer BK, Baker LA, Boyer TH, Drechsel P, Gifford M, Hanjra MA, Parameswaran P, Stoltzfus J, Westerhoff P, Rittmann BE. 2016. Total value of phosphorus recovery. Environ. Sci. Technol. 50:6606–6620.

Mehta CM, Batstone DJ. 2013. Nucleation and growth kinetics of struvite crystallization. Water Res. 47:2890–2900.

Nagajyoti PC, Lee KD, Sreekanth TVM. 2010. Heavy metals, occurrence and toxicity for plants: A review. Environ. Chem. Lett. 8:199–216.

Parhad NM, Rao NU. 1974. Effect of pH on survival of Escherichia coli. Water Environ. Fed. 46:980–986.

Parsons SA, Doyle JD. 2002. Struvite scale formation and control. Water Sci. Technol. 49:177–182.

Qiao G, Li H, Xu D-H, Il Park S. 2012. Modified a colony forming unit microbial adherence to hydrocarbons assay and evaluated cell surface hydrophobicity and biofilm production of Vibrio scophthalmi. J. Bacteriol. Parasitol. 3:1–6.

De Sanctis M, Del Moro G, Chimienti S, Ritelli P, Levantesi C, Di Iaconi C. 2017. Removal of pollutants and pathogens by a simplified treatment scheme for municipal wastewater reuse in agriculture. Sci. Total Environ. 580:17–25.

Seib MD, Berg KJ, Zitomer DH. 2016. Reduced energy demand for municipal wastewater recovery using an anaerobic floating filter membrane bioreactor. Environ. Sci. Water Res. Technol. 2:290–297.

Shih Y-J, Abarca RRM, de Luna MDG, Huang Y-H, Lu M-C. 2017. Recovery of phosphorus from synthetic wastewaters by struvite crystallization in a fluidized-bed reactor: Effects of pH, phosphate concentration and coexisting ions. Chemosphere

173:466–473.

Standard Methods Committee. 1997. Method 5220: Chemical oxygen demand (COD).

Tang P. 2016. Effects of solution pH and seed material on MAP crystallization. Int. J. Environ. Prot. Policy 4:171–177.

US. EPA. 2007. Method 3051A - Microwave assisted acid digestion of sediments, sludges, soils and oils.

Wang J, Burken JG, Zhang X, Surampalli R. 2005. Engineered struvite precipitation: impacts of component-ion molar ratios and pH. J. Environ. Eng. 131:1433–1440.

WHO. 2016. Global priority list of antibiotic-resistant bacteria to guide research, discovery, and development of new antibiotics.

Wiencek KM, Klapes NA, Foegeding PM. 1990. Hydrophobicity of Bacillus an Clostridium spores. Appl. Environ. Microbiology 56:2600-2605.

Yee R., Leifels M, Scott C, Ashbolt N., Liu Y. 2018. Evaluating microbial and chemical hazards in commercial struvite recovered from wastewater. In progres.

Chapter 6 - Overall Conclusions and Direction for Future Work

6.1 Overall Conclusions

The major focus of this work was to determine if co-precipitation should be a concern in struvite recovered from blackwater. Though struvite precipitation from wastewater is not a new process, Chapter 4 highlighted the potential risks that exist within struvite products that are produced from pilot and full scale plants for commercial use. Viable and detected FIB were demonstrated as well as human enteric viruses, with some potential infectivity. Detected ARGs indicate that AMR could be a concern downstream and that HGT should be considered as a mechanism of spread. Additionally, metal detection shows the impurity associated with recovered struvite products, but as they were within appropriate limits, their presence could be beneficial for agriculture. From the first part of the study, it is concluded that there is a potential public health risk with both biological and chemical contaminants, but quantification of the risk was not undertaken in this study.

With knowledge that biological and chemical wastewater components can co-precipitate with struvite, the focus of the second part of this study was to demonstrate that there are optimal conditions that can address enhanced phosphorus recovery and reduced co-precipitation. Although synthetic blackwater was used as the feed source, Chapter 5 shows that there are certain conditions and factors that will affect the physical and chemical nature of collected struvite. With the results of the batch experiments, it was determined that the conditions that best support enhanced PO_4^{3-} recovery along with reduced co-precipitation from blackwater are pH of 9, Mg^{2+}:PO_4^{3-} molar ratio of 1.5:1 and $MgCl_2$ dosing rate of 24 mL/min. Metal co-precipitation played a role in accounting for co-precipitation, with Ca^{2+}, Ni^{2+} and K^{+} dominating detection, and demonstrating that there is a competition between ions in the precipitation process. Along with this data, the microbial analysis showed that spiked bacterial cells remained viable through the precipitation process with a high detection of ARGs. The risk behind these results can only be clarified through additional tests, but based on literature, residual microbial co-precipitates can be problematic.

6.2 Future Work

This work focused solely on bacteria, select ARGs and some metals. Viruses were also briefly examined in Chapter 4. However, to further understand the role of biological and chemical hazards in recovered struvite, the evaluation of other hazards not assessed in this project could provide a more holistic look at the risk involved. These hazards would include personal care products, other pharmaceuticals, heavy metals and other microbial pathogens. Additionally, the FIB and micro- and macronutrients tested are only indicative of the risks as micro- and macronutrients are not toxic and FIB are not pathogenic, thus the need to assess other hazards.

The co-precipitation of bacteria (*E. coli*, *E. faecalis* and *C. perfringens*) and some metals examined in Chapter 5 show that the precipitation process does not effectively eliminate the presence of hazards. Therefore, it is imperative that the post-processing methods, such as drying and storage are assessed to determine the potential risk reduction. It is likely that methods such as drying and storage will be important in reducing the viability of microbes. Additionally, with this information, a quantitative microbial risk assessment (QMRA) could be undertaken to model the risk at each step of the process. Further downstream studies will also be important for a QMRA as the effects of applying recovered struvite to crops that will be consumed can be evaluated. Previous studies have shown that struvite can spread ARGs, but as limited data exists, the environmental and public health risk is largely unknown. The role of HGT within WWTPs as well as within soils would assist in understanding if there is a concern with the ARGs that will likely be present in the recovered product.

Furthermore, as the experiments were conducted in a batch system, they are not completely reflective of a reactor or pilot scale system. A reactor operated with real anaerobically digested blackwater would be useful to determine if similar optimization would be observed at a larger scale and with a more complex feed.

Evaluation of solubility product values for each struvite sample collected at varying water chemistry conditions could also be conducted. This could help strengthen the optimization conditions to form a struvite product that acts as a slow release fertilizer.

References

Ajonina C, Buzie C, Rubiandini RH, Otterpohl R. 2015. Microbial pathogens in wastewater treatment plants (WWTP) in Hamburg. J. Toxicol. Environ. Health 78:381–387.

Al-hamzah AA, Smith EJ, Fellows CM. 2015. Inhibition of homogeneous formation of magnesium hydroxide by low-molar-mass poly(acrylic acid) with different end-groups. Ind. Eng. Chem. Res. 54:2201–2207.

Alp Ö, Yazgan B, Söhmen U, Gulyas H, Otterpohl R. 2008. Recovery of phosphorus as struvite from source-separated blackwater.

Bambic DG, Kildare-Hann BJ, Rajal VB, Sturm BSM, Minton CB, Schriewer A, Wuertz S. 2015. Spatial and hydrologic variation of Bacteroidales, adenovirus and enterovirus in a semi-arid, wastewater effluent-impacted watershed. Water Res. 75:83–94.

Batstone DJ, Hülsen T, Mehta CM, Keller J. 2015. Platforms for energy and nutrient recovery from domestic wastewater: A review. Chemosphere 140:2–11.

Bajaj P, Singh NS, Virdi JS. 2016. Escherichia coli β-lactamases: what really matters. Front. Microbiol. 7:1–14.

Baquero F, Martínez JL, Cantón R. 2008. Antibiotics and antibiotic resistance in water environments. Curr. Opin. Biotechnol. 19:260–265.

Başakçılardan-Kabakcı S, Thompson A, Cartmell E, Le Corre K. 2007. Adsorption and precipitation of tetracycline with struvite. Water Environ. Res. 79:2551–2556.

Bender JK, Kalmbach A, Fleige C, Klare I, Fuchs S, Werner G. 2016. Population structure and acquisition of the vanB resistance determinant in German clinical isolates of Enterococcus faecium ST192. Sci. Rep. 6:1–13.

Bennett AM, Lobanov S, Koch FA, Mavinic DS. 2017. Improving potassium recovery with new solubility product values for K-struvite. J. Environ. Eng. Sci. 12:93–103.

Berendonk TU, Manaia CM, Merlin C, Fatta-Kassinos D, Cytryn E, Walsh F, Bürgmann H, Sørum H, Norström M, Pons M-N, et al. 2015. Tackling antibiotic resistance: the environmental framework. Nat. Rev. Microbiol. 13:310–317.

Berglund B, Dienus O, Sokolova E, Berglind E, Matussek A, Pettersson T, Lindgren PE. 2017. Occurrence and removal efficiency of parasitic protozoa in Swedish wastewater treatment plants. Sci. Total Environ. 598:821–827.

Berglund B, Gengler S, Batoko H, Wattiau P, Errampalli D, Leung K, Cassidy MB, Kostrzynska M, Blears M, Lee H, et al. 2015. Environmental dissemination of antibiotic

resistance genes and correlation to anthropogenic contamination with antibiotics. J. Microbiol. Methods 113:28564–28574.

Bhuiyan MIH, Mavinic DS, Koch FA. 2008. Thermal decomposition of struvite and its phase transition. Chemosphere 70:1347–1356.

Bischel HN, Schindelholz S, Schoger M, Decrey L, Buckley CA, Udert KM, Kohn T. 2016. Bacteria inactivation during the drying of struvite fertilizers produced from stored urine. Environ. Sci. Technol. 50:13013–13023.

Borjesson S, Dienues O, Jarnheimer P-A, Olsen B, Matussek A, Lindgren P-E. 2009. Quantification of genes encoding resistance to aminoglycosides, beta-lactams and tetracyclines in wastewater environments by real-time PCR. Int. J. Environ. Health Res. 19:219–230.

Buckwalter SP, Sloan LM, Cunningham SA, Espy MJ, Uhl JR, Jones MF, Vetter EA, Mandrekar J, Cockerill FR, Pritt BS, et al. 2014. Inhibition controls for qualitative real-time PCR assays: Are they necessary for all specimen matrices? J. Clin. Microbiol. 52:2139–2143.

Butkovskyi A, Leal LH, Zeeman G, Rijnaarts HHM. 2017. Micropollutants in source separated wastewater streams and recovered resources of source separated sanitation. Environ. Res. 156:434–442.

Byappanahalli MN, Nevers MB, Korajkic A, Staley ZR, Harwood VJ. 2012. Enterococci in the environment. Microbiol. Mol. Biol. Rev. 76:685–706.

Canadian Food Inspection Agency. 2017. T-4-93 - Safety Guidelines for Fertilizers and Supplements.

Cetinkaya Y, Falk P, Mayhall CG. 2000. Vancomycin-resistant enterococci. Clin. Microbiol. Rev. 13:686–707.

Chen Q, An X, Zhu Y, Su J, Gillings MR, Ye Z. 2017. Application of struvite alters the antibiotic resistome in soil, rhizosphere, and phyllosphere. Environ. Sci. Technol. 51:8149–8157.

Cherkinskii SN, Gabrilevskaia LN, Klimenkova KM, Kozlova MV. 1978. Substantiation of the standard indices for the chlorine decontamination of afterpurified municipal sewage. Gig. Sanit. 5:25–28.

Christou A, Agüera A, Bayona JM, Cytryn E, Fotopoulos V, Lambropoulou D, Manaia CM, Michael C, Revitt M, Schröder P, et al. 2017. The potential implications of reclaimed wastewater reuse for irrigation on the agricultural environment: the knowns and unknowns of the fate of antibiotics and antibiotic resistant bacteria and resistance genes – A review. Water Res. 123:448–467.

Clasen T, Pruss-Ustun A, Mathers CD, Cumming O, Cairncross S, Colford JM. 2014. Estimating the impact of unsafe water, sanitation and hygiene on the global burden of disease: evolving and alternative methods. Trop. Med. Int. Heal. 19:884–893.

Chopra I, Roberts M. 2001. Tetracycline antibiotics: mode of action, applications , molecular biology, and epidemiology of bacterial resistance. Microbiol. Mol. Biol. Rev. 65:232–260.

Choubert JM, Pomiès M, Martin Ruel S, Coquery M. 2011. Influent concentrations and removal performances of metals through municipal wastewater treatment processes. Water Sci. Technol. 63:1967–1973.

Cordell D, Schmid-Neset T, White S, Drangert J-O. 2009. Preferred future phosphorus scenarios: A framework for meeting long-term phosphorus needs for global food demand. Ashley K, Mavinic D, Koch F, editors. London, UK: IWA Publishing.

Cordell D, Neset TSS. 2014. Phosphorus vulnerability: A qualitative framework for assessing the vulnerability of national and regional food systems to the multi-dimensional stressors of phosphorus scarcity. Glob. Environ. Chang. 24:108–122.

Cordell D, Schmid-Neset T, White S, Drangert J-O. 2009. Preferred future phosphorus scenarios: A framework for meeting long-term phosphorus needs for global food demand. Ashley K, Mavinic D, Koch F, editors. London, UK: IWA Publishing.

Culyba MJ, Mo CY, Kohli RM. 2015. Targets for Combating the Evolution of Acquired Antibiotic Resistance. Biochemistry 54:3573–3582.

Da Silva MF, Tiago I, Verissimo A, Boaventura RA, Nunes OC, Manaia CM. 2006. Antibiotic resistance of enterococci and related bacteria in an urban wastewater treatment plant. FEMS Microbiol. Ecol. 55:322–329.

Davies CM, Long, JAH, Donald, M, Ashbolt, NJ. 1995. Survival of fecal microorganisms in marine and freshwater sediments. Appl. Environ. Microbiol. 61: 1888-1896.

Deer DM, Lampel KA, González-Escalona N. 2010. A versatile internal control for use as DNA in real-time PCR and as RNA in real-time reverse transcription PCR assays. Lett. Appl. Microbiol. 50:366–372.

Decrey L, Udert KM, Tilley E, Pecson BM, Kohn T. 2011. Fate of the pathogen indicators phage ΦX174 and Ascaris suum eggs during the production of struvite fertilizer from source-separated urine. Water Res. 45:4960–4972.

de Graaff MS, Temmink H, Zeeman G, Buisman CJN. 2010. Anaerobic treatment of concentrated black water in a UASB reactor at a short HRT. Water 2:101–119.

de Graaff MS, Temmink H, Zeeman G, Buisman CJN. 2011. Energy and phosphorus recovery from black water. Water Sci. Technol. 63:2759–2765.

de Graaff MS, Temmink H, Zeeman G, van Loosdrecht MCM, Buisman CJN. 2011. Autotrophic nitrogen removal from black water: calcium addition as a requirement for settleability. Water Res. 45:63–74.

Degryse F, Baird R, da Silva RC, McLaughlin MJ. 2017. Dissolution rate and agronomic effectiveness of struvite fertilizers – effect of soil pH, granulation and base excess. Plant Soil 410:139–152.

De Sanctis M, Del Moro G, Chimienti S, Ritelli P, Levantesi C, Di Iaconi C. 2017. Removal of pollutants and pathogens by a simplified treatment scheme for municipal wastewater reuse in agriculture. Sci. Total Environ. 580:17–25.

Di Cesare A, Eckert EM, D'Urso S, Bertoni R, Gillan DC, Wattiez R, Corno G. 2016. Co-occurrence of integrase 1, antibiotic and heavy metal resistance genes in municipal wastewater treatment plants. Water Res. 94:208–214.

Dinh Thanh M, Agustí G, Mader A, Appel B, Codony F. 2017. Improved sample treatment protocol for accurate detection of live Salmonella spp. in food samples by viability PCR. PLoS One 12:1–13.

Dillon B, Thomas L, Mohmand G, Zelynski A, Iredell J. 2005. Multiplex PCR for screening of integrons in bacterial lysates. J. Microbiol. Methods 62:221–232.

Drozdova J, Raclavska H, Skrobankova H. 2015. A survey of heavy metals in municipal wastewater in combined sewer systems during wet and dry weather periods. Urban Water J. 12:131–144.

Dunkin N, Weng SC, Coulter CG, Jacangelo JG, Schwab KJ. 2018. Impacts of virus processing on human norovirus GI and GII persistence during disinfection of municipal secondary wastewater effluent. Water Res. 134:1–12.

ECDC EFSA & EMA. 2017. ECDC, EFSA and EMA joint scientific opinion on a list of outcome indicators as regards surveillance of antimicrobial resistance and antimicrobial consumption in humans and food-producing animals. EFSA J. 15.

Fattah KP. 2012. Assessing struvite formation potential at wastewater treatment plants. Int. J. Environ. Sci. Dev. 3:548–552.

Ferreira Da Silva M, Vaz-Moreira I, Gonzalez-Pajuelo M, Nunes OC, Manaia CM. 2007. Antimicrobial resistance patterns in Enterobacteriaceae isolated from an urban wastewater treatment plant. FEMS Microbiol. Ecol. 60:166–176.

Gall AM, Mariñas BJ, Lu Y, Shisler JL. 2015. Waterborne viruses: a barrier to safe

drinking water. PLoS Pathog. 11:1–8.

Gallagher N, Sharvelle S. 2010. Decentralized anaerobic treatment of blackwater: a sustainable development technology concept for urban water management. World Environ. Water Resour. Congr.:4118–4128.

Gao M, Zhang L, Florentino AP, Liu Y. Anaerobic treatment of blackwater collected from different toliet flushing systems: can we achieve both energy recovery and water conservation? In progress.

Gell K, Ruijter FJ d., Kuntke P, Graaff M De, Smit AL. 2011. Safety and effectiveness of struvite from black water and urine as a phosphorus fertilizer. J. Agric. Sci. 3:67–80.

Gillings MR. 2017. Class 1 integrons as invasive species. Curr. Opin. Microbiol. 38:10–15.

Guo J, Li J, Chen H, Bond PL, Yuan Z. 2017. Metagenomic analysis reveals wastewater treatment plants as hotspots of antibiotic resistance genes and mobile genetic elements. Water Res. 123:468–478.

Hamza IA, Jurzik L, Stang A, Sure K, Überla K, Wilhelm M. 2009. Detection of human viruses in rivers of a densly-populated area in Germany using a virus adsorption elution method optimized for PCR analyses. Water Res. 43:2657–2668.

Hamza IA, Jurzik L, Überla K, Wilhelm M. 2011. Evaluation of pepper mild mottle virus, human picobirnavirus and Torque teno virus as indicators of fecal contamination in river water. Water Res. 45:1358–1368.

Haramoto E, Kitajima M, Hata A, Torrey JR, Masago Y, Sano D, Katayama H. 2018. A review on recent progress in the detection methods and prevalence of human enteric viruses in water. Water Res. 135:168–186.

Harwood VJ, Levine AD, Scott TM, Chivukula V, Lukasik J, Farrah SR, Rose JB. 2005. Validity of the indicator organism paradigm for pathogen reduction in reclaimed water and public health protection. Appl. Environ. Microbiol. 71:3163–3170.

Haugland RA, Siefring SD, Varma M, Dufour AP, Brenner KP, Wade TJ, Sams E, Cochran S, Braun S, Sivaganensan M. 2014. Standardization of enterococci density estimates by EPA qPCR methods and comparison of beach action value exceedances in river waters with culture methods. J. Microbiol. Methods 105:59–66.

Heim A, Ebnet C, Harste G, Pring-Åkerblom P. 2003. Rapid and quantitative detection of human adenovirus DNA by real-time PCR. J. Med. Virol. 70:228–239.

Hooper DC. 2001. Mechanisms of action of antimicrobials: focus on fluoroquinolones. Clin. Infect. Dis. 32:S9–S15.

Huang H, Song Q, Wang W, Wu S, Dai J. 2012. Treatment of anaerobic digester effluents of nylon wastewater through chemical precipitation and a sequencing batch reactor process. J. Environ. Manage. 101:68–74.

Huang HM, Song QW, Xu CL. 2011. The mechanism and influence factors of struvite precipitation for the removal of ammonium nitrogen. Adv. Mater. Res. 189–193:2613–2620.

Huchzermeier MP, Tao W. 2012. Overcoming challenges to struvite recovery from anaerobically digested dairy manure. Water Environ. Res. 84:34–41.

Iaconelli M, Muscillo M, Della Libera S, Fratini M, Meucci L, De Ceglia M, Giacosa D, La Rosa G. 2017. One-year surveillance of human enteric viruses in raw and treated wastewaters, downstream river waters, and drinking waters. Food Environ. Virol. 9:79–88.

Jian Z, Hejing W. 2003. The physical meanings of 5 basic parameters for an x-ray diffraction peak and their application. Chinese J. Geochemistry 22:38–44.

Jimenez-Cisneros BE. 2006. Helminth ova control in wastewater and sludge for agricultural reuse. In: Encylopedia of Life Support Systems. Vol. II. p. 12.

Johnson L, Atheesha G. 2013. Water quality indicators: bacteria, coliphage, enteric viruses. Int. J. Environ. Res. Public Health 23:484–506.

Kageyama T, Kojima S, Shinohara M, Uchida K, Fukushi S, Hoshino FB, Takeda N, Katayama K. 2003. Broadly reactive and highly sensitive assay for Norwalk-like viruses based on real-time quantitative reverse transcription-PCR. J. Clin. Microbiol. 41:1548–1557.

Karabegovic L, Uldal M, Werker A, Morgan-Sagastume F. 2013. Phosphorus recovery potential from a waste stream with high organic and nutrient contents via struvite precipitation. Environ. Technol. 34:871–883.

Karkman A, Do TT, Walsh F, Virta MPJ. 2018. Antibiotic resistance genes in waste water. Trends Microbiol. 26:220–228.

Karpowicz E, Novinscak A, Bärlocher F, Filion M. 2010. qPCR quantification and genetic characterization of Clostridium perfringens populations in biosolids composted for 2 years. J. Appl. Microbiol. 108:571–581.

Kauppinen A, Miettinen I. 2017. Persistence of norovirus GII genome in drinking water and wastewater at different temperatures. Pathogens 6: 3-11.

Kemacheevakul P, Chuangchote S, Otani S, Matsuda T, Shimizu Y. 2015. Effect of magnesium dose on amount of pharmaceuticals in struvite recovered from urine. Water Sci. Technol. 72:1102–1110.

Kim D, Min KJ, Lee K, Yu MS, Park KY. 2017. Effects of pH, molar ratios and pre-treatment on phosphorus recovery through struvite crystallization from effluent of anaerobically digested swine wastewater. Environ. Eng. Res. 22:12–18.

Kim D, Ryu H-D, Kim M-S, Kim J, Lee S-I. 2007. Enhancing struvite precipitation potential for ammonia nitrogen removal in municipal landfill leachate. J. Hazard. Mater. 146:81–85.

Kim H, Sudduth A, Hummel JW. 2009. Soil macronutrient sensing for precision agriculture. J. Environ. Monit. 11:1810–1824.

Koeleman JGM, Stoof J, Van der bijl MW, Vandenbroucke-Grauls CMJE, Savelkoul PHM. 2001. Identification of epidemic strains of Acinetobacter baumannii by integrase gene PCR. J. Clin. Microbiol. 39:8–13.

Korajkic A, McMinn BR, Shanks OC, Sivaganesan M, Fout GS, Ashbolt NJ. 2014. Biotic interactions and sunlight affect persistence of fecal indicator bacteria and microbial source tracking genetic markers in the upper mississippi river. Appl. Environ. Microbiol. 80:3952–3961.

Krasowska A, Sigler K. 2014. How microorganisms use hydrophobicity and what does this mean for human needs? Front. Cell. Infect. Microbiol. 4:1–7.

Kujawa-Roeleveld K, Zeeman G. 2006. Anaerobic treatment in decentralised and source-separation-based sanitation concepts. Rev. Environ. Sci. Biotechnol. 5:115–139.

Laridi R, Auclair JC, Benmoussa H. 2005. Laboratory and pilot-scale phosphate and ammonium removal by controlled struvite precipitation following coagulation and flocculation of swine wastewater. Environ. Technol. 26:525–536.

Larsson DGJ, Andremont A, Bengtsson-Palme J, Brandt KK, de Roda Husman AM, Fagerstedt P, Fick J, Flach C-F, Gaze WH, Kuroda M, et al. 2018. Critical knowledge gaps and research needs related to the environmental dimensions of antibiotic resistance. Environ. Int. 117:132–138.

Le Corre KS, Valsami-Jones E, Hobbs P, Jefferson B, Parsons SA. 2007. Struvite crystallisation and recovery using a stainless steel structure as a seed material. Water Res. 41:2449–2456.

Le Corre KS, Valsami-jones E, Hobbs P, Parsons SA. 2005. Impact of calcium on struvite crystal size, shape and purity. J. Cryst. Growth 283:514–522.

Le Corre KS, Valsami-Jones E, Hobbs P, Parsons SA. 2009. Phosphorus recovery from wastewater by struvite crystallization: a review. Crit. Rev. Environ. Sci. Technol. 39:433–477.

Le Corre KS, Valsami-Jones E, Hobbs P, Parsons SA. 2007a. Impact of reactor operation on success of struvite precipitation from synthetic liquors. Environ. Technol. 28:1245–56.

Le Corre KS, Valsami-Jones E, Hobbs P, Parsons SA. 2007b. Kinetics of struvite precipitation: effect of the magnesium dose on induction times and precipitation rates. Environ. Technol. 28:1317–1324.

Le Corre KS, Valsami-Jones E, Hobbs P, Parsons SA. 2009. Phosphorus recovery from wastewater by struvite crystallization: a review. Crit. Rev. Environ. Sci. Technol. 39:433–477.

Legros S, Levard C, Marcato-Romain CE, Guiresse M, Doelsch E. 2017. Anaerobic digestion alters copper and zinc speciation. Environ. Sci. Technol. 51:10326–10334.

Leifels M, Hamza IA, Krieger M, Wilhelm M, Mackowiak M, Jurzik L. 2016. From lab to lake - Evaluation of current molecular methods for the detection of infectious enteric viruses in complex water matrices in an urban area. PLoS One 11:1–16.

Leifels M, Jurzik L, Wilhelm M, Hamza IA. 2015. Use of ethidium monoazide and propidium monoazide to determine viral infectivity upon inactivation by heat, UV-exposure and chlorine. Int. J. Hyg. Environ. Health 218:686–693.

Li D, De Keuckelaere A, Uyttendaele M. 2015. Fate of Foodborne Viruses in the "Farm to Fork" Chain of Fresh Produce. Compr. Rev. Food Sci. Food Saf. 14:755–770.

Li J, Cheng W, Xu L, Strong PJ, Chen H. 2014. Antibiotic-resistant genes and antibiotic-resistant bacteria in the effluent of urban residential areas, hospitals, and a municipal wastewater treatment plant system. Environ. Sci. Pollut. Res. 22:4587–4596.

Li Z, Ren X, Zuo J, Liu Y, Duan E, Yang J, Chen P, Wang Y. 2012. Struvite precipitation for ammonia nitrogen removal in 7-aminocephalosporanic acid wastewater. Molecules 17:2126–2139.

Liu Y, Qu H. 2017. Interplay of digester supernatant composition and operating pH on impacting the struvite particulate properties. J. Environ. Chem. Eng. 5:3949–3955.

Lizasoain A, Tort LFL, García M, Gillman L, Alberti A, Leite JPG, Miagostovich MP, Pou SA, Cagiao A, Razsap A, et al. 2018. Human enteric viruses in a wastewater treatment plant: evaluation of activated sludge combined with UV disinfection process reveals different removal performances for viruses with different features. Lett. Appl. Microbiol. 66:215–221.

Loisy F, Atmar RL, Guillon P, Le Cann P, Pommepuy M, Le Guyader FS. 2005. Real-time RT-PCR for norovirus screening in shellfish. J. Virol. Methods 123:1–7.

Lowther JA, Bosch A, Butot S, Ollivier J, Mäde D, Rutjes SA, Hardouin G, Lombard B, in't Veld P, Leclercq A. 2017. Validation of ISO method 15216 part 1 – quantification of hepatitis A virus and norovirus in food matrices. Int. J. Food Microbiol.

Luby E, Ibekwe AM, Zilles J, Pruden A. 2016. Molecular methods for assessment of antibiotic resistance in agricultural ecosystems: prospects and challenges. J. Environ. Qual. 45:441–451.

Lucena F, Duran AE, Morón A, Calderón E, Campos C, Gantzer C, Skraber S, Jofre J. 2004. Reduction of bacterial indicators and bacteriophages infecting faecal bacteria in primary and secondary wastewater treatments. J. Appl. Microbiol. 97:1069–1076.

Mackowiak M, Leifels M, Hamza IA, Jurzik L, Wingender J. 2018. Distribution of Escherichia coli, coliphages and enteric viruses in water, epilithic biofilms and sediments of an urban river in Germany. Sci. Total Environ. 626:650–659.

Madoni P. 2011. Protozoa in wastewater treatment processes: a minireview. Ital. J. Zool. 78:3–11.

Mamais D, Pitt PA, Cheng YW, Loiacono J, Jenkins D, Wen Y. 1994. Digesters determination to control in anaerobic of ferric chloride precipitation digesters dose struvite sludge. Water Environ. Res. 66:912–918.

Manser ND, Wald I, Ergas SJ, Izurieta R, Mihelcic JR. 2015. Assessing the fate of Ascaris suum ova during mesophilic anaerobic digestion. Environ. Sci. Technol. 49:3128–3135.

Mayer BK, Baker LA, Boyer TH, Drechsel P, Gifford M, Hanjra MA, Parameswaran P, Stoltzfus J, Westerhoff P, Rittmann BE. 2016. Total value of phosphorus recovery. Environ. Sci. Technol. 50:6606–6620.

Mehta CM, Batstone DJ. 2013. Nucleation and growth kinetics of struvite crystallization. Water Res. 47:2890–2900.

Metcalf & Eddy Inc., Tchobanoglous G, Stensel HD, Tsuchihashi R, Burton F. 2014. Wastewater engineering - treatment and resource recovery.

Miao XS, Bishay F, Chen M, Metcalfe CD. 2004. Occurrence of antimicrobials in the final effluents of wastewater treatment plants in Canada. Environ. Sci. Technol. 38:3533–3541.

Michael I, Rizzo L, McArdell CS, Manaia CM, Merlin C, Schwartz T, Dagot C, Fatta-Kassinos D. 2013. Urban wastewater treatment plants as hotspots for the release of antibiotics in the environment: a review. Water Res. 47:957–995.

Miller WR, Munita JM, Arias CA. 2014. Mechanisms of antibiotic resistance in enterococci. Expert Rev. Anti. Infect. Ther. 12:1221–1236.

Mirzaei B, Farivar TN, Juhari P, Mehr MA, Babaei R. 2013. Investigation of the prevalence of vanA and vanB genes in vancomycin resistant enterococcus (VRE) by Taq Man real time PCR Assay. J. Microbiol. Infect. Dis. 3:192–198.

Moulder JF, Stickle WF, Sobol PE, Bomben KD. 1992. Handbook of X-ray photoelectron spectroscopy.

Munch E V., Barr K. 2001. Controlled struvite crystallisation for removing phosphorus from anaerobic digester sidestreams. Water Res. 35:151–159.

Nagajyoti PC, Lee KD, Sreekanth TVM. 2010. Heavy metals, occurrence and toxicity for plants: A review. Environ. Chem. Lett. 8:199–216.

Ohlinger BKN, Member S, Young TM, Member A, Schroeder ED. 1999. Kinetics effects on preferential struvite accumulation in wastewater. J. Environ. Engin 125:730–737.

O'Neill J. 2016. Tackling drug-resistant infections globally: final report and recommendations. Rev. Antimicrob. Resist.:1–84.
Ostara Nutrient Recovery Technologies Inc. 2017. Ostara delivers a complete resource recovery solution.

Ostara Nutrient Recovery Technologies Inc. 2017. The only nutrient recovery solution that prevents digester struvite build-up. Tech. Factsheet:1–2.

Parhad NM, Rao NU. 1974. Effect of pH on survival of Escherichia coli. Water Environ. Fed. 46:980–986.

Paques. 2017. PHOSPAQ ^{TM} Sustainable phosphorus recovery. Tech. Factsheet:1–4.

Parsons SA, Doyle JD. 2002. Struvite scale formation and control. Water Sci. Technol. 49:177–182.

Payment P, Locas A. 2011. Pathogens in water: value and limits of correlation with microbial indicators. Ground Water 49:4–11.

P-Rex. 2015. AirPrex® Struvite crystallization in sludge. Tech. Factsheet:1–2.

Priya M, Haridas A, Manilal VB. 2007. Involvement of protozoa in anaerobic wastewater treatment process. Water Res. 41:4639–4645.

Pruden A, Alcalde R, Alvarez P, Ashbolt N, Bischel H, Capiro N, Crossette E, Frigon D, Grimes K, Haas CN, et al. 2018. An environmental science and engineering framework for combating antimicrobial resistance. Environ. Eng. Sci. 35:1–7.

Prywer J, Torzewska A, Plociński T. 2012. Unique surface and internal structure of struvite crystals formed by Proteus mirabilis. Urol. Res. 40:699–707.

Qiao G, Li H, Xu D-H, Il Park S. 2012. Modified a colony forming unit microbial adherence to hydrocarbons assay and evaluated cell surface hydrophobicity and biofilm production of Vibrio scophthalmi. J. Bacteriol. Parasitol. 3:1–6.

Rahaman MS, Ellis N, Mavinic DS. 2008. Effects of various process parameters on struvite precipitation. Water Sci. Technol. 57:647–654.

Rahman MM, Salleh MAM, Rashid U, Ahsan A, Hossain MM, Ra CS. 2014. Production of slow release crystal fertilizer from wastewaters through struvite crystallization - a review. Arab. J. Chem. 7:139–155.

Rames E, Roiko A, Stratton H, Macdonald J. 2016. Technical aspects of using human adenovirus as a viral water quality indicator. Water Res. 96:308–326.

Randazzo W, Khezri M, Ollivier J, Le Guyader FS, Rodríguez-Díaz J, Aznar R, Sánchez G. 2018. Optimization of PMAxx pretreatment to distinguish between human norovirus with intact and altered capsids in shellfish and sewage samples. Int. J. Food Microbiol. 266:1–7.

Randazzo W, López-Gálvez F, Allende A, Aznar R, Sánchez G. 2016. Evaluation of viability PCR performance for assessing norovirus infectivity in fresh-cut vegetables and irrigation water. Int. J. Food Microbiol. 229:1–6.

Ranotkar S, Kumar P, Zutshi S, Prashanth KS, Bezbaruah B, Anand J, Lahkar M. 2014. Vancomycin-resistant enterococci: troublemaker of the 21st century. J. Glob. Antimicrob. Resist. 2:205–212.

Risebro HL, Doria MF, Andersson Y, Medema G, Osborn K, Schlosser O, Hunter PR. 2007. Waterborne transmission of protozoan parasites: a worldwide review of outbreaks and lesson learnt. J. Water Health 5:1–18.

Rout GR, Das P. 2003. Effect of metal toxicity on plant growth and metabolism: I. Zinc. Argonomic 23:3–11.

Said L Ben, Klibi N, Lozano C, Dziri R, Ben Slama K, Boudabous A, Torres C. 2015. Diversity of enterococcal species and characterization of high-level aminoglycoside resistant enterococci of samples of wastewater and surface water in Tunisia. Sci. Total Environ. 530–531:11–17.

Sales-Ortells H, Fernandez-Cassi X, Timoneda N, Dürig W, Girones R, Medema G. 2015. Health risks derived from consumption of lettuces irrigated with tertiary effluent containing norovirus. Food Res. Int. 68:70–77.

Seib MD, Berg KJ, Zitomer DH. 2016. Reduced energy demand for municipal wastewater recovery using an anaerobic floating filter membrane bioreactor. Environ. Sci. Water Res.

Technol. 2:290–297.

Sheets JP, Yang L, Ge X, Wang Z, Li Y. 2015. Beyond land application : Emerging technologies for the treatment and reuse of anaerobically digested agricultural and food waste. Waste Manag. 44:94–115.

Shih Y-J, Abarca RRM, de Luna MDG, Huang Y-H, Lu M-C. 2017. Recovery of phosphorus from synthetic wastewaters by struvite crystallization in a fluidized-bed reactor: Effects of pH, phosphate concentration and coexisting ions. Chemosphere 173:466–473.

Sobsey MD, Abebe L, Andremont A, Ashbolt NJ, de Roda Husman AM, Gin KY-H, Hunter PR, Meschke JS, Vilchez S. 2015. Antimicrobial resistance: an emerging water, sanitation and hygiene issue briefing note WHO/FWC/WSH/14.07. World Heal. Organ.

Soller JA, Bartrand T, Ashbolt NJ, Ravenscroft J, Wade TJ. 2010. Estimating the primary etiologic agents in recreational freshwaters impacted by human sources of faecal contamination. Water Res. 44:4736–4747.

Song Y, Yuan P, Zheng B, Peng J, Yuan F, Gao Y. 2007. Nutrients removal and recovery by crystallization of magnesium ammonium phosphate from synthetic swine wastewater. Chemosphere 69:319–324.

Standard Methods Committee. 1997. Method 5220: Chemical oxygen demand (COD).

Stumm W, Morgan JJ. 1981. Aquatic chemistry. Wiley-Interscience.

Szczepanowski R, Linke B, Krahn I, Gartemann KH, Gützkow T, Eichler W, Pühler A, Schlüter A. 2009. Detection of 140 clinically relevant antibiotic-resistance genes in the plasmid metagenome of wastewater treatment plant bacteria showing reduced susceptibility to selected antibiotics. Microbiology 155:2306–2319.

Tang P. 2016. Effects of solution pH and seed material on MAP crystallization. Int. J. Environ. Prot. Policy 4:171–177.

Tansel B, Lunn G, Monje O. 2018. Struvite formation and decomposition characteristics for ammonia and phosphorus recovery: a review of magnesium-ammonia-phosphate interactions. Chemosphere 194:504–514.

Taskin B, Gozen AG, Duran M. 2011. Selective quantification of viable Escherichia coli bacteria in biosolids by quantitative PCR with propidium monoazide modification. Appl. Environ. Microbiol. 77:4329–4335.

Taylor a. W, Frazier a. W, Gurney EL. 1963. Solubility products of magnesium ammonium and magnesium potassium phosphates. Trans. Faraday Soc. 59:1580–1584.

Thanh PM, Ketheesan B, Yan Z, Stuckey D. 2016. Trace metal speciation and bioavailability in anaerobic digestion: a review. Biotechnol. Adv. 34:122–136.

Türker M, Çelen I. 2011. Chemical equilibrium model of struvite precipitation from anaerobic digester effluents. Turkish J. Eng. Environ. Sci. 35:39–48.

U.S. Centers for Disease Control and Prevention. 2013. Antibiotic resistance threats in the United States, 2013.

USEPA. 1998. National Strategy for the Development of Regional Nutrient Criteria.

US. EPA. 1999. Estimating Risk from Contaminants Contained in Agricultural Fertilizers Draft Report.

US. EPA. 2007. Method 3051A - Microwave assisted acid digestion of sediments, sludges, soils and oils.

US. EPA. 2012a. 2012 Recreational Water Quality Criteria.

US. EPA. 2012b. Method 1611: enterococci in water by TaqMan® quantitative polymerase chain reaction (qPCR) assay.

US. EPA. 2007. Method 3051A - Microwave assisted acid digestion of sediments, sludges, soils and oils.

US. EPA. 2016. National rivers and streams assessment 2008-2009: a collaborative survey (EPA/841/R-16/007). Washington, DC.

Van Hoek AHAM, Mevius D, Guerra B, Mullany P, Roberts AP, Aarts HJM. 2011. Acquired antibiotic resistance genes: an overview. Front. Microbiol. 2:1–27.

Vierheilig J, Frick C, Mayer RE, Kirschner AKT, Reischer GH, Derx J, Mach RL, Sommer R, Farnleitner AH. 2013. Clostridium perfringens is not suitable for the indication of fecal pollution from ruminant wildlife but is associated with excreta from nonherbivorous animals and human sewage. Appl. Environ. Microbiol. 79:5089–5092.

Wang J, Burken JG, Zhang X. 2006. Effect of seeding materials and mixing strength on struvite precipitation. Water Environ. Res. 78:125–132.

Wang J, Burken JG, Zhang X, Surampalli R. 2005. Engineered struvite precipitation: impacts of component-ion molar ratios and pH. J. Environ. Eng. 131:1433–1440.

Wen Q, Tutuka C, Keegan A, Jin B. 2009. Fate of pathogenic microorganisms and indicators in secondary activated sludge wastewater treatment plants. J. Environ. Manage. 90:1442–1447.

WHO. 2006. Guidelines for the safe use of wastewater, excreta and greywater. Geneva.

WHO. 2016. Global priority list of antibiotic-resistant bacteria to guide research, discovery, and development of new antibiotics.

Wiencek KM, Klapes NA, Foegeding PM. 1990. Hydrophobicity of Bacillus an Clostridium spores. Appl. Environ. Microbiology 56:2600-2605.

Woodford N, Morrison D, Johnson AP, Bateman AC, Hastings JG, Elliott TS, Cookson B. 1995. Plasmid-mediated vanB glycopeptide resistance in enterococci. Microb. Drug Resist. 1:235–240.

Wose Kinge CN, Ateba CN, Kawadza DT. 2010. Antibiotic resistance profiles of Escherichia coli isolated from different water sources in the Mmabatho locality, Northwest Province, South Africa. S. Afr. J. Sci. 106:44–50.

Wuijts S, van den Berg HHJL, Miller J, Abebe L, Sobsey M, Andremont A, Medlicott KO, van Passel MWJ, de Roda Husman AM. 2017. Towards a research agenda for water, sanitation and antimicrobial resistance. J. Water Health 15:175–184.

Xu K, Li J, Zheng M, Zhang C, Xie T, Wang C. 2015. The precipitation of magnesium potassium phosphate hexahydrate for P and K recovery from synthetic urine. Water Res. 80:71–79.

Yang Y, Li B, Zou S, Fang HHP, Zhang T. 2014. Fate of antibiotic resistance genes in sewage treatment plant revealed by metagenomic approach. Water Res. 62:97–106.

Yee R., Leifels M, Scott C, Ashbolt N., Liu Y. 2018. Evaluating microbial and chemical hazards in commercial struvite recovered from wastewater. In progress.

Yetilmezsoy K, Sapci-Zengin Z. 2009. Recovery of ammonium nitrogen from the effluent of UASB treating poultry manure wastewater by MAP precipitation as a slow release fertilizer. J. Hazard. Mater. 166:260–269.